Regulation of cytoskeletal dynamics leading to axis induction in the early zebrafish embryo

By

Elaine Loye Welch

A dissertation submitted in partial fulfillment of

the requirements for the degree of

Doctor of Philosophy

Genetics

at the

UNIVERSITY OF WISCONSIN-MADISON

2017

Date of final oral examination: 05/10/2017

The dissertation is approved by the following members of the Final Oral Committee:

Francisco Pelegri, Professor, Genetics
Arash Bashirullah, Associate Professor, Genetics
Allen Laughon, Professor, Genetics
Michael Sheets, Professor, Biomolecular Chemistry
Ahna Skop, Associate Professor, Genetics

Dedication

I would like to dedicate the work contained in this dissertation to my wonderful mother Cecile Welch-Graham who has been my driving force from the beginning. She has made endless sacrifices to make sure that, unlike her, I received an education; for this I am eternally grateful. This is also for my siblings Lyndon, Tracean, Patricia, Patrick and Patrice, to let them know that they can achieve anything for which they aspire with hard work and determination.

Acknowledgements

I would like to thank my advisor Francisco Pelegri for giving me the opportunity to work in his lab. He has challenged me to grow and think critically as a scientist and I am forever grateful for his support. He has also encouraged my professional development and supports the avenues that I wish pursue post grad school. To my thesis committee members, thank you for your expertise, encouragement and guidance with my projects and for helping me through the bumps along the way. I would like to thanks members of the genetics department for supporting my academic endeavors and providing opportunities that contribute to where I am now. I would also like to thank my colleague Dr. Celeste Eno who has been a great support system for me throughout my time in the lab. She was always there to lend her scientific expertise and to faithfully go with me to the gym every day. Thanks to Abbey Thompson and Sara Patterson who has provided incredible support for me through the SciMed GRS community, which has been an invaluable part of my experience at UW. There are so many other friends and family that have helped me in tremendous ways throughout this experience with encouragement, prayers and a shoulder to cry on, your efforts have not gone unnoticed. Thank you all!

Table of contents

Abbreviations

DV: Dorsoventral
MTs: Microtubules
tmi: too much information
GP: Germ Plasm
RNPs: Ribonucleoparticles
FISH: Fluorescent in situ hybridization
WMISH: Whole mount in situ hybridization
CPC: Chromosomal passenger complex
FMA: Furrow microtubule array

List of figures and tables

Chapter 1: Reorganization of vegetal cortex microtubules and its role in axis induction in the early vertebrate embryo

Chapter 2: Hecate/Grip2a acts to reorganize the cytoskeleton in the symmetry-breaking event of embryonic axis induction

Chapter 3: Cortical depth and differential transport of vegetally localized dorsal and germ line determinants in the zebrafish embryo

Abstract

Axis induction requires the transport of maternal and zygotic factors from the vegetal pole of the embryo to the dorsal organizer region. This is mediated by a process called the cortical rotation which is mediated by a parallel arrangement of microtubules. These studies describe this process using maternal effect mutations that have been identified from genetic screens, using *Danio rerio* (zebrafish) as a model. *hecate* encodes Glutamate receptor interacting protein 2a which is necessary for microtubule reorganization and formation of dorsoanterior structures. *tmi* encodes Protein regulator of cytokinesis 1-like and is necessary for cell division and cytokinesis, as well as microtubule bundling and alignment necessary for axis induction. Both maternal mutants as well as drug inhibitors of cytoskeletal dynamics reveal important steps to understanding the conserved developmental process of vertebrate axis induction.

Chapter 1: Reorganization of vegetal cortex microtubules and its role in axis induction in the early vertebrate embryo

Elaine L. Welch and Francisco Pelegri*

Laboratory of Genetics, University of Wisconsin-Madison, Madison, WI, USA

*Correspondence to: fjpelegri@wisc.edu

Author contribution: EW wrote the manuscript, FP edited before submission.

Elaine Welch and Francisco Pelegri (2017). *Reorganization of vegetal cortex microtubules and its role in axis induction in the early vertebrate embryo*, **Cytoskeleton: Structure, Dynamics, Function and Disease**, Jose C. Jimenez-Lopez (Ed.), InTech, ISBN 978-953-51-4898-2.

1.1. Abstract

In vertebrate species, induction of the embryonic axis is initiated by the transport of maternally supplied determinants, initially localized to the vegetal pole of the egg, towards the prospective organizer in the animal region. This transport process remains incompletely understood. Here, we review studies involving embryonic manipulations, visualization and functional analysis of the cytoskeleton, and loss- and gain-of-function conditions, which provide insights in this process. Transport of dorsal determinants requires cytoskeletal reorganization of a vegetal array of microtubules, microtubule motors and an off-center movement of the vegetal cortex with respect to the inner egg core, a so-called cortical rotation. Additional mechanisms may be used in specific systems, such as a more general animally-directed movement found in the teleost embryo. Initial polarity of the microtubule movement depends on early asymmetries, which are amplified by the movement of the outermost cortex. An interplay between microtubule organization and axis specification has also been reported in other animal species. Altogether, these studies show the importance of cytoskeletal dynamic changes, such as bundling, force-inducing motor activity, and regulated cytoskeletal growth, for the intracellular transport of maternally-inherited factors to their site of action in the zygote.

Key words: Microtubules, dorsoventral axis, cortical rotation, zebrafish, *Xenopus*, embryo

1.2. Introduction

One of the main events that take place during vertebrate development is the establishment of the dorsoventral (DV) axis. This process has been studied in a variety of vertebrate species, in particular in the amphibian *Xenopus laevis* and the teleost fish *Danio rerio*. In these model systems, embryological manipulations show that the ligation of the vegetal pole of the freshly laid egg results in embryos that lack a primary (dorsal) axis (reviewed in [1]). However, the ligation of the same vegetal region after the second cell cycle does not have this effect. These manipulations allowed to infer the presence of dorsal determinants initially localized to the vegetal pole of the egg, which following fertilization are transported to a more animal region to specify prospective dorsal cells. These determinants, through mechanisms that have not been fully determined, result in the activation of the canonical Wnt/β-catenin signaling pathway, leading to dorsal gene expression and the induction of the dorsal organizer [2–4]. In *Xenopus*, the inferred transport of these determinants is coincident with the shift of the outer cortex, the "cortical rotation", relative to the entire cytoplasm, a shift that is readily apparent due to pigmentation patterns of granules in the cortex.

It has been shown that the process of transport of dorsal determinants is dependent on the microtubule cytoskeleton in the egg cortex, specifically on the reorganization of vegetal microtubules as long tracks of parallel bundles (Figure 1, left and center). In *Xenopus*, this array of aligned microtubule bundles extend the relatively long span from the vegetal pole to the prospective dorsal region near the animal pole, and visualization of particles, vesicles and fluorescently labeled factors suggest that these tracks of microtubules may be acting as a substrate for long range transport [5,6]. Early zebrafish

embryos do not exhibit an outwardly apparent cortical shift [7] and aligned vegetal microtubule tracks appear to span a more restricted area [6,8], yet vegetal cortex microtubules may have similar transport functions as in *Xenopus*. Analysis of dynamic changes during microtubule reorganization in the context of the embryo has led to a model in which cortical rotation and microtubule-dependent transport are interdependent processes that together mediate the transport of dorsal determinants [5] (see below). Forward and reverse genetic approaches in various systems, primarily zebrafish and *Xenopus*, have contributed to our understanding of these processes.

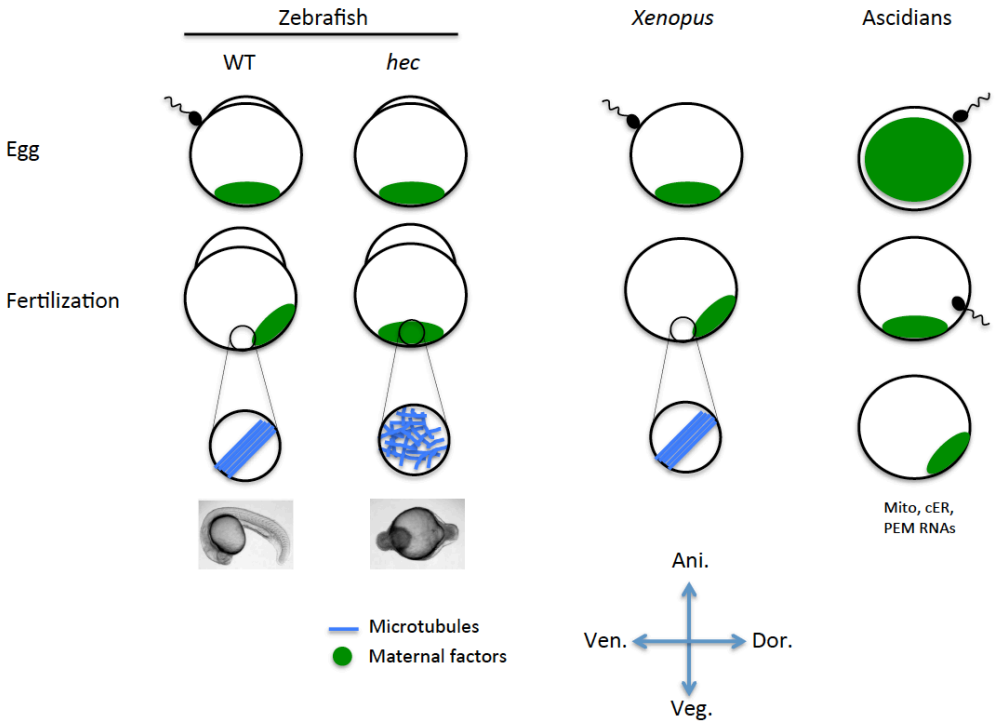

Figure 1: Schematic of early developmental processes in fish, amphibians and ascidians.

Prior to fertilization in zebrafish and Xenopus wild-type embryos, maternal factors are localized at the vegetal pole. Upon fertilization, they are transported to the dorsal region via a parallel array of vegetal microtubules. In zebrafish hecate/grip2a (hec) mutants, this vegetal microtubule array is compromised, preventing an initial early off-center dorsal shift of maternal factors, subsequently leading to a ventralized embryo (bottom row, second from left, compared to wild-type at left). A second phase of animally directed transport in zebrafish (not shown) appears to depend on a more general mechanism, independent of vegetal microtubule alignment [26]. In ascidian embryos, first the egg cortex and plasma membrane contract, resulting in the segregation of microfilaments, mitochondria, cER, postplasmic/PEM RNAs, and muscle-forming and endoderm-forming determinants toward the vegetal pole region. These components subsequently move toward the posterior pole through the attraction of a microtubule aster-based center.

This chapter reviews events involved in the cytoskeletal reorganization required for the movement of determinants leading to axis induction. The outcome of microtubule reorganization in the early embryo is the induction of the dorsal axis and we first briefly review this process in the zebrafish as well as the amphibian *Xenopus leavis*.

1.3. Induction signals for axis specification

A primary event in the establishment of the dorsoventral axis in zebrafish and *Xenopus* is the translocation of the normally cytoplasmic protein β-catenin into the nuclei of dorsal blastomeres during cleavage stages [2,9,10] (Figure 2). In the absence of Wnt signaling, levels of the cytoplasmic pool of β-catenin are reduced by the activity of glycogen synthase kinase 3 (GSK-3), which promotes β-catenin degradation (reviewed in [11]). Accordingly, enrichment of β -catenin in dorsal cell nuclei, as well as dorsal axis induction, is blocked by ectopic expression of GSK-3. Activation of the canonical Wnt signaling pathway, resulting in localized inhibition of GSK-3 on the future dorsal side of the embryo, is thought to promote the accumulation of cytoplasmic β -catenin in the prospective dorsal region. Accumulated β -catenin in turn translocates to the nucleus [3,12], where it can influence gene expression (reviewed in [13,14]).

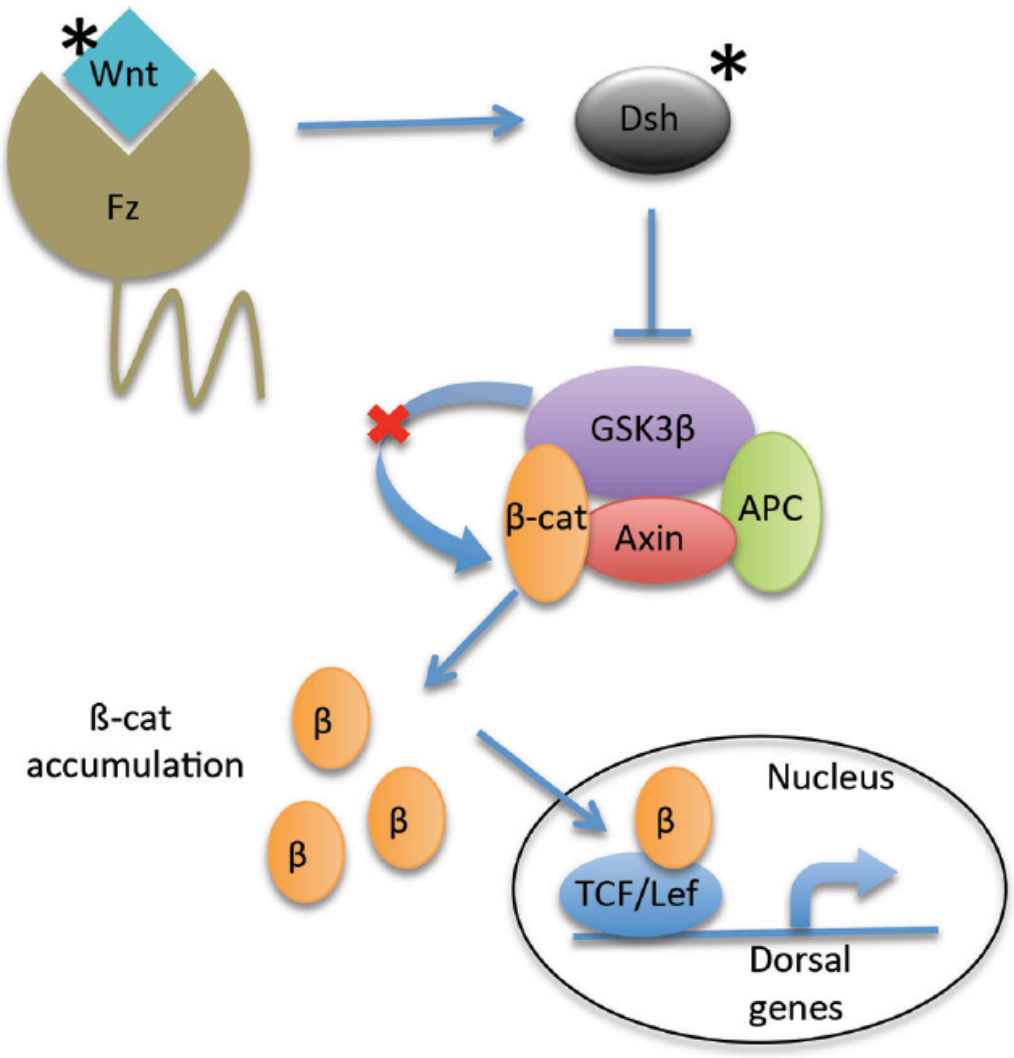

Figure 2: Simplified diagram of Wnt activity involved in axis specification.

In the canonical Wnt signaling pathway, extracellular Wnt protein ligands signal through Frizzled transmembrane receptors to activate the cytoplasmic protein dishevelled (Dsh). Dsh in turn inhibits GSK-3 activity. GSK-3 is part of a complex that normally destabilizes β-catenin protein; hence, inhibition of GSK-3 activity results in β-catenin stabilization and its translocation into the nucleus. β-Catenin forms a complex with the transcription factor Tcf/Lef to activate dorsal-specific gene expression. Asterisk denotes factors thought to undergo a translocation to the prospective dorsal site through a process involving cortical rotation and/or microtubule-dependent transport.

A key mediator of Wnt signaling, when localized to the nuclei, β-catenin acts as a transcriptional effector to activate dorsal-specific genes such as *bozozok/dharma*, *nodal-related 1* and *chordin* [13]. Products expressed from these dorsal genes along with those from their targets antagonize ventralizing signals such as bone morphogenetic proteins (BMPs), thus promoting dorsal cell fate specification (reviewed in [14,15]). Failure of nuclear β-catenin to localize to the nuclei of dorsal blastomeres results in the ventralization of embryos [16].

The intricacies of the Wnt signaling pathway and its role in vertebrate axis induction has been determined through many studies, including functional manipulation of genes through ectopic expression and knock down or expression of dominant-negative constructs (reviewed in [11,17]). For example, overexpression of β-catenin induces a secondary axis in *Xenopus* embryos [18]. When β-catenin is overexpressed in zebrafish embryos, it is able to induce the expression of target genes such as *goosecoid* and *ntl* [19]. Similar results have been observed with the overexpression of some Wnt ligands [20], including overexpression of Wnt8 and Wnt8b in zebrafish embryos [19].

Several mutations in zebrafish have allowed for the confirmation of an endogenous role for Wnt signaling pathway in axis induction in the early embryo. An identified recessive maternal-effect mutant in *ichabod* results in defective dorsal organizer formation and severe ventralization and shows impaired nuclear localization of maternal β-catenin protein [21]. This mutation was found to be closely linked to β-*catenin-2* (ctnnb2), a duplicate copy of the β-catenin gene located on a different linkage group from the previously characterized β-*catenin-1* [22]. It was shown that although the *ichabod* mutation does not functionally alter the β-*catenin-2* open reading frame, the level of maternal β-

catenin-2 transcript, (but not that of the unlinked β-*catenin-1* gene), is substantially lower in *ichabod* mutant embryos. Reduction of β-*catenin-2* function in wild-type embryos by the injection of a gene-specific morpholino antisense oligonucleotide (MO) results in ventralized phenotypes [22], which are similar to those seen in *ichabod* mutant embryos. In contrast, MOs directed against β-*catenin-1* has no ventralizing effect on wild-type embryos. These data strongly suggest that the *ichabod* mutation corresponds to the β-*catenin-2* gene, providing genetic evidence for the role of this factor in axis induction. These results indicate that activation of Wnt signaling via the stabilization of β-catenin is essential for proper organization of the embryonic axis.

Activation of the Wnt/β-catenin signaling pathway, as well as its important role in the expression of dorsal genes, has been extensively studied in a number of cellular systems (reviewed in [11,17]). However, the identity of the molecules thought to activate the pathway in early vertebrate embryos, referred to as dorsal determinants, remain to be fully elucidated. Wnt11 has been proposed to be a dorsal determinant in amphibian species [23]. In *Xenopus*, *wnt11* mRNA is located at the vegetal pole of the mature egg and, after fertilization, becomes enriched at the future dorsal side of the embryo. Thus, the localization of *wnt11* RNA exhibits the expected behavior of the inferred dorsal determinant, as predicted from transplantation of the dorsal-inducing activity. Additionally, it was shown that depletion of *wnt11* mRNA from oocytes results in embryos defective in dorsal axis induction [24]. Further studies have implicated ubiquitously present Wnt5 as acting together with Wnt11 in Wnt/β -catenin activation [23]. Studies in zebrafish have not implicated Wnt11 or Wnt5 function in axis induction. However, a role for zebrafish Wnt8a has been suggested in this process [25,26]. Similarly to *Xenopus wnt11*,

zebrafish *wnt8a* mRNA is localized to the vegetal pole of the egg and can be observed to translocate after fertilization towards the animally-located blastomeres. These studies also indicate that, while Wnt/β-catenin pathway activation may be highly conserved in axis induction across the animal kingdom, there are variations in maternally based mechanisms leading to pathway activation.

Studies in *Xenopus* and zebrafish also showed that the transport of dorsal determinants, which results in the translocation of β-catenin to the nuclei of dorsal blastomeres, requires an array of parallel microtubules originating in the vegetal pole region [6,27]. Miller and colleagues investigated the mechanisms responsible for the dorsal activation of the Wnt signaling pathway in *Xenopus* eggs and the subsequent specification of dorsal cell fates in the embryo. It was shown that Dishevelled (Dsh) protein, a cytoplasmic component of the Wnt pathway that functions upstream of β-catenin [28], is associated with vesicle-like organelles that become enriched in the prospective dorsal side of the egg at the end of the first cell cycle, and that the accumulation of Dsh persists through early cleavage stages [27]. Further experiments revealed that when embryos were UV irradiated at the vegetal hemisphere, the distribution of Dsh was blocked, which also blocked dorsal axis formation. Subsequently, when observing the subcellular localization of Dsh fused to GFP, it was revealed that during cortical rotation Dsh-GFP is translocated toward the future dorsal side via the vegetal cortex microtubule array [27]. Together, these data suggest a model in which dorsal-determining factors including *wnt* gene products and Dsh protein are transported via a microtubule-dependent pathway to the future dorsal side of the embryo, leading to the localized activation of the Wnt signaling pathway, the accumulation of β-catenin in dorsal blastomeres, and the induction of dorsal cell fates [27].

1.4. Transport of dorsal determinants in *Xenopus* and zebrafish

1.4.1. Molecular mechanism underlying cortical rotation

As mentioned above, embryological manipulations showed that, both in *Xenopus* and zebrafish, dorsal determinants are localized to the vegetal pole of the egg at the time of fertilization, but have within several cell cycles moved to an animal region where they influence cell fate. Spatial changes that lead to these determinants translocating to the prospective dorsal region appear to be facilitated by two processes: the rotation of the zygote cortex with respect to the core during cortical rotation, and the intracellular movement of factors (e.g. *wnt* RNA or Dsh-bound vesicles) along aligned vegetal microtubules. These are likely intertwined processes, as tracks of parallel microtubules appear to be required not only for the movement of vegetal factors to the prospective dorsal side but also for cortical rotation [29]. Treatment of the vegetal portion of embryos to prevent microtubule polymerization, such as exposure to nocodazole, cold shock, hydrostatic pressure or UV irradiation [30,31] shows that microtubules are required for cortical rotation in normal conditions [31]. In contrast, cytochalasin D, an inhibitor of actin polymerization, does not interfere with cortical rotation, indicating that microfilaments are not required for this process. Inhibition of protein synthesis with cycloheximide, known to have dramatic effects such as cell cycle arrest [32], also does not inhibit rotation, indicating that the control of cortical rotation is post-translational and depends on pre-formed maternal proteins [32].

Failure of cortical rotation results in a ventralized mutant phenotype in the embryo. However, in embryos treated to inhibit microtubules, a cortical rotation can be artificially induced by gravity after immobilizing the embryo in a matrix and physically turning it 90

degrees. This manipulation results in the formation of dorsal structures, albeit delayed [33]. Under these conditions, gravity leads to a rearrangement of the heavier yolk-containing core of the embryo relative to the cortex. This is thought to increase the proximity of vegetally localized cortical signals to internal regions in the more animally-located prospective dorsal region. The ability of the entire cortex to move as a whole relative to the embryonic core contrasts with the visualization of moving particles along microtubule tracks. These observations suggest that both transport along cortical microtubules and a cortical shift relative to the embryonic core contribute to the redistribution of signals involved in axis induction during the early embryonic cell cycles. We subsequently address each of these processes.

1.4.2. Relocalization of RNA determinants during oogenesis and early embryogenesis

The mRNA for the putative zebrafish dorsal determinant *wnt8a* is localized to the Balbiani body during oogenesis. The zebrafish Balbiani body [34] is a mitochondria-rich subcellular structure in the forming oocyte shown to be essential for the creation of animal-vegetal polarity in the oocyte. This structure, thought to be homologous to the early messenger transport organizer (METRO) pathway of localization in *Xenopus* [35], constitutes a crucial component of a vegetally-directed transport pathway that entraps mRNAs and other gene products necessary for patterning of the embryo and germ cell formation [34,35]. Association of *wnt8a* RNA with the Balbiani body leads to the localization of this RNA to the vegetal pole of the mature zebrafish oocyte [25]. Thus, fertilized embryos initiate development with *wnt8a* RNA localized to the vegetal pole.

However, in wild type embryos starting at 30 minutes, this mRNA experiences an asymmetric movement toward a more animal region that will become the prospective organizer region [25,26].

In addition to *wnt8a*, genetic studies in zebrafish have allowed the identification of other maternally inherited factors involved in the transport of determinants essential for dorsal axis induction, such as *hecate/grip2a* mRNA and Tokkaebi/Syntabulin proteins. Molecular characterization of the three independent mutant alleles of the zebrafish maternal effect gene *hecate/grip2a* shows that loss of function for its product results in embryos with reduced dorsal gene expression and concomitant defects in forming dorso-anterior structures [26]. Similar effects are caused by a single mutation in *tokkaebi* [36]. Mutations in genes coding for either *hecate/grip2a* or *tokkaebi/syntabulin* do not interfere with vegetal pole localization of *wnt8a* RNA during oogenesis, but abolish the animally-directed asymmetric movement of this RNA that normally occurs after fertilization [25,36,37]. Given the proposed role for Wnt8a as the dorsal determinant in zebrafish [25], the post-fertilization defect in *wnt8a* RNA asymmetric movement in *hecate* and *tokkaebi* mutants explains axis induction defects observed in these mutants.

Positional cloning of *hecate* shows that this gene encodes Glutamate receptor interacting protein (Grip) 2a, a factor whose *Drosophila* homolog protein is associated with membrane vesicles in postsynaptic neuronal cells, where it acts in the reception of Wnt signals across the synapse [38]. Zebrafish Grip2a protein has four PDZ domains, which are known to interact with membrane-associated factors including members of the Wnt signaling pathway. Mutant alleles in this protein exhibit a range of phenotypes whose severity roughly correlates with the extent of unaffected protein, with the strongest allele

causing a premature stop codon that truncates the Grip2a protein, removing all 4 PDZ domains [26]. The mutation in *tokkaebi* corresponds to syntabulin, which codes for a linker of the kinesin I motor protein [36], and acts as a linker molecule that attaches mitochondria to the kinesin-1 motor, thereby contributing to anterograde trafficking of mitochondria to neuronal processes [39]. The known roles for Grip and syntabulin in the transport of membranous organelles and signaling in neuronal types begins to draw similarities between microtubule-based transport of vesicles in neurons and the transport of dorsal determinants, also thought to at least partially associate with vesicles (as highlighted by Dsh-GFP movement [27]), in early vertebrate embryos.

Consistent with the effect of maternal-effect mutations in *hecate/grip2a* and *tokkaebi/syntabulin* on the formation of dorsal structures, products of these genes are localized in patterns that likely facilitate the movement of dorsal determinants [26,36,40]. In wild-type embryos, *grip2a* mRNA, like *wnt8a*, is localized via a Balbiani Body-dependent mechanism to the vegetal pole of the oocyte and early embryo, and following egg activation and fertilization the localization of this mRNA shifts off-center about 30 degrees from the vegetal pole. During oogenesis, as in the case of *grip2a* RNA, *syntabulin* RNA becomes localized to the vegetal pole of the oocyte via a Balbiani body-dependent pathway, resulting in the localization of both syntabulin mRNA and protein to the vegetal pole of the egg. After fertilization, as in the case of *wnt8a* RNA and *grip2a* RNA, Syntabulin protein (but not its RNA) exhibits an off-center shift upon egg activation [36]. The off-center shift from the vegetal pole exhibited by *wnt8a* and *grip2a* mRNAs and Syntabulin protein roughly corresponds to a 30 degree arc offset from the vegetal pole that contains an aligned set of arrayed microtubules in the zebrafish embryo and which has been observed to contain

moving subcellular particles [8]. Thus, the movement of these mRNAs roughly corresponds to a region in the teleost early embryo thought to undergo mass movements toward the future dorsal side, reminiscent of the amphibian cortical rotation. The coordinated asymmetric movement of vegetally localized products such as *wnt8a* RNA*, grip2a* RNA and Syntabulin protein is consistent with the observed mass transport of particles in the vegetal cortex [8], although they may also reflect specialized transport mechanisms involving microtubule tracks, Syntabulin-mediated motor movement and *wnt8* RNA- and *grip2a* RNA-containing RNPs.

Genetic analysis indicates that the Hecate/Grip2a and Tokkaebi/Syntabulin products are required for the off-center, asymmetric shift of vegetally localized determinants that follows fertilization. *hecate/grip2a* mutants show defects in this off-center movement for vegetally localized products such as *wnt8a* RNA and Syntabulin protein, as well as *grip2a* RNA itself [26]. Mutations in *tokkaebi/syntabulin* also result in defects in *wnt8a* RNA and Syntabulin protein asymmetric movement [36]. However, in both of these mutants, localization of dorsal factors (*wnt8a* RNA, *hecate/grip2a* RNA and *tokkaebi* products) during oogenesis remains unaffected. Localization of these factors during oogenesis is instead dependent on the function of Bucky Ball [25,26,36], a novel protein required for Balbiani body formation [34,41]. Thus, localization of dorsal factors to the vegetal pole of the oocyte relies on a Balbiani body-dependent pathway, and the asymmetric movement of these factors after fertilization, which is required for axis induction, depends on the subsequent action of *hecate* and *tokkaebi.* As discussed below, these functions rely on microtubule-dependent reorganization and transport processes.

Additional studies have shown that, as in *Xenopus*, zebrafish vegetal cortex microtubules become reorganized into parallel bundles [6,8] (Figure 3). The studies paint a picture of translocation of dorsal axis determinants that is remarkably similar to that of the known *Xenopus* cortical rotation. However, transport of dorsal determinants in zebrafish appears to use a dual system, in which microtubule alignment initiates an off-center shift, and other cytoskeletal processes mediate long-range transport (see below). In spite of observed differences, these studies show that microtubule-dependent transport of dorsal determinants plays an essential role in canonical Wnt pathway activation and dorsal axis determination in teleost embryos, as in amphibians.

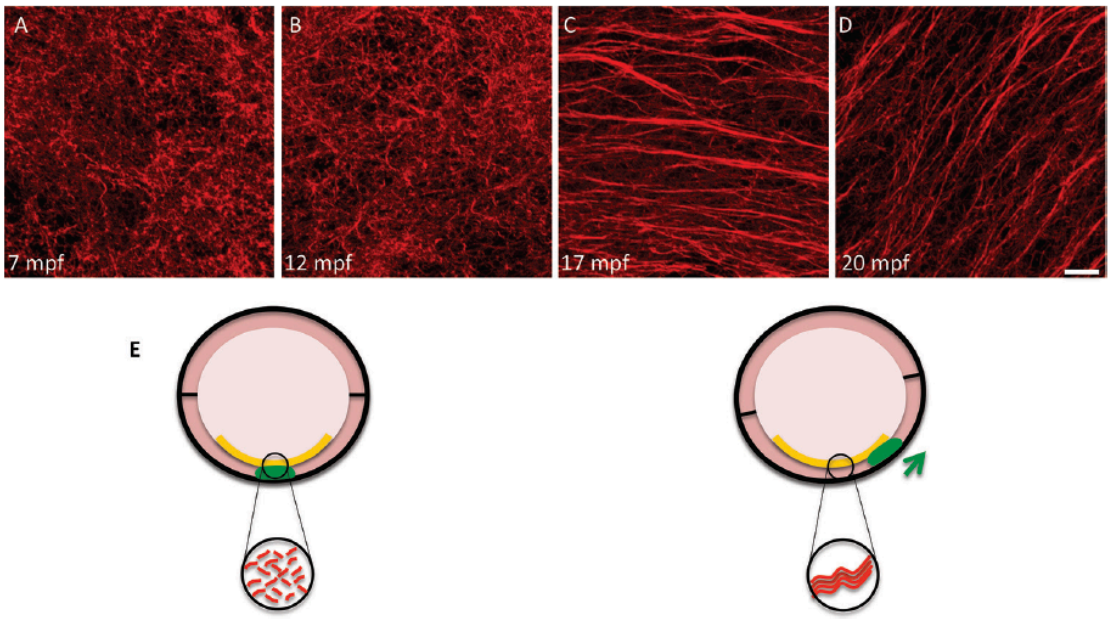

Figure 3: Alignment of microtubules at the vegetal cortex in wild-type zebrafish embryos.

(A–B) Between 7 and 12 min postfertilization (mpf), microtubules at the vegetal cortex start to become reorganized to form parallel bundles. (C–D) Around 17 mpf, microtubules become organized into parallel bundles. This organization facilitates the movement of dorsal determinants from the base of the vegetal pole to the dorsal region. Scale bar in D represents two microns for all panels. (E) Diagrammatic representation of dorsal determinants (green) with respect to more internally located determinants, such as vegetally localized germplasm determinants in the zebrafish (orange), depicting microtubule reorganization (red lines), before (left) and after (right) cortical rotation.

Interestingly, the RNA for the *grip2* homolog in *Xenopus*, *XGRIP2* is, like its zebrafish homologue *grip2a*, localized to the mitochondrial cloud (the Balbiani body in zebrafish) during *Xenopus* oocyte development and subsequently to the vegetal pole of the mature oocyte. However, in contrast to zebrafish *grip2a* RNA, *Xenopus XGRIP2* RNA does not have an apparent role in axis induction, and after fertilization its RNA becomes localized to germ plasm masses that coalesce in the embryo [42–44] (see below).

Altogether, these studies indicate key roles for RNA localization pathways during oogenesis leading to the localization of factors required for axis induction to the vegetal pole of the egg. Initially localized to the vegetal pole through the action of the mitochondrial cloud during oogenesis, after fertilization and egg activation these factors exhibit an off-center shift dependent on the function of vegetally localized factors, such as Grip2a and the kinesin motor adaptor protein Syntabulin.

1.4.3. Reorganization of microtubules during cortical rotation

At least in the case of *Xenopus* it is clear that the rotation of the cortex facilitates the relocation of dorsalizing factors from the vegetal pole to the presumptive future dorsal side, or to a more animal (equatorial in the case of *Xenopus*) region, where they act to initiate gene expression programs corresponding to the body axis, at a signaling center known as the Spemann's, organizer [45]. Following fertilization in the *Xenopus* egg, the cortex rotates an average of 30 degrees within the first cell cycle, relative to the inner cytoplasm [29,46], a rotation mediated by an array of aligned microtubules beneath the vegetal cortex [47]. At the same time, these microtubules become aligned in a parallel

arrangement with plus ends directed toward the direction of cortical translocation [48], a reorganization that coincides with the initiation of cortical rotation [30].

In the early *Xenopus* embryo, microtubule nucleation occurs deep within the animal hemisphere [49] by the sperm-derived centriole near the site of sperm entry. These microtubules extend through the cytoplasm towards the vegetal pole, where they contribute to the formation of the vegetal microtubule array [50] (Figure 4, top left). Thus, in *Xenopus*, rotation (and dorsal site formation) typically occurs away from the sperm site of entry. On the other hand, the orientation of the vegetal microtubule array can occur in potentially any direction with respect to the cleavage site [5,29], so that it is unlikely that there is an intrinsic preexisting dorsal asymmetry in the egg with respect to the site of cellular cleavage, itself determined by the orientation of the spindle [51,52]. Studies have also shown that cortical rotation can occur toward the sperm entry point in specific cases, such as when the sites of meiotic spindle assembly and polar body extrusion are oppositely located [53], suggesting the existence of additional unknown variables that influence the orientation of the vegetal microtubule array. In *Xenopus*, cortical rotation is halted right before the first cellular cleavage occurs [47], when the microtubules of the vegetal microtubule array are depolymerized under the influence of M-phase promoting factor [54].

A morphologically apparent cortical rotation, observed through changes in the position of an outer cortex relative to an inner core as observed in *Xenopus*, is not readily apparent in the zebrafish embryo. However, studies have indicated the existence of processes in the zebrafish embryo that share similarities with the amphibian cortical rotation. Early studies showed that fluorescent polystyrene beads injected at the vegetal

pole were transported animally along microtubule-based cortical tracks in a microtubule dependent manner [6], and that this movement had temporal dynamics and functional requirements similar to that of the movement of putative dorsal determinants as defined by embryological manipulations. However, this movement was shown to occur by visualizing injected fluorescent beads, as opposed to an entire cortex, consistent with translocation along microtubule arrays but not necessarily a shift of the outer cortex analogous to a cortical rotation. A cortical rotation process in the zebrafish was later suggested by the observation of coordinated movement of optically visible particles in the vegetal cortex, and that long-term tracking of these particles occurs towards the presumed dorsal side, as expected from a cortical rotation [8].

A cortical rotation-like process is also consistent with differences in the changes in RNP particle distribution at different cortical depths, as visualized by fluorescent in situ hybridization, since RNPs located at the outermost cortex undergo a spatial shift with respect to more internally located RNPs [55] (Figure 3E). To understand the basis of transport for differentially localizing factors at the zebrafish vegetal-most embryo cortex, double fluorescence in situ hybridization (FISH) was used to detect pairs of RNAs for factors involved in axis induction (*wnt8a* and *grip2a*) and RNAs for vegetally localized germ cell specification factors (*dazl*). Localization of these three factors occurs in different RNPs at the vegetal cortex. Moreover, RNAs for dorsal factors, *wnt8a* and *grip2a*, are enriched in the outermost layer of the cortex, whereas RNPs for the primordial germ cell determining factor *dazl* are present in more internal regions [55]. Although domains containing RNPs for these two sets of vegetally-localized factors are both centered at the vegetal pole in the egg, upon fertilization the domain containing the outer-cortex RNPs, coding for dorsal

induction factors, shifts relative to the more internal domain containing germ plasm determinant RNPs. RNPs in the outer cortex have a function in axis determination and need to experience a relative shift to generate an asymmetry in the embryo, facilitated by the cortical rotation-like movement. These observations further add to the finding of bulk particle movement at the zebrafish embryo vegetal cortex [8] and are consistent with a cortical rotation-like process in the early zebrafish embryo. As in amphibians, this teleost cortical rotation-like process may be involved in generating an asymmetry in the location and function of dorsal determinants.

Thus, both in amphibians and teleost, an array of aligned microtubules is associated with the movement of RNA molecules and the vegetal cortex itself with respect to the inner egg core, which altogether mediates the transport of dorsal determinants towards the prospective dorsal site.

1.4.4. Long-range vs. short-range transport

In both *Xenopus* and zebrafish, the process of cortical rotation appears to be an important part of the mechanism that directs dorsal determinants to their final destination at the animal pole. However, zebrafish and *Xenopus* embryos display some differences in mechanism of animally-directed transport. In the *Xenopus* embryo, aligned tracks of microtubules appear to span most if not all of the space between the vegetal pole and the prospective dorsal region. In zebrafish, in contrast, transport with an end-point in blastomeres at the animal pole of the embryo appears to depend on two sequential steps: an initial short-range transport of vegetal localizing factors generating a slight off-center shift toward the animal pole, followed by animally-directed transport via a more general

mechanism. The first, off-center asymmetry, is revealed by changes in the distribution of RNAs such as *wnt8a* and *grip2a* in a process that appears to correspond to a cortical rotation-like event. As in *Xenopus*, the initial cortical rotation-like event in zebrafish depends on the alignment of microtubules in parallel bundles at the vegetal cortex. The microtubule reorganization into parallel bundles in turn is dependent on the function of Grip2a (Figure 1, left). Short-range shift in vegetal signals are affected in homozygous *hecate/grip2a* mutant embryos, evidenced by defective off-center shift of RNAs such as *wnt8a* and other factors [26].

The second step involves a long-range transport along the medio-lateral region of the embryo to the base of the blastomeres by a mechanism that is neither restricted to the dorsal side, nor dependent on Grip2a function [6,26]. The presence of such a second transport mechanism can be inferred by the observation that *hecate/grip2a* mutants do not exhibit a defect in the long-range animally-directed translocation of vegetally injected beads, indicating that animally-directed movement occurring in mediolateral regions is independent of *hecate* function. Indeed, injection of beads in opposite sides of the embryo indicates that animally-directed travel along the mediolateral region of the yolk cortex occurs in both injected sides, implying that, as opposed to *Xenopus*, the entirety of the zebrafish mediolateral cortex, and not only the prospective dorsal region, is competent for long-range movement [26]. It is possible that the second step in zebrafish depends on a more general transport mechanism associated with animally-directed transport in meroblastic embryos, through which other factors with a function unrelated to dorsal axis induction, such as vegetally localized germ plasm RNAs [56], need to travel animally towards the forming blastodisc. Thus, both *Xenopus* and zebrafish experience animally-

directed movement of dorsal determinants facilitated by a microtubule-dependent cortical rotation-like process. However, the *Xenopus* embryo uses a mechanism in which cortical rotation and microtubule alignment into parallel tracks together implement long-range movement of dorsal determinants through an apparently seamless mechanism. In teleost embryos, on the other hand, embryonic-scale differences along the dorsoventral axis are generated by the sequential action of a short-range off-center movement mediated by less expansive vegetal microtubule array, which is subsequently amplified by a more general animally-directed system.

1.4.5. Other factors involved in vegetal microtubule reorganization

Additional factors have been identified to be important for dorsal axis induction. A mutation in the maternal-effect mutant *brom bones*, which has a nonsense mutation in the gene *hnRNP I*, shows egg activation defects, disorganized vegetal microtubule array formation, and subsequently defects in axis formation [16]. Additionally, these mutant embryos display egg activation defects as evidenced by failure of cortical granule exocytosis and chorion expansion. In zebrafish, cortical granule exocytosis is one of the first cellular responses to egg activation, and is initiated by a wave of elevated cytoplasmic calcium that is impaired in *brom bones* mutants [16]. It is possible that the defect in vegetal microtubule alignment in *brom bones* is similarly based on the calcium release defects after egg activation, which is required for vegetal microtubule array formation [8].

Studies have also revealed that an ubiquitin ligase, *tripartite motif-containing 36* (*trim36*) is required for vegetal microtubule reorganization mediating axis induction. *Xenopus trim36* is maternally expressed, with mRNA enrichment at the Balbiani body in

stage 1 oocytes and localization to the vegetal cortex of stage VI oocytes. *trim36* mRNA is also detectable in the germ plasm of fertilized eggs and cleavage stage embryos [57] . Embryos depleted of *trim36* function by injection of antisense oligos into oocytes exhibit defects in vegetal microtubule reorganization and cortical rotation, leading to reduced organizer formation and severe embryo ventralization at later stages [57]. As expected, injection of *wnt11* mRNA rescues this effect, confirming that Trim36 functions upstream of Wnt/β-catenin activation. Recent studies have shown that Trim36 attenuates the growth of plus ends of vegetal microtubules during array formation [58] (see below), indicating a role for this factor, possibly through the mediation of protein degradation, in the regulation of microtubule dynamics essential for array formation.

The mRNA for *dead end*, which codes for an RNA binding protein initially shown to be essential for the development of the germ line [59–68], has been shown to have a role in vegetal microtubule array formation. In *Xenopus,* the mRNA for *dead end1*, like that of *trim36*, is localized to the vegetal pole of the oocyte [61]. Early embryos depleted of dead end exhibit an unexpected defect in the formation of arrays of parallel vegetal microtubules and consequently axis specification [69]. This requirement appears to depend on the function of Dead end protein to directly bind *trim36* mRNA and anchor it to the oocyte vegetal pole, likely increasing Trim36 protein local concentration in this region [46].

Thus, a variety of factors are required for the reorganization of vegetal cortex microtubules leading to dorsal determinant transport. In some cases, these factors are important for general processes essential for the microtubule reorganization, such as in the case of *hnRNP I* and dependent-calcium signaling. In other cases, these factors begin to

delineate a pathway for microtubule reorganization, as in the case of *dead end* and *trim36*, involved in the regulation of vegetal microtubule growth.

1.4.6. Mechanism of microtubule alignment during cortical rotation

Even though it has been shown that microtubule-dependent cortical rotation is important for axis formation, the molecular mechanisms underlying the organization and orientation of cortical microtubule have not been fully elucidated. The process of cortical rotation is highly conserved, and it likely requires the embryo to use a significant amount of energy. Weaver and Kimelman [70] asked the question that if dorsal determinants can travel along microtubules, then what is the purpose of the cortical rotation? As described above, cortical rotation might directly contribute to the overall animally-directed movement of the dorsalizing activity. However, studies have also suggested that cortical rotation might serve to facilitate aligning the polymerizing microtubules into parallel bundles and orienting their plus ends towards the dorsal side. One favored model for the orientation of the microtubule array is a positive feedback mechanism where initial random asymmetry in microtubule growth is amplified by continuous movement of the cortex [31,58].

Microtubules that form the vegetal microtubule array appear to arise from several sources [70]. Some are nucleated by the centriole of the sperm, which acts as a minus-end microtubule organizing center, others extend towards the periphery from unknown sources deep in the cytoplasm and bend into the vegetal shear zone, and finally, some arrays appear to polymerize spontaneously in the vegetal shear zone [49,50]. As the vegetal microtubule array begins to form, it becomes progressively stabilized by movement

of the cortex during cortical rotation, which provides an amplifying loop for microtubule alignment [58]. The precise manner by which this cortical movement contributes to microtubules alignment and stabilization is not fully understood. Suggested mechanisms, described below, include a combing process mediated by cortically anchored kinesin-related proteins [54,70] or the stabilization of microtubules by membrane compartments such as the endoplasmic reticulum and vesicles [58].

Vegetal microtubules originally appear with their plus ends in a random orientation, yet subsequently become aligned in parallel arrays with plus ends directed towards the dorsal side (reviewed in [70], see also [58]) (Figure 4). Marrari and colleagues suggested how microtubules could become aligned through cortical motor proteins and the process of the cortical rotation [54] (reviewed in [70]). They proposed that cortically anchored plus end directed motor proteins, such as kinesins, move toward microtubule plus ends, generating a cortical displacement with respect to the inner core [47,54,71]. The attachment of plus ends to the moving cortex mediates aligning of microtubules in the same direction. Thus, the movement and action of these kinesin related proteins could potentially align the microtubules as well as generate the pulling force that is needed to translocate the cortex relative to the cytoplasm [54,70]. This positive feedback loop also allows amplifying an original small asymmetry into the observed prominent array of parallel microtubule bundles.

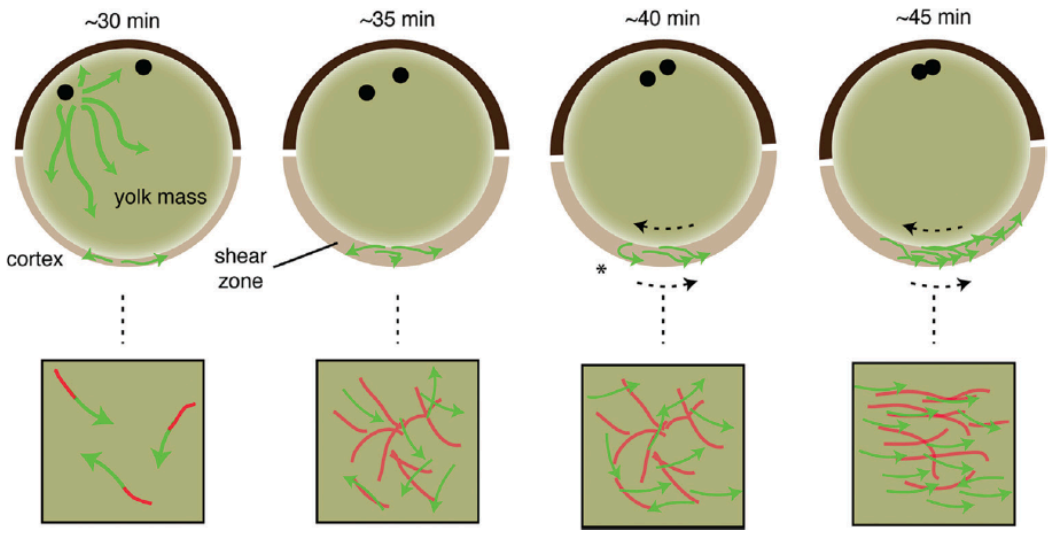

Figure 4: Microtubule dynamics during cortical rotation.

In the *Xenopus* embryo, microtubule polymerization is initiated approximately 30 min after fertilization at the vegetal cortex, when astral microtubules derived from sperm components at the animal pole reach the vegetal cortex. Microtubule polymerization also occurs at the vegetal pole (growing microtubule (plus) ends indicated by green arrows and preformed microtubules by red lines). Relative movement between the yolk cell and the cortex (dashed arrows), initiated by the asymmetry conferred by the sperm-derived asters, facilitates the alignment of both growing and preformed microtubules in the direction of movement. Microtubule alignment in turn contributes to cortical movement. Microtubules oriented toward the dorsal side, the direction in which the cortex rotates (Reprinted from Ref. [58], with permission).

Marrari and colleagues also investigated the role of kinesin and dynein motors in the formation of the cortical microtubule array as well as their role in the translocation of the vegetal cortex [47,54,71]. The function of kinesin was inhibited using an antibody against a highly conserved peptide of the kinesin motor domain, LAGSE. Anti-LAGSE antibodies block spindle elongation in semi-*in vitro* systems [47,54,71,72] , and successfully interfere with kinesin function [47,54,71]. The function of dynein was inhibited by microinjection of p50/dynamitin beneath the vegetal cortex [54]. In *Xenopus* egg extracts as well as cells, excess dynamitin inhibits processes dependent on dynein function by disrupting the dynactin complex [73].

Inhibition of kinesin related function results not only in expected defects in mitosis and cell cleavage but also in disruptions in the array of vegetal microtubules and cortical rotation [71]. On the other hand, inhibition of dynein causes an inward shift in the distribution of microtubules with respect to the cortex, indicating that dynein functions to move microtubules outward, into the vegetal subcortical layer [47]. Moreover, these experiments showed that the formation of the vegetal microtubule array (and therefore cortical rotation) is sensitive to dynein inhibition prior to array formation, but that cortical rotation remains sensitive to inhibition of kinesin function throughout the normal period of rotation [47]. Together, these data suggest that kinesin and dynein motors have different functions during cortical rotation [47] (Figure 5). In this model, dynein motors anchored to internal elements generate an outward force to facilitate bringing microtubules from the inner egg core region to the vegetal cortex. Kinesins, on the other hand, are thought to act by tethering microtubule plus ends to the cortex, thus generating a pulling force on microtubule arrays, mediating the rotation of the cortex itself, and favoring further parallel

alignment of microtubules within the array. It is important to note that, after the vegetal microtubule array has formed, further microtubule alignment and cortical rotation can occur independent of dynein function, but motors of the kinesin related protein family are needed for the movement of the cortex [47]. Thus, kinesin motor function appears to be essential for *Xenopus* cortical rotation, whereas the role of dynein appears to be more indirect. Altogether, these data suggest that both motor proteins interact early in the process of vegetal microtubule array, followed by a period in which kinesin-dependent translocation is sufficient to generate cortical movement.

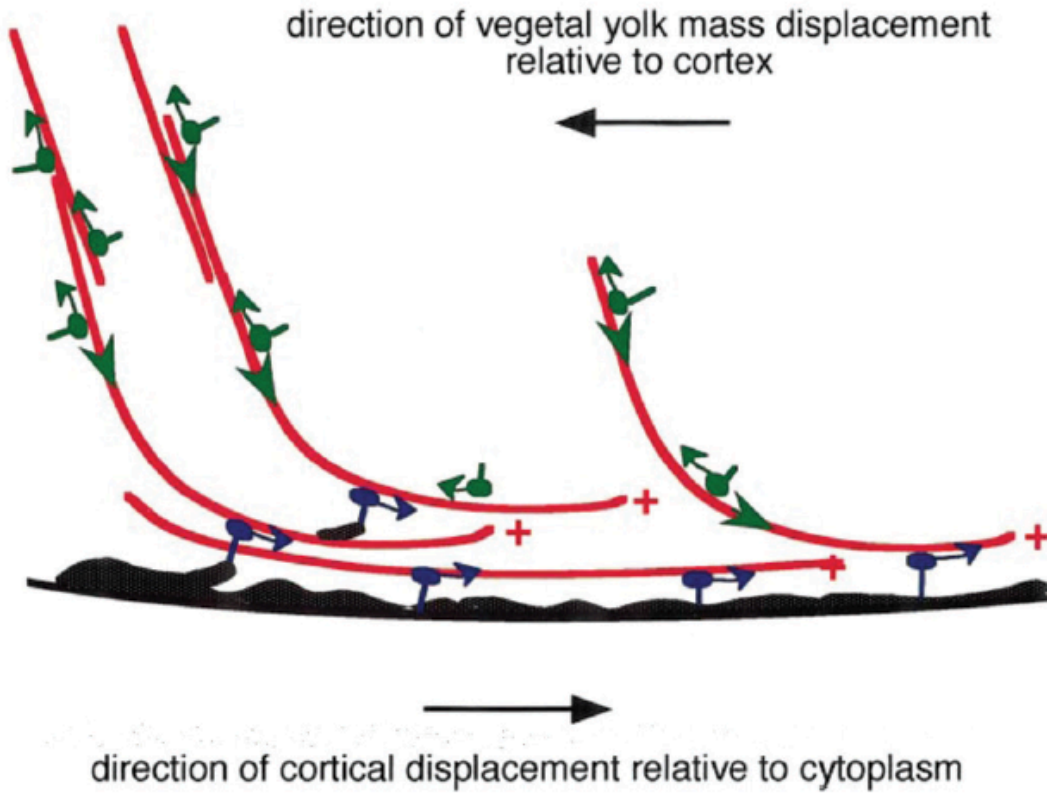

Figure 5: Proposed role of microtubule-dependent motors on the rotation of the vegetal cortex, as suggested by inhibitor studies.

[47, 54, 71]. A pushing force from the minus-end-directed microtubule motor dynein (green; green arrows show direction of motor movement relative to microtubules) helps translocate microtubules (depicted in red) from the inner cytoplasm outward onto the cortical surface (green arrowheads indicate direction of microtubule movement). Plus-end directed microtubule motors such as kinesins (blue) anchor microtubules to the cortex and facilitate cortical movement relative to the yolk mass (blue arrows show direction of motor movement relative to microtubules). (Reprinted from Ref. [71], with permission. The original image has been rotated horizontally for a better comparison to others in this chapter.)

Olson and colleagues performed experiments that would characterized microtubule plus-end dynamics in *Xenopus* oocytes and eggs, identified changes in microtubule stability and plus end flux during the oocyte to egg transition, and characterized behaviors that are present at the onset of cortical rotation [58] (Figure 4). They showed that the initial phase of microtubule assembly is between 25-35 minutes post egg activation. During this time, microtubules are short and dynamic with a low initial density that increases rapidly [58]. In the second phase of assembly, microtubules polymerize rapidly from sites within the vegetal cortex. Microtubules became thinner or less bundled, and the entire network appears to sink deep into the cytoplasm. At this time the microtubule array is referred to as exhibiting a "fine-combed" appearance, which is thought to be the result of the continual action of cortical kinesin-related proteins that straighten microtubules as the cortex moves along them [47,58,70]. At the same time, at approximately 36 minutes post activation, the cortical shift in relation to the egg core becomes apparent [58]. These studies also reveal that microtubule directed growth, occurring after the initial cortical microtubule alignment, has an important contribution to the formation of the vegetal array of parallel microtubules, which powers cortical rotation.

It was previously noted that the direction of microtubule polymerization in cultured cells depends on the arrangement of elongated tubes of endoplasmic reticulum [74]. Endoplasmic reticulum, vesicles and tubes possess kinesin-like microtubule associated proteins that associate with microtubules during transport and elongation, and it is possible that similar membrane organelles are attached to the vegetal cortex and facilitate kinesin-mediated anchoring of microtubules during cortical rotation [31]. A precedent for this is the association of cortical ER with aligned microtubules in early ascidian embryos

[75] (see below). Further studies will be required to address a potential role for membrane organelle attachment in *Xenopus* vegetal microtubule array formation and cortical rotation, such as membrane organelle sliding between membrane organelles and microtubules, or associations of ER extensions with growing microtubule tips [76].

Studies in zebrafish are consistent with mechanisms for cortical microtubule array formation and alignment as detailed in amphibians, including the presence of early internal microtubules, increase in cortical microtubule polymerization concomitant with microtubule alignment and bulk movement of the cortex, and the aligned orientation of microtubule plus ends towards the prospective dorsal site [8].

Altogether, these studies suggest that the formation of the vegetal microtubule array is dependent on the orchestration of various influences, including dynein-dependent outward translocation of existing microtubule, kinesin-dependent vegetal anchoring of cortical microtubules, and microtubule polymerization at the vegetal cortex. Vegetal microtubule and cortical rotation are interdependent and enhance each other, resulting in the alignment of preexisting and new microtubules and allowing dorsal determinant transport.

1.5. Cortical rotation and cytoskeletal dynamics in invertebrate and proto-vertebrate systems

As described above, a cortical rotation process has been described in amphibians, and a related process proposed in teleosts. However, other studies have described processes of cytoskeletal reorganization that serve a similar purpose as the cortical rotation, namely the early distribution of cellular determinants that will help pattern the

egg or embryonic axis. We briefly discuss three such examples below, in ascidians (a chordate proto-vertebrate), the nematode *Caenorhabditis elegans* and the dipteran *Drosophila melanogaster,* highlighting similarities with cortical rotation-like processes in lower vertebrates. For a more in-depth description of these processes, the reader if referred to [77–81] .

1.5.1 Ascidians

In ascidians, gastrulation and neurulation involve cellular rearrangements that are comparable to those in vertebrates, with the exception that ascidians are composed of just a few hundred cells, while vertebrate embryos contain thousands of cells [82]. In fact, the very first classical evidence that localized determinants control cell fate specification was found in ascidians [82,83].

The ascidian egg undergoes dramatic cytoplasmic and cortical reorganizations between fertilization and the beginning of the first cleavage, a process that has been referred to as ooplasmic segregation [83–85]. Ascidian ooplasmic segregation occurs in two major phases (Figure 1, right). The first phase occurs shortly after fertilization. The first consequence of fertilization is that a calcium wave is initiated from the site where the sperm and egg fuses [86]. Upon fertilization, the sperm activates the stage IV oocyte, which was arrested in metaphase I of meiosis, resulting in the contraction of the egg cortex and the plasma membrane as a wave that travels across the egg in the animal to vegetal direction. It was suggested early on that an oocyte actomyosin cortical network can only contract in a general animal to vegetal direction regardless of the sperm entry site, because of it being less dense around the animal pole, in a basket-like arrangement [86,87]. This

animal-to-vegetal contraction in turn causes the segregation of cortical and subcortical components including microfilaments, mitochondria, and the cortical endoplasmic reticulum (cER), [77,88,89].

Unfertilized eggs after the first phase of ooplasmic segregation are radially symmetrical along the animal-vegetal (A-V) axis. This symmetry is broken in the second phase of reorganization after the movement of cortical and subcortical components from the vegetal pole toward the posterior pole occurs, generating an antero-posterior asymmetry, and eggs become bilaterally symmetrical [77]. In this second ooplasmic segregation phase, a number of cellular organelles such as the ER and mitochondria are brought toward the future posterior pole [90]. These organelles also anchor specific RNAs, termed postplasmic/PEM, which are important for muscle determination and the specification of the posterior germ cell fate, in particular the germ line [91]. Other factors involved in endoderm formation and gastrulation do not move toward the future posterior pole and instead expand their distribution to the vegetal hemisphere [77] (see Figure 1). Reminiscent of asymmetry development in *Xenopus*, it has been suggested that also in the ascidian egg, reorganization of plus end directed motors attached to the ER could provide the major force to move the vegetal cortex dorsally to a more equatorial location [48,92].

Ascidian embryonic polarity is directed by a posteriorly located centrosome, introduced through sperm entry in this region [77,93,94] . In contrast to the first phase which is driven by microfilaments, and where the sperm triggers a cortical contraction [88], the second phase is mediated by anchoring of one of the centrosomes of the bipolar spindle to the vegetal posterior cortex resulting in the posterior asymmetric localization of

germ line-determining components. Spindle pole posterior anchoring also results in the eccentric, posteriorly located placement of the spindle, which in turn (because of the influence of the spindle midzone on furrow induction) [51,52], results in asymmetric division [75,77]. In this manner, the embryo generates sets of smaller posterior cells fated to become the germ line.

Thus, in both *Xenopus* and ascidians, microtubule-dependent function results in the redistribution of embryonic determinants just before the onset of embryonic mitoses, the posterior-specifying cytoplasmic components such as the cER-mRNA and myoplasm domains being displaced posteriorly in ascidians, and dorsalizing factors being translocated toward the future dorsal side in *Xenopus* [89,95].

1.5.2. *Caenorhabditis elegans*

In the nematode *C. elegans,* a role for PAR proteins in anterior-posterior (AP) axis specification is well documented [96]. In contrast, dorsal-ventral (DV) patterning in this system is less understood. It was recently reported that the so-called cytokinetic midbody remnant (MBR), a thus-far poorly studied organelle, acts as a polarity cue to define the *C. elegans* DV axis [97]. The MBR is an organelle that forms from the cytokinetic midbody when the fully constricted actomyosin furrow embraces the condensed material of the spindle midzone [98,99]. To understand the role of the MBR in DV axis specification, Singh and Pohl [100] analyzed the pattern of segregation and the movements of the MBR during the first divisions of the *C. elegans* embryo. The AP axis of the *C. elegans* embryo is established by the asymmetric distribution of PAR proteins during the P0 division producing an anterior AB and a posterior P1 blastomere. Subsequently, the DV axis is

established in the transition from the two-cell to the four-cell stage [101]. During prophase of the second cell division in the P1 cell, a 90 degree rotation of the nucleus-centrosome complex relative to the AP axis takes place, and is regarded as a key event in DV axis formation [102,103]. It was not clear as to what generates this movement, which has long been a point of interest. The authors showed that the MBR was displaced toward the ventral side of the embryo and that it acts as a positional cue for mitotic spindle rotation in the P1 cell, thereby establishing DV axis patterning. Importantly, the authors demonstrated that ventral displacement of the MBR is directed by Myosin II cortical flow [97,100]. In this system, again microtubules together with coordinated actomyosin regulation are important for symmetry breaking events in the embryo.

1.5.3. *Drosophila melanogaster*

In *D. melanogaster*, the transition from a round to an elongated egg is driven by the rearrangement of the polar arrays of microtubules [80,81], a process that is again facilitated by the actomyosin cytoskeleton [81]. As in *C. elegans* and ascidians this reorganization results in the segregation of cell determinants to the posterior pole of the egg, except that in the case of *Drosophila*, these changes occur during oogenesis and not early embryogenesis.

Altogether, these studies show that the microtubule cytoskeleton, and in some cases the actomyosin cortex, is used to generate axis asymmetry in various organisms, although the precise details of the interactions, and whether microtubules act as tracks that mediate transport or attraction centers, are specific to different species [97,104].

1.6. Relationship between axis induction and germ cell specification

As mentioned above, in addition to dorsal determinants, anuran and teleost embryos contain other vegetally localized factors, particularly RNAs that become associated with the germ plasm. The germ plasm, also referred to as nuage, is a maternally inherited cytoplasmic structure containing RNPs present in some animal species. Through a mechanism referred to a preformation, inherited germ plasm determines the germ cell fate [105]. Evidence for preformation mechanism for PGC induction in anurans was originally shown by the inheritance of electron dense cytoplasm, corresponding to germ plasm, into the primordial germ cells of this organism [106]. This electron dense cytoplasm was later shown to contain specialized mRNAs involved in germ cell specification [107]. Similarly, RNAs involved in germ cell development in zebrafish, such as for the gene *vasa* [108] and subsequently other mRNAs [56,59,109], were shown to localize in electron dense particles and become segregated to primordial germ cells.

Maternally-inherited germ plasm in *Xenopus* and zebrafish contains shared sets of factors for primordial germ cell specification, such as *deleted in azoospermia-like (dazl)* and *Xcat2*/*nanos*. Zebrafish and *Xenopus* additionally share similarities in the way in which germ plasm masses are assembled and segregated, including the gradual condensation of germ plasm masses from smaller particles, the formation of four germ masses, and their asymmetric segregation during cell division in the cleavage stages [110,111].

Recent studies in these systems have begun to suggest a functional connection between axis induction and germ cell determination. As described above, during oogenesis both dorsal determinants are transported to the vegetal pole of the egg through the mitochondrial cloud in *Xenopus* and its equivalent structure, the Balbiani body, in zebrafish

[111,112]. Moreover, during early embryogenesis, genes acting in dorsal induction functionally overlap and share localization patterns with genes involved in germ cell determination. For example, the germ plasm component *dead end,* which has been well characterized as a germ plasm-specific transcript both in *Xenopus* [61] and zebrafish [59] and is known to function in germ cell migration and survival, has been shown in *Xenopus* to have an unexpected role in axis induction [46]. *XDead end* localizes to the vegetal pole in oocytes beginning at early stage III to stage VI, when it becomes transported to the vegetal pole via the late RNA transport pathway [61]. It has recently been shown that maternal XDead end plays a role in vegetal microtubule reorganization required for dorsal axis induction [46]. When XDead end function is disrupted, the expression of dorsal-specific genes is reduced and embryos become ventralized, due to the disruption in vegetal microtubule reorganization [46]. As mentioned above, this requirement appears to be due to a role for XDead end function in the vegetal cortex anchoring of the RNA for the Trim36 Ubiquitin ligase [46], itself needed for growth regulation of the vegetal microtubule array [58].

Conversely, factors known to be involved in dorsal axis induction also function in germ cell development. One example is maternal Syntabulin, which as mentioned above is important for vegetal microtubule array reorganization and axis induction in both zebrafish and *Xenopus* [36,113]. Recently, *syntabulin* mRNA has been shown to localize in *Xenopus* cleaving embryos to clusters near the cleavage furrow on the vegetal hemisphere of the early embryo, consistent with germ plasm localization and colocalization with *Xpat* RNA, a germ cell marker, during later stages [113]. *Xenopus* Syntabulin is also expressed in scattered cells localized along the posterior endoderm, presumably primordial germ cells

[113]. These data suggest that, in addition to a role in DV patterning, Syntabulin may have a role in germ cell development.

Similarly, *grip2a*, which as mentioned above is required for vegetal cortex microtubule reorganization in zebrafish [26], has gene homologs involved in germ cell development in the *Xenopus* embryo [43,44], suggesting a potential scenario in which an ancestral *grip* gene had a role in both processes. Altogether, these findings suggest that there is functional overlap between factors involved in germ plasm segregation and axis induction. Whether this functional overlap is caused by evolutionary history or convergent evolution remains to be determined.

It is important to note, as stated above, that there is a difference with respect to cortical depth between the factors that are localized to the vegetal pole. Those that are important for microtubule reorganization and thereby patterning the embryonic axis, namely *grip2a* and *wnt8a*, are located toward the outer most region of the cortex. This allows them to be transported from the vegetal to the prospective dorsal region of the egg and embryo through a cortical rotation-like process. Those factors that are important for germ cell specification, such as *dazl* RNA, are localized deeper within the embryo and are transported via the actin cytoskeleton to the animal pole, where they become localized to the aggregating zebrafish germ plasm [55]. Thus, RNA localization at the cortex reflects transport mechanisms consistent with the function of the localized product.

These set of studies highlight commonalities between processes and factors involved in axis induction and germ cell specification. Factors such as Dead end, Grip2 and Syntabulin may form a core gene set with a current or ancestral function in both axis induction and germ cell determination.

1.7. Conclusion: Challenges and future directions

The cytoskeleton plays an essential role in axis specification, through its role mediating the movement of maternal factors within the early zygote. Studies have shown that the reorganization of the microtubule cytoskeleton is important for the transport of factors from the vegetal pole of the embryo to the future dorsal side in both zebrafish and *Xenopus*, in a process associated with the shift of the outer-most cortical layer of the embryo – a cortical rotation. This cytoskeletal reorganization allows for the asymmetric transport of localized dorsal determinants, involved in the specification of the main embryonic axis. Precise mechanisms for microtubule reorganization remain incompletely understood, although are known to involve microtubule dependent motors and a positive feedback loop in which an early asymmetry and microtubule alignment triggers the rotation of the cortex, which in turn amplifies and stabilizes the incipient cytoskeletal rearrangement. Anurans and teleosts show similarities in the use of microtubule arrays and a cortical rotation-like mechanism, although they also exhibit differences in the spatial extent implemented by these coordinated processes, variations that may be related to the different cleavage type of these embryos. Components of the germ plasm, which also become localized to the vegetal pole of the fertilized embryo, may escape cortical rotation by virtue of differential localization in more internal regions of the embryo. A comparison of early cytoplasmic segregation events in other species, such as ascidians, nematodes and dipterans, highlights the importance of microtubule- and other cytoskeletal-dependent processes in the generation of early asymmetries in the embryos. Further studies will allow better understanding for mechanisms of microtubule generation, bundling and alignment that

drive the movement of cellular determinants in the early vertebrate embryo, and their relation to similar processes in other animal lineages.

1.8. Acknowledgements

We would like to thank the members of the Pelegri lab for feedback and encouragement. This work was supported by NIH grants 5RO1GM065303 and 3RO1GM65303-10A1S1. E.W. received additional support from NIH Training Grant 2 T32 GM007133 to the Laboratory of Genetics.

1.9. References

1. Sive HL. The frog prince-ss: A molecular formula for dorsoventral patterning in Xenopus. Genes Dev. 1993;7: 1–12. doi:10.1101/gad.7.1.1
2. Schneider S, Steinbeisser H, Warga RM, Hausen P. B-Catenin Translocation Into Nuclei Demarcates the Dorsalizing Centers in Frog and Fish Embryos. Mech Dev. 1996;57: 191–198. doi:10.1016/0925-4773(96)00546-1
3. Larabell CA, Torres M, Rowning BA, Yost C, Miller JR, Wu M, et al. Establishment of the dorso-ventral axis in Xenopus embryos is presaged by early asymmetries in β-catenin that are modulated by the Wnt signaling pathway. J Cell Biol. 1997;136: 1123–1136. doi:10.1083/jcb.136.5.1123
4. Petersen CP, Reddien PW. Wnt Signaling and the Polarity of the Primary Body Axis. Cell. 2009;139: 1056–1068. doi:10.1016/j.cell.2009.11.035
5. Houston DW. Cortical rotation and messenger RNA localization in Xenopus axis formation. Wiley Interdiscip Rev Dev Biol. 2012;1: 371–388. doi:10.1002/wdev.29
6. Jesuthasan S, Strähle U. Dynamic microtubules and specification of the zebrafish embryonic axis. Curr Biol. 1997;7: 31–42. doi:10.1016/S0960-9822(06)00025-X
7. Kimmel CB, Ballard WW, Kimmel SR, Ullmann B, Schilling TF. Stages of embryonic development of the zebrafish. Dev Dyn. 1995;203: 253–310. doi:10.1002/aja.1002030302
8. Tran LD, Hino H, Quach H, Lim S, Shindo a., Mimori-Kiyosue Y, et al. Dynamic microtubules at the vegetal cortex predict the embryonic axis in zebrafish. Development. 2012;139: 3644–3652. doi:10.1242/dev.082362
9. Fagotto F, Funayama N, Glück U, Gumbiner BM. Binding to cadherins antagonizes the signaling activity of β-catenin during axis formation in Xenopus. J Cell Biol. 1996;132:

1105–1114. doi:10.1083/jcb.132.6.1105
10. Heasman J, Ginsberg D, Geiger B, Goldstone K, Pratt T, Yoshida-Noro C, et al. A functional test for maternally inherited cadherin in Xenopus shows its importance in cell adhesion at the blastula stage. Development. 1994;120: 49–57.
11. Clevers H. Wnt/beta-Catenin Signaling in Development and Disease. Cell. 2006. pp. 469–480. doi:10.1016/j.cell.2006.10.018
12. Yost C, Torres M, Miller JR, Huang E, Kimelman D, Moon RT. The axis-inducing activity, stability, and subcellular distribution of beta-catenin is regulated in Xenopus embryos by glycogen synthase kinase 3 [Internet]. Genes and Development. 1996. pp. 1443–1454. doi:10.1101/gad.10.12.1443
13. Schier AF, Talbot WS. Molecular genetics of axis formation in zebrafish. Annu Rev Genet. 2005;39: 561–613. doi:10.1146/annurev.genet.37.110801.143752
14. Langdon YG, Mullins MC. Maternal and Zygotic Control of Zebrafish Dorsoventral Axial Patterning. Annu Rev Genet. 2011;45: 357–377. doi:10.1146/annurev-genet-110410-132517
15. Little SC, Mullins MC. Extracellular modulation of BMP activity in patterning the dorsoventral axis. Birth Defects Res Part C - Embryo Today Rev. 2006;78: 224–242. doi:10.1002/bdrc.20079
16. Mei W, Lee KW, Marlow FL, Miller AL, Mullins MC. hnRNP I is required to generate the Ca2+ signal that causes egg activation in zebrafish. Development. 2009;136: 3007–3017. doi:10.1242/dev.037879
17. Clevers H, Nusse R. Wnt/β-catenin signaling and disease. Cell. 2012. pp. 1192–1205. doi:10.1016/j.cell.2012.05.012
18. Funayama N, Fagotto F, McCrea P, Gumbiner BM. Embryonic Axis Induction by the Armadillo Repeat Domain of β-catenin : Evidence for Intracellular Signaling. 1995;128: 959–968.
19. Kelly GM, Erezyilmaz DF, Moon RT. Induction of a secondary embryonic axis in zebrafish occurs following the overexpression of β-catenin. Mech Dev. 1995;53: 261–273. doi:10.1016/0925-4773(95)00442-4
20. Du SJ, Purcell SM, Christian JL, McGrew LL, Moon RT. Identification of distinct classes and functional domains of Wnts through expression of wild-type and chimeric proteins in Xenopus embryos. Mol Cell Biol. 1995;15: 2625–34. doi:10.1128/MCB.15.5.2625
21. Kelly C, Chin a J, Leatherman JL, Kozlowski DJ, Weinberg ES. Maternally controlled β-catenin-mediated signaling is required for organizer formation in the zebrafish. Development. 2000;127: 3899–3911.
22. Bellipanni G, Varga M, Maegawa S, Imai Y, Kelly C, Myers AP, et al. Essential and opposing roles of zebrafish beta-catenins in the formation of dorsal axial structures and neurectoderm. Development. 2006;133: 1299–1309. doi:10.1242/dev.02295
23. Cha S, Tadjuidje E, White J, Wells J, Mayhew C, Wylie C. Wnt11 / 5a Complex Formation Caused by Tyrosine Sulfation Increases Canonical Signaling Activity. Curr Biol. Elsevier Ltd; 2009;19: 1573–1580. doi:10.1016/j.cub.2009.07.062
24. Tao Q, Yokota C, Puck H, Kofron M, Birsoy B, Yan D, et al. Maternal Wnt11 activates the canonical Wnt signaling pathway required for axis formation in Xenopus embryos. Cell. 2005;120: 857–871. doi:10.1016/j.cell.2005.01.013
25. Lu F, Thisse C, Thisse B. Identification and mechanism of regulation of the zebrafish

dorsal determinant. Proc Natl Acad Sci U S A. 2011;108: 15876–15880. doi:10.1073/pnas.1106801108/-/DCSupplemental.www.pnas.org/cgi/doi/10.1073/pnas.1106801108

26. Ge X, Grotjahn D, Welch E, Lyman-Gingerich J, Holguin C, Dimitrova E, et al. Hecate/Grip2a Acts to Reorganize the Cytoskeleton in the Symmetry-Breaking Event of Embryonic Axis Induction. PLoS Genet. 2014;10. doi:10.1371/journal.pgen.1004422
27. Miller JR, Rowning B a, Larabell C a, Yang-snyder J a, Bates RL, Moon RT. Establishment of the Dorsal – Ventral Axis in Xenopus Embryos Coincides. J Cell Biol. 1999;146: 427–437.
28. Nordermeer J, Klingensmith J, Perrimon N, Nusse R. dishevelled and armadillo act in the wingless sinaling pathway in Drosophila. Nature. 1994;367: 80–83. doi:doi:10.1038/367080a0
29. Moon RT, Kimelman D. From cortical rotation to organizer gene expression: Toward a molecular explanation of axis specification in Xenopus. BioEssays. 1998;20: 536–545. doi:10.1002/(SICI)1521-1878(199807)20:7<536::AID-BIES4>3.0.CO;2-I
30. Elinson RP, Rowning B. A transient array of parallel microtubules in frog eggs: Potential tracks for a cytoplasmic rotation that specifies the dorso-ventral axis. Dev Biol. 1988;128: 185–197. doi:10.1016/0012-1606(88)90281-3
31. Gerhart J, Danilchik M, Doniach T, Roberts S, Rowning B, Stewart R. Cortical rotation of the Xenopus egg: consequences for the anteroposterior pattern of embryonic dorsal development. Development. 1989;107 Suppl: 37–51. Available: http://www.ncbi.nlm.nih.gov/pubmed/2699856
32. Gerhardt J, Wu M, Kirschner MW. Cell cycle dynamics of an M-phase specific cytoplasmic factor in Xenopus laevis oocytes and eggs. J Cell Biol. 1984;98: 1247–1255.
33. Scharf SR, Gerhart JC. Determination of the dorsal-ventral axis in eggs of Xenopus laevis: complete rescue of uv-impaired eggs by oblique orientation before first cleavage. Dev Biol. 1980;79: 181–198. doi:10.1016/0012-1606(80)90082-2
34. Marlow FL, Mullins MC. Bucky ball functions in Balbiani body assembly and animal-vegetal polarity in the oocyte and follicle cell layer in zebrafish. Dev Biol. 2008;321: 40–50. doi:10.1016/j.ydbio.2008.05.557
35. Kloc M, Etkin LD. RNA localization mechanisms in oocytes. J Cell Sci. 2005;118: 269–282. doi:10.1242/jcs.01637
36. Nojima H, Rothhämel S, Shimizu T, Kim C-H, Yonemura S, Marlow FL, et al. Syntabulin, a motor protein linker, controls dorsal determination. Development. 2010;137: 923–933. doi:10.1242/dev.046425
37. Ge X, Grotjahn D, Welch E, Lyman-gingerich J, Holguin C, Dimitrova E, et al. Hecate / Grip2a Acts to Reorganize the Cytoskeleton in the Symmetry-Breaking Event of Embryonic Axis Induction. 2014;10. doi:10.1371/journal.pgen.1004422
38. Ataman B, Ashley J, Gorczyca D, Gorczyca M, Mathew D, Wichmann C, et al. Nuclear trafficking of Drosophila Frizzled-2 during synapse development requires the PDZ protein dGRIP. Proc Natl Acad Sci U S A. 2006;103: 7841–7846. doi:10.1073/pnas.0600387103
39. Cai Q, Gerwin C, Sheng ZH. Syntabulin-mediated anterograde transport of mitochondria along neuronal processes. J Cell Biol. 2005;170: 959–969.

doi:10.1083/jcb.200506042
40. Nojima H, Shimizu T, Kim CH, Yabe T, Bae YK, Muraoka O, et al. Genetic evidence for involvement of maternally derived Wnt canonical signaling in dorsal determination in zebrafish. Mech Dev. 2004;121: 371–386. doi:10.1016/j.mod.2004.02.003
41. Bontems F, Stein A, Marlow F, Lyautey J, Gupta T, Mullins MC, et al. Bucky Ball Organizes Germ Plasm Assembly in Zebrafish. Curr Biol. Elsevier Ltd; 2009;19: 414–422. doi:10.1016/j.cub.2009.01.038
42. Kaneshiro K, Miyauchi M, Tanigawa Y, Ikenishi K, Komiya T. The mRNA coding for Xenopus glutamate receptor interacting protein 2 (XGRIP2) is maternally transcribed, transported through the late pathway and localized to the germ plasm. Biochem Biophys Res Commun. 2007;355: 902–906. doi:10.1016/j.bbrc.2007.02.059
43. Tarbashevich K, Koebernick K, Pieler T. XGRIP2.1 is encoded by a vegetally localizing, maternal mRNA and functions in germ cell development and anteroposterior PGC positioning in Xenopus laevis. Dev Biol. 2007;311: 554–565. doi:10.1016/j.ydbio.2007.09.012
44. Kirilenko P, Weierud FK, Zorn AM, Woodland HR. The efficiency of Xenopus primordial germ cell migration depends on the germplasm mRNA encoding the PDZ domain protein Grip2. Differentiation. International Society of Differentiation; 2008;76: 392–403. doi:10.1111/j.1432-0436.2007.00229.x
45. Elinson RP, Holowacz T. Specifying the Dorsoanterior Axis in Frogs: 70 Years since Spemann and Mangold. Curr Top Dev Biol. 1995;30: 253–285. doi:10.1016/S0070-2153(08)60569-4
46. Mei W, Jin Z, Lai F, Schwend T, Houston DW, King M Lou, et al. Maternal Dead-End1 is required for vegetal cortical microtubule assembly during Xenopus axis specification. Development. 2013;140: 2334–44. doi:10.1242/dev.094748
47. Marrari Y, Rouvière C, Houliston E. Complementary roles for dynein and kinesins in the Xenopus egg cortical rotation. Dev Biol. 2004;271: 38–48. doi:10.1016/j.ydbio.2004.03.018
48. Houliston E, Elinson RP. Evidence for the involvement of microtubules, ER, and kinesin in the cortical rotation of fertilized frog eggs. J Cell Biol. 1991;114: 1017–1028. doi:10.1083/jcb.114.5.1017
49. Schroeder MM, Gard DL. Organization and regulation of cortical microtubules during the first cell cycle of Xenopus eggs. Development. 1992;114: 699–709.
50. Houliston E, Elinson RP. Patterns of microtubule polymerization relating to cortical rotation in Xenopus laevis eggs. Development. 1991;112: 107–17. Available: http://www.ncbi.nlm.nih.gov/pubmed/1769322
51. Rappaport R. Experiments Concerning the Cleavage Stimulus in Sand Dollar Eggs. 1961;148: 81–89. doi:10.1002/jez.1401480107
52. Oegema K, Mitchison TJ. Rappaport rules: cleavage furrow induction in animal cells. Proc Natl Acad Sci U S A. 1997;94: 4817–4820. doi:10.1073/pnas.94.10.4817
53. Brown EE, Margelot KM, Danilchik M V. Provisional bilateral symmetry in Xenopus eggs is established during maturation. 1994;2: 213–220.
54. Marrari Y, Clarke EJ, Rouvière C, Houliston E. Analysis of microtubule movement on isolated Xenopus egg cortices provides evidence that the cortical rotation involves dynein as well as Kinesin Related Proteins and is regulated by local microtubule polymerisation. Dev Biol. 2003;257: 55–70. doi:10.1016/S0012-1606(03)00057-5

55. Welch E, Pelegri F. Cortical depth and differential transport of vegetally localized dorsal and germ line determinants in the zebrafish embryo. Bioarchitecture. 2015;5: 13–26. doi:10.1080/19490992.2015.1080891
56. Theusch E V., Brown KJ, Pelegri F. Separate pathways of RNA recruitment lead to the compartmentalization of the zebrafish germ plasm. Dev Biol. 2006;292: 129–141. doi:10.1016/j.ydbio.2005.12.045
57. Cuykendall TN, Houston DW. Vegetally localized Xenopus trim36 regulates cortical rotation and dorsal axis formation. Development. 2009;136: 3057–65. doi:10.1242/dev.036855
58. Olson DJ, Oh D, Houston DW. The dynamics of plus end polarization and microtubule assembly during Xenopus cortical rotation. Dev Biol. Elsevier; 2015;401: 249–263. doi:10.1016/j.ydbio.2015.01.028
59. Weidinger G, Stebler J, Slanchev K, Dumastrei K, Wise C, Lovel-Badge R, et al. dead end a novel vertebrate germ plasm component is required fir zebrafish primordial germ cell migration and survival. Curr Biol. 2003;13: 1429–143478. doi:http://dx.doi.org/10.1016/S0960-9822(03)00537-2
60. Youngren KK, Coveney D, Peng X, Bhattacharya C, Schmidt LS, Nickerson ML, et al. The Ter mutation in the dead end gene causes germ cell loss and testicular germ cell tumours. Nature. 2005;435: 360–4. doi:10.1038/nature03595
61. Horvay K, Claußen M, Katzer M, Landgrebe J, Pieler T. Xenopus Dead end mRNA is a localized maternal determinant that serves a conserved function in germ cell development. Dev Biol. 2006;291: 1–11. doi:10.1016/j.ydbio.2005.06.013
62. Aramaki S, Sato F, Kato T, Soh T, Kato Y, Hattori MA. Molecular cloning and expression of dead end homologue in chicken primordial germ cells. Cell Tissue Res. 2007;330: 45–52. doi:10.1007/s00441-007-0435-1
63. Kedde M, Strasser MJ, Boldajipour B, Vrielink JAFO, Slanchev K, le Sage C, et al. RNA-Binding Protein Dnd1 Inhibits MicroRNA Access to Target mRNA. Cell. 2007;131: 1273–1286. doi:10.1016/j.cell.2007.11.034
64. Lam MYJ, Heaney JD, Youngren KK, Kawasoe JH, Nadeau JH. Trans-generational epistasis between Dnd1Ter and other modifier genes controls susceptibility to testicular germ cell tumors. Hum Mol Genet. 2007;16: 2233–2240. doi:10.1093/hmg/ddm175
65. Zhu R, Bhattacharya C, Matin A. The role of dead-end in germ-cell tumor development. Ann N Y Acad Sci. 2007;1120: 181–186. doi:10.1196/annals.1411.006
66. Koebernick K, Loeber J, Arthur PK, Tarbashevich K, Pieler T. Elr-type proteins protect Xenopus Dead end mRNA from miR-18-mediated clearance in the soma. Proc Natl Acad Sci U S A. 2010;107: 16148–16153. doi:10.1073/pnas.1004401107
67. Cook MS, Coveney D, Batchvarov I, Nadeau JH, Capel B. BAX-mediated cell death affects early germ cell loss and incidence of testicular teratomas in Dnd1 Ter / Ter mice. Dev Biol. Elsevier Inc.; 2009;328: 377–383. doi:10.1016/j.ydbio.2009.01.041
68. Cook MS, Munger SC, Nadeau JH, Capel B. Regulation of male germ cell cycle arrest and differentiation by DND1 is modulated by genetic background. Development. 2011;138: 23–32. doi:10.1242/dev.057000
69. Mei W, Jin Z, Lai F, Schwend T, Houston DW, King M Lou. Maternal Dead-End1 is required for vegetal cortical microtubule assembly during Xenopus axis specification. 2013;2344: 2334–2344. doi:10.1242/dev.094748

70. Weaver C, Kimelman D. Move it or lose it: axis specification in Xenopus. Development. 2004;131: 3491–9. doi:10.1242/dev.01284
71. Marrari Y, Terasaki M, Arrowsmith V, Houliston E. Local inhibition of cortical rotation in Xenopus eggs by an anti-KRP antibody. Dev Biol. 2000;224: 250–262. doi:10.1006/dbio.2000.9773
72. Hogan CJ, Wein H, Wordeman L, Scholey JM, Sawin KE, Cande WZ. Inhibition of anaphase spindle elongation in vitro by a peptide antibody that recognizes kinesin motor domain. Proc Natl Acad Sci U S A. 1993;90: 6611–5. Available: http://www.pubmedcentral.nih.gov/articlerender.fcgi?artid=46982&tool=pmcentrez&rendertype=abstract
73. Echeverri CJ, Paschal BM, Vaughan KT, Vallee RB. Molecular characterization of the 50-kD subunit of dynactin reveals function for the complex in chromosome alignment and spindle organization during mitosis. J Cell Biol. 1996;132: 617–633. doi:10.1083/jcb.132.4.617
74. Terasaki M, Chen LB, Fujiwara K. Microtubules and the endoplasmic reticulum are highly interdependent structures. J Cell Biol. 1986;103: 1557–1568. doi:10.1083/jcb.103.4.1557
75. Sawada T, Schatten G. Microtubules in ascidian eggs during meiosis, fertilization, and mitosis. Cell Motil Cytoskeleton. 1988;9: 219–30. doi:10.1002/cm.970090304
76. Gurel PS, Hatch AL, Higgs HN. Connecting the cytoskeleton to the endoplasmic reticulum and Golgi. Curr Biol. Elsevier Ltd; 2014;24: R660–R672. doi:10.1016/j.cub.2014.05.033
77. Nishida H. Specification of embryonic axis and mosaic development in ascidians. Dev Dyn. 2005;233: 1177–1193. doi:10.1002/dvdy.20469
78. Hyman A a. Centrosome movement in the early divisions of Caenorhabditis elegans: a cortical site determining centrosome position. J Cell Biol. 1989;109: 1185–1193.
79. Hird S, White J. Cortical and Cytoplasmic Flow in Early C. elegans Embryos. J Cell Biol. 1993;121: 1343–1355. Available: http://jcb.rupress.org/content/121/6/1343.long
80. Viktorinová I, Dahmann C. Microtubule polarity predicts direction of egg chamber rotation in Drosophila. Curr Biol. 2013;23: 1472–1477. doi:10.1016/j.cub.2013.06.014
81. Haigo SL, Bilder D. Global Tissue Revolutions in a Morphogenetic Movement Controlling Elongation. Science (80-). 2011;331: 1071–1074. doi:10.1126/science.1199424
82. Corbo JC, Di Gregorio A, Levine M. The Ascidian as a model organism in developmental and evolutionary biology. Cell. 2001;106: 535–538. doi:10.1016/S0092-8674(01)00481-0
83. Conklin EG. The Organization and Cell-Lineage of the Ascidian Egg. Proceedings of the Academy of Natural Sciences of Philadelphia. 1905. doi:10.1126/science.23.583.340
84. Sardet C, Dru P, Prodon F. Maternal determinants and mRNAs in the cortex of ascidian oocytes, zygotes and embryos. [Internet]. Biology of the cell / under the auspices of the European Cell Biology Organization. 2005. pp. 35–49. doi:10.1042/BC20040126
85. Ishii H, Shirai T, Makino C, Nishikata T. Mitochondrial inhibitor sodium azide inhibits the reorganization of mitochondria-rich cytoplasm and the establishment of the

anteroposterior axis in ascidian embryo. Dev Growth Differ. 2014;56: 175–188. doi:10.1111/dgd.12117
86. Sardet C, Paix A, Dru P, Chenevert J. From Oocyte to 16-Cell Stage : Cytoplasmic and Cortical Reorganizations That Pattern the Ascidian Embryo PRIMARY. 2007; 1716–1731. doi:10.1002/dvdy.21136
87. Sardet C, Speksnijder J, Terasaki M, Chang P, Biologie U De, Marine C, et al. Polarity of the ascidian egg cortex before fertilization. 1992;237: 221–237.
88. Roegiers F, Djediat C, Dumollard R, Rouvière C, Sardet C. Phases of cytoplasmic and cortical reorganizations of the ascidian zygote between fertilization and first division. Development. 1999;126: 3101–3117.
89. Prodon F, Dru P, Roegiers F, Sardet C. Polarity of the ascidian egg cortex and relocalization of cER and mRNAs in the early embryo. J Cell Sci. 2005;118: 2393–2404. doi:10.1242/jcs.02366
90. Nishida H. Cell-fate specification by localized cytoplasmic determinants and cell interaction in ascidian embryo. Int Rev Cytol. 1997;176: 245–306. doi:10.1126/scisignal.2001449.Engineering
91. Prodon F, Yamada L, Shirae-Kurabayashi M, Nakamura Y, Sasakura Y. Postplasmic/PEM RNAs: A class of localized maternal mRNAs with multiple roles in cell polarity and development in ascidian embryos. Developmental Dynamics. 2007. pp. 1698–1715. doi:10.1002/dvdy.21109
92. Houliston E, Le Guellec R, Kress M, Philippe M, Le Guellec K. The kinesin-related protein Eg5 associates with both interphase and spindle microtubules during Xenopus early development. Dev Biol. 164: 147–159. Available: http://dx.doi.org.ezproxy.library.wisc.edu/10.1006/dbio.1994.1187
93. Sardet C, Speksnijder J, Inoue S, Jaffe L. Fertilization and ooplasmic movements in the ascidian egg. Development. 1989;105: 237–249. doi:10.1142/9789812790866_0049
94. Roegiers F, McDougall A, Sardet C. The sperm entry point defines the orientation of the calcium-induced contraction wave that directs the first phase of cytoplasmic reorganization in the ascidian egg. Development. 1995;121: 3457–3466.
95. Weaver C, Farr GH, Pan W, Rowning BA, Wang J, Mao J, et al. GBP binds kinesin light chain and translocates during cortical rotation in Xenopus eggs. Development. 2003;130: 5425–36. doi:10.1242/dev.00737
96. Ja K, Ra N. Asymmetric cell division : recent developments and their implications for tumour biology . Dividing cellular asymmetry : asymmetric cell division and its implications for stem cells and cancer . Mechanisms of asymmetric stem cell division . Nat Rev Mol Cell Biol. 2010;11: 849–860. doi:10.1038/nrm3010.
97. Singh D, Pohl C. A function for the midbody remnant in embryonic patterning. Commun Integr Biol. 2014;7: 1–3. doi:10.4161/cib.28533
98. Fededa JP, Gerlich DW. Molecular control of animal cell cytokinesis. Nat Cell Biol. Nature Publishing Group; 2012;14: 440–7. doi:10.1038/ncb2482
99. Green RA, Mayers JR, Wang S, Lewellyn L, Desai A, Audhya A, et al. The midbody ring scaffolds the abscission machinery in the absence of midbody microtubules. J Cell Biol. 2013;203: 505–520. doi:10.1083/jcb.201306036
100. Singh D, Pohl C. Coupling of Rotational Cortical Flow, Asymmetric Midbody Positioning, and Spindle Rotation Mediates Dorsoventral Axis Formation in C. elegans. Developmental Cell. 2014. pp. 253–267. doi:10.1016/j.devcel.2014.01.002

101. Pinheiro D, Bellaïche Y. Making the Most of the Midbody Remnant: Specification of the Dorsal-Ventral Axis. Dev Cell. 2014;28: 219–220. doi:10.1016/j.devcel.2014.01.026
102. Hyman AA, White J. Determination of cell division axes in the early embryogenesis of Caenorhabditis elegans. J Cell Biol. 1987;105: 2123–2135. doi:10.1083/jcb.105.5.2123
103. Keating HH, White JG. Centrosome dynamics in early embryos of Caenorhabditis elegans. J Cell Sci. 1998;111 (Pt 2: 3027–3033.
104. Singh D, Pohl C. Coupling of Rotational Cortical Flow, Asymmetric Midbody Positioning, and Spindle Rotation Mediates Dorsoventral Axis Formation in C. elegans. Dev Cell. Elsevier Inc.; 2014;28: 253–267. doi:10.1016/j.devcel.2014.01.002
105. Wylie C. Germ cells. CurrOpinGenetDev. 2000;10: 410–413. doi:http://dx.doi.org/10.1016/S0092-8674(00)80557-7
106. Extavour CG, Akam M. Mechanisms of germ cell specification across the metazoans: epigenesis and preformation. Development. 2003;130: 5869–5884. doi:10.1242/dev.00804
107. Elinson RP, Sabo MC, Fisher C, Yamaguchi T, Orii H, Nath K. Germ plasm in Eleutherodactylus coqui, a direct developing frog with large eggs. Evodevo. BioMed Central Ltd; 2011;2: 20. doi:10.1186/2041-9139-2-20
108. Yoon C, Kawakami K, Hopkins N. Zebrafish vasa homologue RNA is localized to the cleavage planes of 2- and 4-cell-stage embryos and is expressed in the primordial germ cells. Development. 1997;124: 3157–65. Available: http://www.ncbi.nlm.nih.gov/pubmed/9272956
109. Köprunner M, Thisse C, Thisse B, Raz E. A zebrafish nanos-related gene is essential for the development of primordial germ cells. Genes Dev. 2001;15: 2877–2885. doi:10.1101/gad.212401
110. Pelegri F, Knaut H, Maischein HM, Schulte-Merker S, Nüsslein-Volhard C. A mutation in the zebrafish maternal-effect gene nebel affects furrow formation and vasa RNA localization. Curr Biol. 1999;9: 1431–1440. doi:10.1016/S0960-9822(00)80112-8
111. Eno C, Pelegri F. Germ Cell Determinant Transmission , Segregation , and Function in the Zebrafish Embryo. In: Carreira RP, editor. Intec. 2016. Available: http://dx.doi.org/10.5772/62207
112. Minakhina S, Steward R. Axes formation and RNA localization. Curr Opin Genet Dev. 2005;15: 416–421. doi:10.1016/j.gde.2005.06.006
113. Colozza G, De Robertis EM. Maternal syntabulin is required for dorsal axis formation and is a germ plasm component in Xenopus. Differentiation. Elsevier; 2014;88: 17–26. doi:10.1016/j.diff.2014.03.002

Chapter 2: Hecate/Grip2a acts to reorganize the cytoskeleton in the symmetry-breaking event of embryonic axis induction

Xiaoyan Ge[1#], Danielle Grotjahn[1*], **Elaine Welch[1*]**, Jamie Lyman-Gingerich[1], Christiana Holguin[1], Eva Dimitrova[1], Elliot W. Abrams[2], Tripti Gupta [2], Florence L. Marlow[2], Taijiro Yabe[1], Anna Adler[1], Mary C. Mullins[2], Francisco Pelegri[1].

1. Laboratory of Genetics
University of Wisconsin – Madison
425-G Henry Mall
Madison, WI 53706
USA

2. Department of Cell and Developmental Biology
Perelman School of Medicine at the University of Pennsylvania
421 Curie Blvd.
1233 BRB II/III
Philadelphia, PA 19104-6058
USA

* These authors contributed equally to the work

Current address: Division of Medical Genetics, Department of Pediatrics and Institute for Human Genetics, University of California San Francisco, San Francisco, California 94143

Corresponding author: fjpelegri@wisc.edu

PLoS Genet 10(6): e1004422. doi:10.1371/journal.pgen.1004422, 2014.

Author contribution: Elaine Welch performed experiments and revised the manuscript.

2.1. Abstract

Maternal homozygosity for three independent mutant *hecate* alleles results in embryos with reduced expression of dorsal organizer genes and defects in the formation of dorsoanterior structures. A positional cloning approach identified all *hecate* mutations as stop codons affecting the gene, revealing that *hecate* encodes the Glutamate receptor interacting protein 2a (Grip2a), a gene containing multiple PDZ domains known to interact with membrane-associated factors including components of the Wnt signaling pathway. We find that *grip2a* mRNA is localized to the vegetal pole of the oocyte and early embryo, and that during egg activation this mRNA shifts to an off-center vegetal position corresponding to the previously proposed teleost cortical rotation. *hecate* mutants show defects in the alignment and bundling of microtubules at the vegetal cortex, which result in defects in the asymmetric movement of *wnt8a* mRNA as well as anchoring of the dynein-associated cargo adaptor Syntabulin. We also find that, although short-range shifts in vegetal signals are affected in *hecate* mutant embryos, these mutants exhibit normal long-range, animally directed translocation of cortically injected dorsal beads that occurs in lateral regions of the yolk cortex. Furthermore, we show that such animally-directed movement along the lateral cortex is not restricted to a single arc corresponding to the prospective dorsal region, but occur in multiple meridional arcs even in opposite regions of the embryo. Together, our results reveal a role for Grip2a function in the reorganization and bundling of microtubules at the vegetal cortex to mediate a symmetry-breaking short-range shift corresponding to the teleost cortical rotation. The slight asymmetry achieved by this

directed process is subsequently amplified by a general cortical animally-directed transport mechanism that is neither dependent on *hecate* function nor restricted to the prospective dorsal axis.

Key words: zebrafish, embryo, maternal, transport, microtubule

2.2. Introduction

Dorsoventral axis formation is a fundamental process in early vertebrate embryogenesis. In many vertebrates such as amphibians and teleosts, evidence indicates that maternally-supplied dorsal determinants trigger the formation of the future dorsal organizer. Embryological manipulations have indicated that the dorsal determinants are initially localized to the vegetal pole and subsequently translocate animally to the prospective dorsal side in a microtubule-dependent process in both amphibians (reviewed in [1]) and teleosts [2]–[4]. In amphibians, translocation of the signal from the vegetal pole to the dorsal side is initiated by cortical rotation, the microtubule-dependent movement of the egg cortex with respect to its core that is triggered by fertilization and is implemented by transport along microtubule tracks (reviewed in [1]).

Although not readily apparent in the zebrafish embryo, detailed analysis has indicated the existence of processes that share similarities with the amphibian cortical

rotation. Early studies showed that fluorescent polystyrene beads injected at the vegetal pole were transported animally along microtubule-based cortical tracks in a microtubule dependent manner [2], and that this movement had temporal dynamics and functional requirements similar to that of the movement of putative dorsal determinants as defined by embryological manipulations [3], [4]. Subsequent work showed that maternal factors such as Syntabulin and Wnt8a, involved in axis induction, localized to the vegetal pole of the egg and upon fertilization and egg activation shifted animally towards the presumed prospective dorsal region of the embryo [5]–[7]. Further studies of microtubule rearrangements in live embryos confirmed that the tracks of bundled microtubules that form at the zebrafish vegetal pole upon egg activation become aligned in the direction of the future dorsal side of the embryo, and showed bulk cortical particle movement analogous to a cortical rotation [8].

The movement of the dorsal determinant results in the activation of the Wnt/βcatenin signaling pathway and the activation of β-catenin-dependent targets [1]. This well-known pathway is characterized by the activation of Frizzled receptors by the Wnt ligand, and an intracellular cascade involving the activation of Dishevelled and the downregulation of a β-catenin degradation complex that includes GSK3, Axin and Adenomatous polyposis coli (APC), leading to the accumulation of β-catenin in the nucleus [9]. Nuclear β-catenin in turn interacts with transcription factors of the Tcf family to activate transcription of target genes. Wnt/βcatenin pathway components and/or nuclear accumulation of β-catenin have been shown to be involved in embryonic axis determination in diverse deuterostomes such as fish, amphibians, mammals and amphioxus, as well as in lineages as basal as echinoderms, Cnidarians and planaria

(reviewed in [10]) implying that the pathway was recruited for axis determination very early in animal evolution.

Although the involvement of Wnt/βcatenin activation across species is well documented, the identity of the molecules that activate the pathway in the early embryo, often referred to as dorsal determinants, remains unknown in most cases.
In *Xenopus*, *wnt11* mRNA is first located at the vegetal pole and becomes enriched at the future dorsal side after fertilization, and depletion of *wnt11* mRNA results in embryos defective in dorsal axis induction [11]. Thus, Wnt11, together with ubiquitously present Wnt5 [12], [13] has been proposed to be the dorsal determinant in this amphibian species. Studies in the zebrafish exclude a function for Wnt11 or Wnt 5 in axis induction but suggest a role for Wnt8a in this process [7]. Maternal zebrafish *wnt8a* mRNA is localized during oogenesis to the vegetal pole of the oocyte and, upon fertilization, *wnt8a* mRNA experiences a shift from its original location at the vegetal pole to an off-center region thought to correspond to the dorsal side [7]. These studies suggest that, while Wnt/β-catenin pathway activation may be highly conserved in axis induction across the animal kingdom, maternally-based mechanisms that lead to the activation of the pathway vary.

Efforts from several laboratories have used forward genetics approaches to identify maternal factors essential for various aspects of early embryonic development in the zebrafish [5], [14]–[18]. Several reports have documented maternal-effect mutations affecting zebrafish dorsal axis induction [5], [15], [17], [18]. Mutations in three maternal-effect genes, *ichabod*, *tokkaebi* and *hecate*, cause specific ventralized phenotypes, consistent with a role for these genes in axis induction. Overexpression of Wnt signaling pathway

components in *ichabod*mutant embryos indicate that this mutation acts within the Wnt/β-catenin signaling pathway at a level downstream of the β-catenin degradation complex [15]. These and other results show that *ichabod* corresponds to a β-catenin-2 gene expressed maternally and involved in axis induction [19].

Similar overexpression analysis has shown that *tokkaebi* and *hecate*, in contrast to *ichabod*, act upstream of the β-catenin-degradation machinery [5], [20]. Specifically, overexpression of components that activate the pathway at multiple points can rescue the *hecate* and *tokkaebi*mutant phenotypes. Rescue by an exogenous Wnt ligand suggests that the Wnt/β-catenin pathway is intact in *tokkaebi* and *hecate* mutant embryos, and suggests that, rather than being required for an integral component of Wnt/β-catenin signaling, these genes are required to regulate an endogenous signal that activates this pathway. Consistent with such a proposed role, positional cloning reveals that *tokkaebi* corresponds to the *syntabulin* (*sybu*) gene, which codes for a linker of the kinesin I motor protein involved in cargo transport along microtubules [6]. Both *sybu* mRNA and protein are localized to the vegetal pole of the egg, and Sybu protein exhibits a slight off-center shift upon egg activation [6]. These data suggest a role for Sybu in the microtubule-dependent transport of vegetally localized dorsal determinants.

Here, we present the molecular characterization of the zebrafish maternal-effect gene *hecate (hec)*. Maternal homozygosity for three independent mutant *hec* alleles results in embryos with reduced expression of dorsal organizer genes and defects in the formation of dorsoanterior structures ([20]; this report). Positional cloning reveals that *hec* encodes the Glutamate receptor interacting protein 2a (Grip2a). We find that *grip2a* mRNA,

like *wnt8a* mRNA and Sybu protein, is localized to the vegetal pole of the oocyte and early embryo, where during egg activation it is shifted off-center corresponding to the previously proposed teleost cortical rotation [8]. The Drosophila Grip homologue has recently been shown to potentiate Wnt signaling at the neuromuscular junction by interacting with the Frizzled receptor on the cytoplasmic side of endocytosing membrane vesicles [21], [22], suggesting a potential mechanism of action for zebrafish Grip2a in axis induction at the level of Frizzled receptor regulation. Unexpectedly, however, we find that *hec* mutants show defects in the alignment and bundling of microtubules at the vegetal cortex, which result in corresponding defects in the asymmetric movement of *wnt8a* mRNA and are sufficient to explain the observed axis induction defects.

The short-range shift in vegetally localized factors such as *grip2a* mRNA also led us to re-examine the functional significance of the previously observed animally-directed cortical transport on axis induction. We find that, although short-range shifts in vegetal signals are affected in *hec* mutant embryos, these mutants do not exhibit a defect in the long-range, animally directed translocation of cortically injected dorsal beads that occurs in lateral regions of the yolk cortex. Furthermore, we show that, contrary to our expectations, such movements are not restricted to a single arc corresponding to the prospective dorsal region, but occur in multiple meridional arcs even in opposite regions of the embryo. Together, our results propose a role for *hec* function in the reorganization and bundling of microtubules at the vegetal cortex to mediate a symmetry-breaking event likely corresponding to the teleost cortical rotation. This asymmetry is subsequently amplified by a cortical animally-directed transport mechanism that is neither dependent on *hec* function nor restricted to the prospective dorsal axis.

2.3. Results

2.3.1. Maternal-effect mutations in *hecate* affect dorsoanterior development

Embryos from mothers homozygous for the mutant *hec* allele, for simplicity referred to here as *hec* mutant embryos, display a range of ventralized phenotypes [17], [20], [23] (Figure 1A–E; Table 1). In the most severe cases, 24-hour mutant embryos exhibit a severe radial ventralization and lack all dorsoanterior-derived structures (V4 class, according to criteria in [24]; Figure 1A). More moderate phenotypes can also be observed, such as embryos that lack all anterior structures as well as the notochord (a dorsally-derived structure), and display an expansion of posterior somites (V3 class; Figure 1B). More weakly ventralized embryos are also observed that lack the anterior-most head structures and the notochord and exhibit expanded posterior somites (V2 class; Figure 1C), and embryos with reduced eyes and some notochord defects (class V1; Figure 1D). In many clutches, a fraction of embryos from mutant mothers are indistinguishable from wild-type embryos (Figure 1E). Such variability in phenotypes can be observed in maternal-effect mutants (some examples can be found in [17], [25], [26]), in particular those exhibiting axis induction defects [5], [15], [27], possibly by inherent variation in the maternal composition of individual eggs coupled to gene or pathway redundancy (see also Discussion). In mutant clutches with a weak expression of the phenotype, a small and variable fraction of embryos exhibits axis duplication phenotypes (Figure 1F) instead of axis formation defects (see Discussion).

Figure 1: Axis induction defects in embryos from mothers homozygous for three different *hecate* mutant alleles.

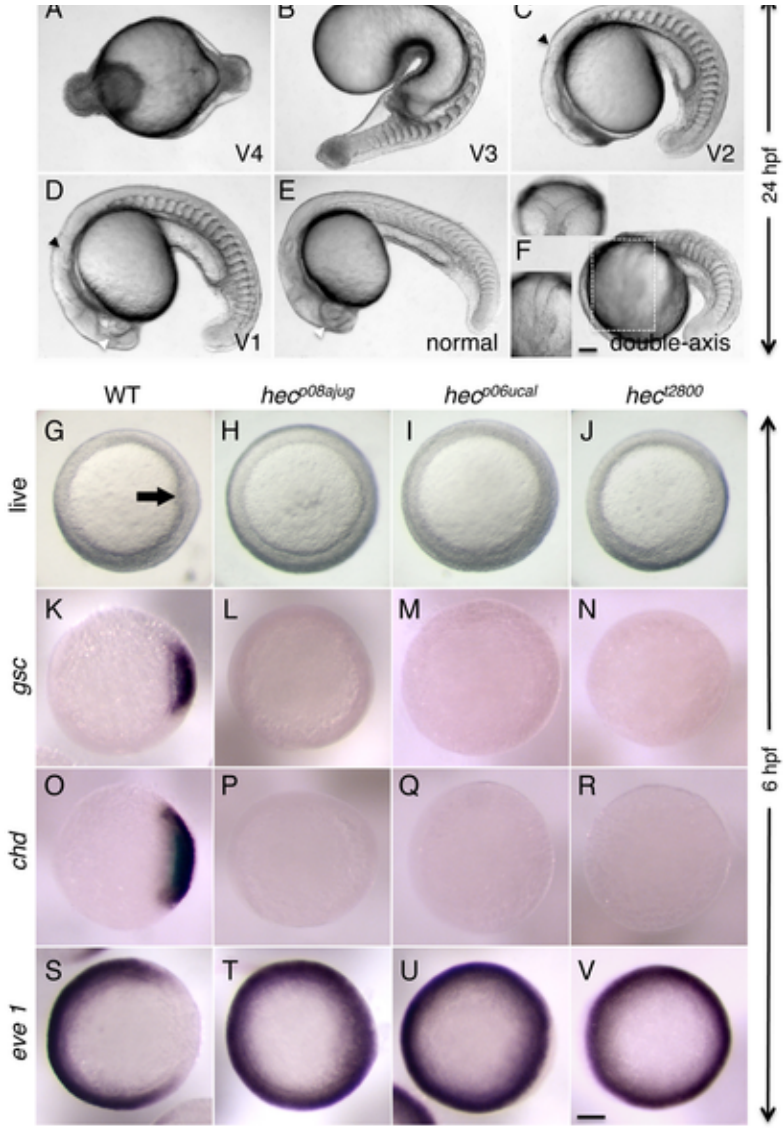

(A-F) Side views (except as indicated in (F)) of live embryos at 24 hpf showing a range of phenotypes from most severe (A) to normal (E) and double-axis embryos (F). A) Class V4 embryo exhibiting complete radially symmetry and lacking all anterior (e.g. head structures) or dorsal most (e.g. notochord) structures. B) Class V3 embryo exhibiting a rudimentary axis but lacking all anterior and dorsal most structures. C) Class V2 embryo lacking anterior most structures such as the eyes, but showing formation of more posterior head structures such as the otic vesicles (black arrowhead, also indicated in D). D) Class V1 embryo with a relatively complete axis but reduced anterior structures, such as the eyes (white arrowhead, also labeled in E), and lacking a properly formed notochord. E) Normal embryo derived from *hec* mutant females indistinguishable from wild-type. Note somites in (E) are chevron-shaped, while they are blocky in (B-D) indicative of defects in notochord formation, or encircling the entire embryo in (A). F) A double-axis embryo found in *hec* mutant clutches exhibiting weak expressivity. Insert in the lower left shows the left axis indicated by the dashed rectangle, out of focus in the main image. Insert in the upper left panel shows a dorsal view, showing the bifurcated axis. Note the lack of defined anterior structures in both axes, as well as the lack of a notochord along the trunl, also reflected by block-shaped somites in this region. Images in A-F are side views, except for upper left insert in (F). (G-I) Animal views of live wild-type embryos (G) and embryos from females homozygous for each of the three *hec* mutant alleles. The dorsal thickening or shield (arrow) is absent in mutant embryos. (K-V) In situ hybridization analysis to detect expression of dorsally-expressed genes (*gsc*, *chd*) and ventrally-expressed genes (*eve 1*). The expression domains of *gsc* and *cho* is reduced in *hec* mutant embryos, while the expression domain of *eve* is expanded in these embryos. (K-V) are animal view of embryos, dorsal to the right when identifiable, at the shield stage (6 hpf). Magnification bars in (F) and (V) correspond to 100 μm for panels sets (A-F) and (G-V), respectively. Dorsal view insert in panel (F, upper left) has been reduced to 75% size.

The *hec*^{t2800} allele was originally isolated in an early-pressure-based screen for recessive maternal-effect mutations [14], [17] and its effects described previously [20], [23]. Two additional alleles, *hec*^{p08ajug} and *hec*^{p06ucal} were identified in another maternal-effect mutant screen, based on a four-generation scheme [16], [18]. Using DNA markers linked to the *hec*^{t2800} allele [20], we determined that the *hec*^{p08ajug}and *hec*^{p06ucal} alleles were linked to the same SSLP markers, z59658 and z24511 on chromosome 8. In addition, we carried out pair-wise crosses between individuals carrying the three mutant alleles to test for non-complementation. All crosses resulted in females that exhibited the *hec* mutant phenotype in their offspring in the expected proportions, i.e. Mendelian for F_1 females (approximately 50% in crosses between homozygous males and heterozygous females of all allelic combinations) and maternal-dependent (near 100%) for F_2 embryos (Table S1), indicating that all three mutations are part of the same complementation group.

A comparison of the phenotypes for the three *hec* alleles suggests that they fall within an allelic series. Embryos from mutant females carrying each of the three alleles were classified and scored at 24 hours post-fertilization (hpf; Table 1). The *hec*^{p06ucal} allele shows the strongest average phenotype among the three alleles, where most embryos (76.3% from 3-month females) exhibit the strongest (V4) phenotype, while *hec*^{t2800} mutants exhibit intermediate phenotype (46.7% V4 class) and *hec*^{p08ajug} mutants show the weakest phenotype (10.9% V4 class). Double-axis embryos are observed only in offspring derived from females mutant for the two weaker alleles *hec*^{p08ajug} and *hec* ^{t2800}, and only in clutches with weak penetrance and expressivity (Table 1 and data not shown). In the case of *ichabod* and *tokkaebi* mutations [5], [15] axis induction defects have been reported to

vary with maternal age, with younger females exhibiting stronger phenotypes. We tested embryos from 3 month old and 12 month old mutant females and find a similar trend for the effects of the three *hec* alleles on axis induction (Figure S1).

Previous studies have shown that the ventralized phenotype of *hec* mutant embryos is associated with a reduction in the embryonic shield and changes in patterns of gene expression in dorsal- and ventral-specific genes in the late blastula embryo. Expression of gene markers of the various germ layers, such as *bmp2* and *gata2* (ectoderm), *no tail* (mesendodermal precursors), and *foxa2* (endoderm) was unaffected, other than regional differences due to predicted changes in dorsoventral specification [20]. As expected, embryos from females mutant for the newly isolated *hec* alleles, $hec^{p06ucal}$ and $hec^{p08ajug}$, similar to the hec^{t2800} allele [20], exhibit a reduction in the shield region corresponding to the dorsal organizer at the incipient dorsal region (Figure 1G–J), as well as a reduction in dorsal-specific gene expression (*goosecoid*, Figure 1K–N; *chordin*, Figure 1O–R) and a concomitant expansion of a ventrally-expressed gene (*eve 1*) (Figure 1S–V). Together, phenotypic, linkage and complementation analysis indicate that these three mutations are alleles of the same gene.

2.3.2. *hecate* encodes the zebrafish Glutamate receptor interacting protein 2a (Grip2a)

To better understand the function of the *hec* gene, we determined its molecular identity using a positional cloning approach. We initially identified linkage of the *hec* locus between SSLP markers z59658 and z24511 on chromosome 8 through mapping of the hec^{t2800} allele [20]. Homozygous mutant males were crossed to heterozygous females to generate large numbers of fish for fine mapping. Fine mapping analysis of 1762 meioses

with newly identified RFLP markers further narrowed the critical region containing *hec* to a genomic region between *gpd1a-1* and the zC150E8y RFLP in the Ensembl database, corresponding to an interval of 383 Kb (Figure 2A). Five overlapping BAC clones were identified and aligned as a contig covering the whole critical region (Figure 2B). Within this critical region, there are 11 predicted genes according to the Ensembl database of the zebrafish genome and the GENSCAN program. Sequencing of cDNA products from wild-type and mutant alleles revealed the presence of mutations in all three *hec* alleles in the gene *glutamate receptor interacting protein 2a* (*grip2a*, NP_001116760.1), one of two *grip2* genes in the zebrafish genome [28].

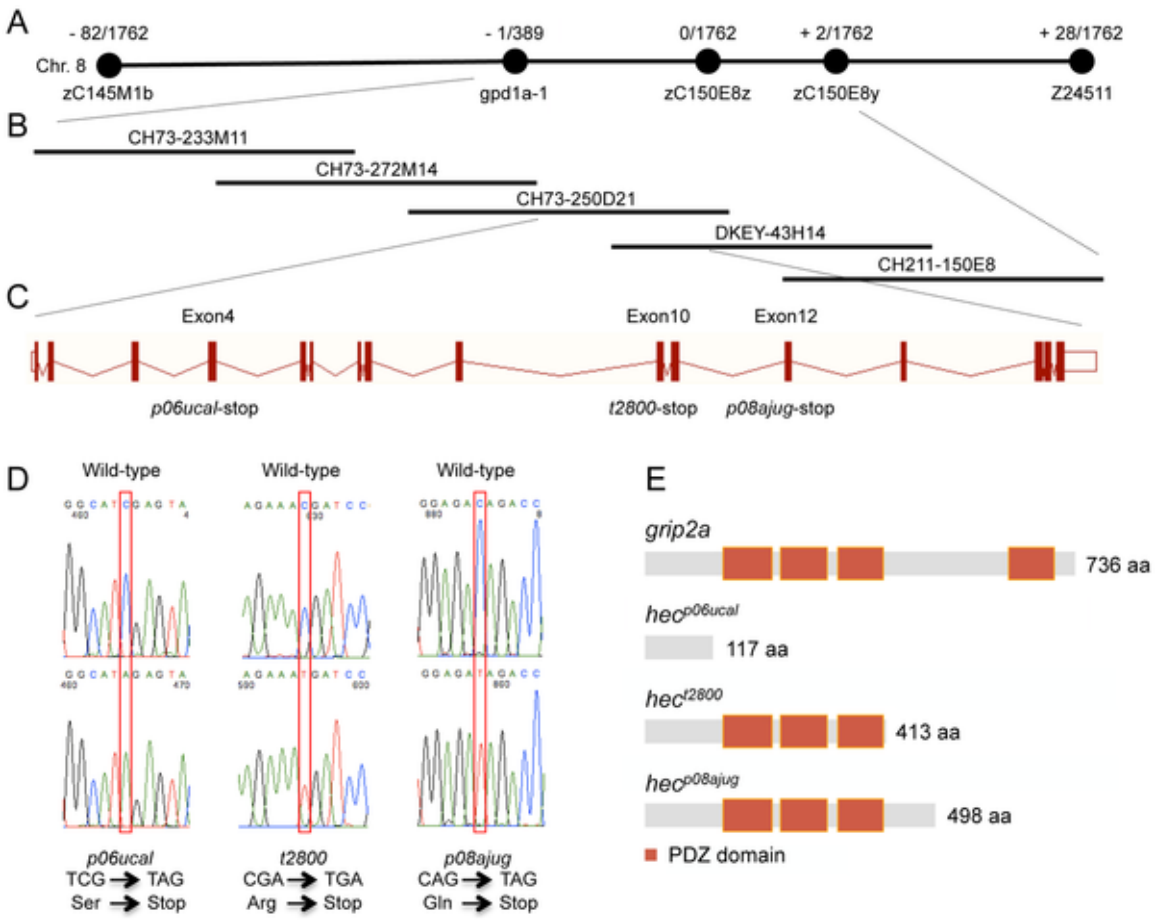

Figure 2: Molecular identification of the *hecate* locus.

A) Linkage map of the *hec* locus. The number or recombinants over the total number of analyzed meiosis is indicated. *hec* linkage was initially identified between SSLP markers z59658 and z24511 on chromosome 8. Fine mapping analysis with newly identified RFLP markers further narrowed the region between the gene *gpd1a-1* and the RFLP zC150E8y. B) Contig of five BAC clones covering the *hec* critical region. CH73-233M11, CH73-272M14, CH73-250D21, DKEY-43H14 and CH211-150E8 are five sequenced and overlapping BAC clones in this interval. C) Exon-intron structure of the *hec/grip2a* gene, which contains 16 exons. The $hec^{p06ucal}$, hec^{t2800} and $hec^{p08ajug}$ alleles each cause a premature stop-codon in exon 4, exon 10 and exon 12, respectively. D) Sequence traces of the cDNA productsfrom wild-type and the three mutant *hec* alleles. Nucleotide substitutions are indicated by the red box. Mutant cDNAs show s C-A transversion in codon 118 ($hec^{p06ucal}$), a C-T transversion in codon 414 (hec^{t2800}), or a C-T transversion in codon 499 ($hec^{p08ajug}$), all creating premature STOP codons. E) Schematic diagram showing the protein domain structures of Grip2a in the wild-type and mutant alleles. Red boxes represent conserved PDZ domains.

The zebrafish *grip2a* gene has 16 exons, which produces a 3,124 bp transcript and a 736 amino acid protein (Figure 2C). The three mutant alleles result in truncated forms of the Grip2a protein: *hec*^{p06ucal} allele has a C-A transversion in codon 118 in exon 4, *hec*^{t2800} has a C-T transversion in codon 414 in exon 10, and *hec*^{p08aju}*g* has a C-T transversion in codon 499 in exon 12, and these three mutations generate premature nonsense (stop) codons (Figure 2D). A search in the Conserved Domain Database (CDD) in NCBI [29] indicates that Grip2a protein has four PDZ domains. The premature stop-codons for these different alleles delete the most C-terminal PDZ domain in the *hec*^{t2800} and *hec*^{p08ajug} alleles, and all four PDZ domains in the *hec*^{p06ucal} allele (Figure 2E). The retention of PDZ domains and size of the predicted truncated proteins roughly correlates with the observed phenotypic strength in the various mutant allele backgrounds (Table 1, Figure S1), although we have not determined expression levels for the mutant proteins to confirm their relative activities. The identification of mutations in these three independently isolated alleles indicates that *hec* encodes Grip2a. This is further substantiated by the localization of *grip2a* mRNA in the region of the embryo affected by the *hec* mutation (see below).

Using BLAST searches on Ensembl and NCBI genome databases, homologous *grip1* and *grip2*genes were found for all vertebrate species, such as fish, amphibians, birds, and mammals. In invertebrate lineages, a distantly related *Grip* gene was identified only in Drosophila. Grip1 and Grip2 protein sequences among eight representative species were used to construct a phylogenetic tree using ClustalW (Figure S2). *grip2* occurs as a single copy in amphibians, birds and mammals but is duplicated in the zebrafish and other fish species such as fugu and medaka, likely a consequence of an

extra round of whole genome duplication in the ray-finned fish lineage [30], [31]. Drosophila and all vertebrate Grip1 and Grip2 proteins contain PDZ domains but zebrafish Hec/Grip2a and Fugu Grip2b contain 4 predicted PDZ domains instead of the 7 PDZ domains predicted in other members of this family (Figure S2 and not shown).

2.3.3. *grip2a* mRNA is localized to the vegetal region of the oocyte, developing an early asymmetry upon egg activation

Quantitative RT-PCR analysis of mRNA from wild-type embryos spanning early development indicates highest levels of *grip2a* mRNA in the 1-cell stage embryo, gradually declining to negligible levels at 50% epiboly (5.25 hpf) and thereafter (Figure S3). In adults, expression can be detected in wild-type females and isolated ovaries, but not in males or female carcasses where the ovaries have been removed (Figure S3). Thus, at our level of analysis, *hec/grip2a* is specifically expressed in ovaries as a maternal-specific transcript, which is consistent with the strict maternal effect observed in females homozygous for the three *hec* mutant alleles.

We examined the spatial expression pattern of *hec/grip2a* at various developmental stages during embryogenesis using whole mount in situ hybridization (Figure 3). *grip2a* mRNA is detected in the vegetal pole region of the yolk in early zygotes and cleavage-stage embryos (Figure 3A–E). Similar to the case of *wnt8a* mRNA [7] and Sybu protein [6], the *grip2a* mRNA localization domain is not precisely aligned with the vegetal pole in activated eggs or early embryos. Instead, *grip2a* mRNA is consistently located slightly off-center in the post-activation stages examined, from the early 1-cell stage embryo 10 minutes post-fertilization (mpf) until late cleavage stages (Figure 3A–D). This off-center shift is not observed in manually extruded mature, inactive eggs, where

the *grip2a* mRNA localization domain is instead located at the vegetal pole in a radially symmetric manner (data not shown). In early embryos the extent of asymmetry of the *grip2a* mRNA localization domain, appears similar throughout the cleavage and blastula stages until mRNA levels become markedly reduced in the late blastula embryo (sphere stage; 4 hpf; Figure 3E). Localized *grip2a* mRNA can no longer be detected starting at the onset of epiboly (30% epiboly; 4.66 hpf; not shown). In contrast to its *Xenopus* homologue [32], zebrafish *grip2a* mRNA does not localize to the zebrafish germ plasm (Figure 3C and data not shown), present at the furrows corresponding to the first and second blastomeric divisions [33]–[37], nor does it become incorporated into the primordial germ cells (Figure 3D,E and data not shown), which form four cell clusters during the late cleavage stages ([33], [35], [38]; see below).

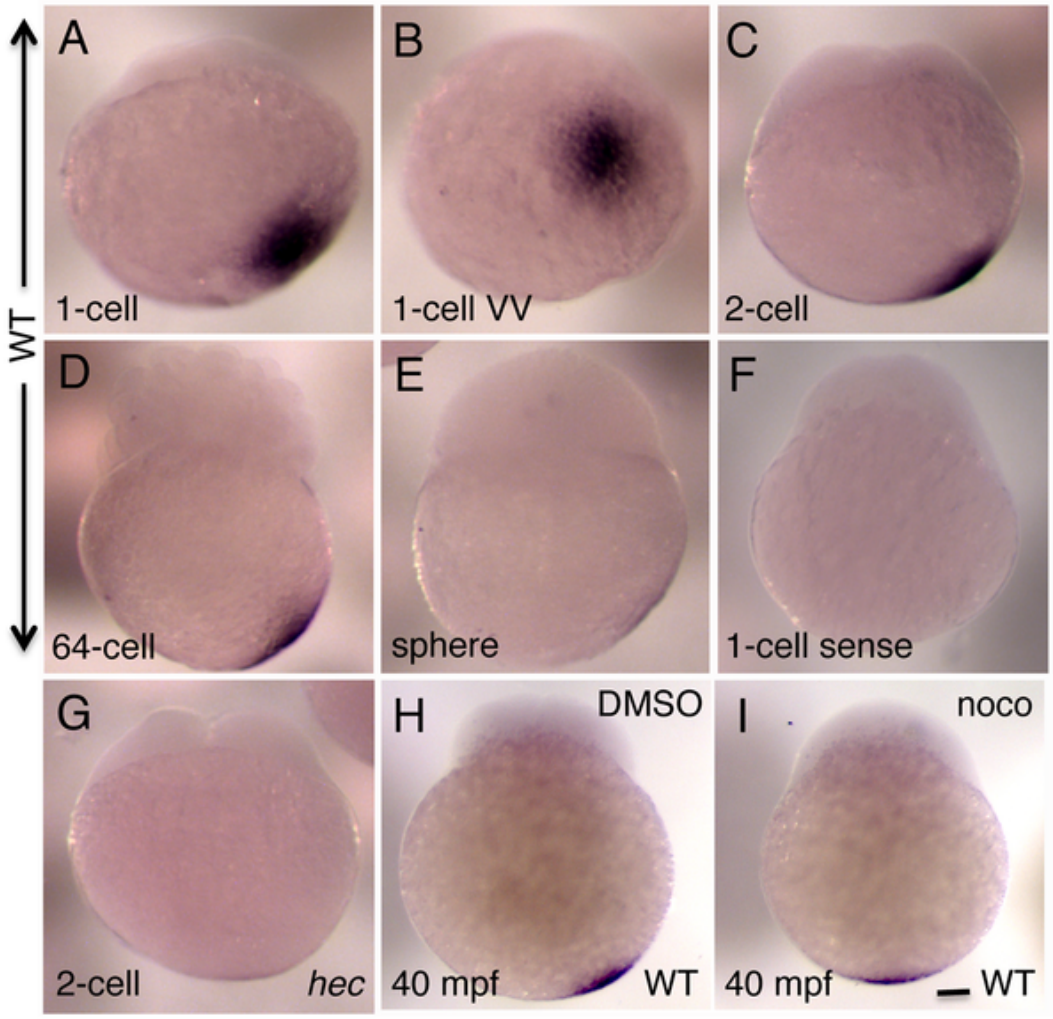

Figure 3: Whole mount in situ hybridization analysis of the expression of zebrafish *grip2a* mRNA in early embryos.

(A-E) *grip2a* mRNA is localized in a slightly off-center position at the vegetal pole of early embryos, and remains in that position until the sphere stage when it becomes undetectable. (F) Control sense probe. G) The domain of *grip2a* mRNA localization in *hec* mutants is reduced in intensity and appears to lack an off-center shift. Panel shows an embryo from females homozygous for the *hec*^{p06ucal} allele. (H,I) Representative control (DMSO)- and nocodazole-treated embryos showing the lack of off-center shift in nocodazole-treated embryos (see Figure S4 for details). All panels are side views (except for (B), which is a vegetal view of the embryo in (A)) at the following stages: A,B) 1-cell (20 mpf), C,F,G) 2-cell (45 mpf), D: 64-cell (2hpf), E: sphere (4hpf), H,I) are at 40 mpf, which approximately corresponds to the 2-cell stage (C) in untreated embryos. Magnification bar in (I) corresponds to 100 μm for all panels.

To further confirm the slight, off-center shift in the *grip2a* mRNA localization domain, and to determine whether this shift, like that of Sybu protein and *wnt8a* mRNA, depends on an intact microtubule network, we tested the effect of early nocodazole treatment on the *grip2a* mRNA localization pattern in wild-type embryos. Embryos were treated at 5 mpf and fixed at 30 and 40 mpf for in situ hybridization. For both time points, control (solvent-treated) embryos show an off-center shift in the domain of *grip2a* mRNA localization so that it is located within an arc at 0–20° from the true vegetal pole of the embryo, while nocodazole-treated embryos do not exhibit a discernable shift in mRNA localization (Figure 3H, 3I; Figure S4). Thus, *grip2a* mRNA is located at the vegetal pole of the embryo in mature oocytes, but upon egg activation (typically coupled to fertilization) this mRNA exhibits a short-range, off-center translocation within the vegetal region of the embryo. Once in an off-center position *grip2a* mRNA remains static until its degradation at late cleavage stages.

Whole mount in situ hybridization of embryos from mutant female mothers homozygous for each of the three *hec* alleles show significantly reduced levels of localized *grip2a* mRNA during the early cleavage stages, ranging from reduced to nearly undetectable levels (Figure 3G and data not shown). In those embryos where *grip2a* mRNA localization can be discerned, the domain of localization appears centered at the vegetal pole, consistent with the absence of an off-center shift for vegetally localized products in *hec* mutants (see below). Quantitation of total *grip2a* mRNA levels in mutant embryos at the 2-cell stage indicates that, for all alleles, *grip2a*mRNA abundance is drastically reduced to approximately 15–25% that in wild-type embryos (Figure S3). It is possible that *hec/grip2a* function is required for the localization of its own mRNA, which when not

localized is unstable. Alternatively, the reduction in apparent *grip2a*mRNA localization in *hec* mutant embryos might be a consequence of a decrease in *grip2a*mRNA abundance in these embryos, possibly by non-sense mediated mRNA decay as has been proposed for other maternal transcripts [39], [40].

2.3.4. Vegetal localization of *grip2a* mRNA is initiated during oogenesis and depends on oocyte polarity genes

To visualize how the pattern of *grip2a* mRNA localization is established during oogenesis, we carried out in situ hybridization analysis of wild-type oocytes at various stages using a *grip2a*antisense probe (Figure 4). In early stage I oocytes, *grip2a* transcripts appear sharply localized to a compact, spherical region at one region of the oocyte (Figure 4A, 4D). By late stage I, *grip2a* mRNA acquires a more spread, subcortical localization pattern still centered in one region of the oocyte (Figure 4A, 4E). This cortical localization is maintained until the end of oogenesis (Figure 4A, 4F and data not shown).

Figure 4: Localization of *grip2a* mRNA in wild-type and mutant oocytes.

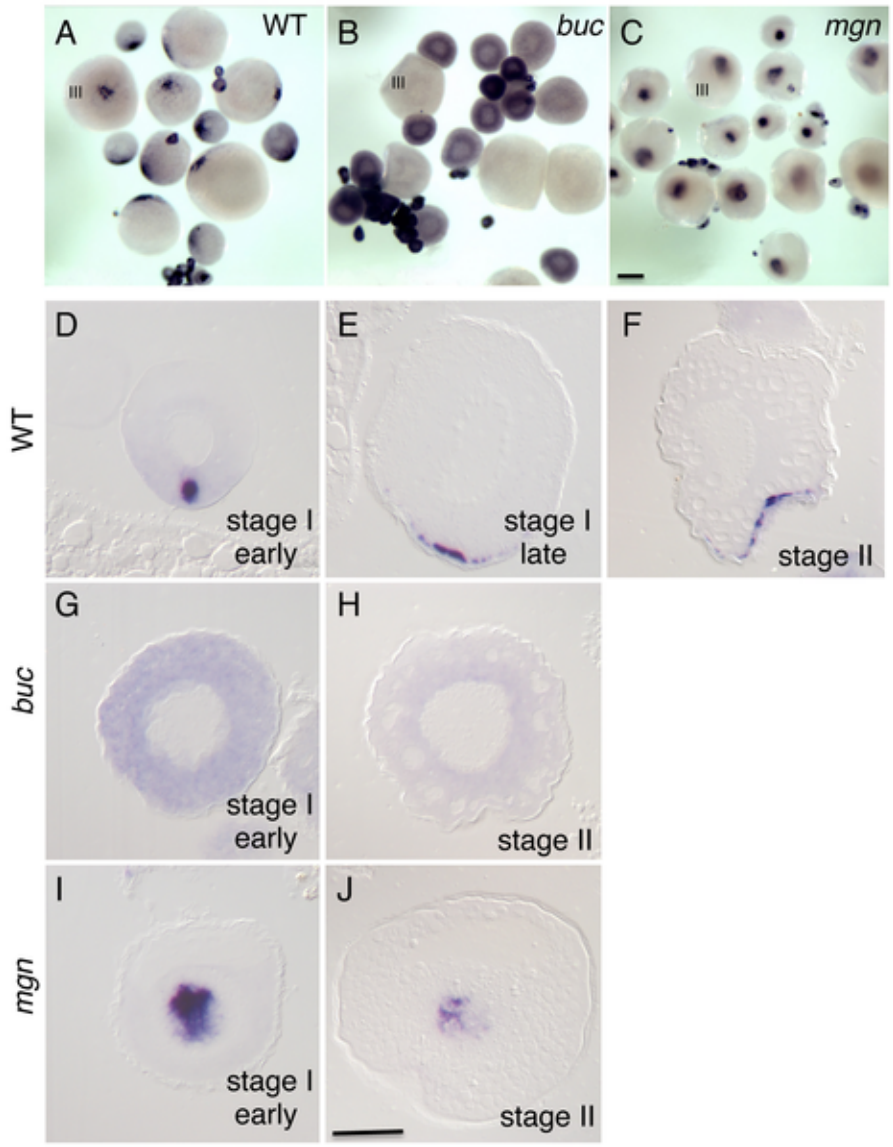

(A-C) Whole mount in situ hybridization of dissected ovaries from wild-type (A), *bucky ball (buc,* B*)* and *magellan (mgn,* C*)* mutant females. In (A-C) oocytes at stage III of development are indicated. Smaller oocytes are at stages I and II, which are difficult to differentiate in whole mounts at this magnification. The *grip2a* mRNA localization domain is observed in an asymmetric cortical position in wild-type oocytes (A) but is unlocalized and diffuse in *buc* oocytes B) and internally-located in *mgn* mutants (C). *(D-J)* Sections of wild-type and mutant oocytes at the indicated stages after labeling to detect *grip2a* mRNA. Stages are as indicated in the panel and were determined by size and oocyte morphology according to {Selman, 1993 #167}. (D-F) Wild-type oocytes showing localization to the presumptive Balbiani Body (D) and subsequent localization to a cortical domain of the oocyte corresponding to the presumptive vegetal pole (E-F). (G,H) *buc* mutant oocytes lack the Balbiani body {Marlow, 2008 #4627}{Bontems, 2009 #4911} and the *grip2a* mRNA subcellular localization domain in stage I and II oocytes. (I) *mgn* mutant stage I oocytes exhibit an enlarged Balbiani body {Gupta, 2010 #5769} and displayed an enlarged *grip2a* mRNA localization domain. (J) Stage II mgn mutant oocytes fail to localize transcripts to the vegetal pole which instead persist in an internal domain {Gupta, 2010 #5769}, as observed also for *grip2a* mRNA. Number of oocytes examined were as follows: wild-type: early stage I: 13, stage II: 12; *buc:* early stage I: 35, stage II: 26; *mgn:* early stage I: 23, stage II: 18. Magnification bar in (C) corresponds to 250 μm for panels (A-C), and in (J) to 50 μm for panels (D-J).

The localization pattern of *grip2a* mRNA in stage I oocytes is reminiscent of the zebrafish Balbiani body, a conserved aggregate of organelles present in animal oocytes shown to anchor subcellularly localized oocyte mRNAs [41]–[43]. We therefore tested whether *grip2a* mRNA localization is dependent on Balbiani body formation, using zebrafish mutants that affect this structure. Oocytes mutant for the gene *bucky ball* lack the Balbiani body [39], [43], and we found that *bucky ball* mutant oocytes lack *grip2a* mRNA subcellular localization during oogenesis (Figure 4B, 4G, 4H). Moreover, oocytes mutant for the cytoskeletal linker protein *magellan* (*macf1*), which exhibit an enlarged Balbiani body with an abnormal location [40], exhibit *grip2a* mRNA mislocalization (Figure 4C, 4I, 4J) similar to other Balbiani-localized transcripts. These results indicate that *grip2a* mRNA becomes localized to the vegetal cortex during oogenesis by a Balbiani body-dependent mechanism.

2.3.5. *hecate/grip2a* is required for microtubule rearrangements at the vegetal pole

The rescue of *hec* mutant embryos by overexpression of Wnt pathway components has suggested that *hec* likely activates signaling at an upstream step of the pathway [20]. Given that an early event in the pathway leading to Wnt signaling activation is the reorganization of microtubules at the vegetal pole required for the transport of local determinants, we tested whether this reorganization is affected in *hec* mutant embryos (Fig. 5; Figure S5). Consistent with previous studies [2], [8], [27], we find that microtubules at the vegetal cortex in wild-type appear as parallel tracks of bundled microtubules at 20 mpf (Figure 5A). In *hec* mutant embryos, such parallel tracks of bundled microtubules are not observed (Figure 5B). In these mutants, unbundled microtubules typically appear to

radially emanate from one or more aster-like structures at the vegetal pole region (Figure 5C–F). Exposure to the microtubule-stabilizing drug taxol [44] during the first cell cycle (5 to 35 mpf) does not influence the degree of residual axis induction in *hec* mutants (Figure S6), suggesting that the observed defects may not be simple consequence of altered microtubule dynamics. Labeling of the F-actin cortical network in the vegetal cortex region shows a similar appearance in wild-type and mutant embryos (Figure S7), including the presence of F-actin rich protrusions as previously described [45].

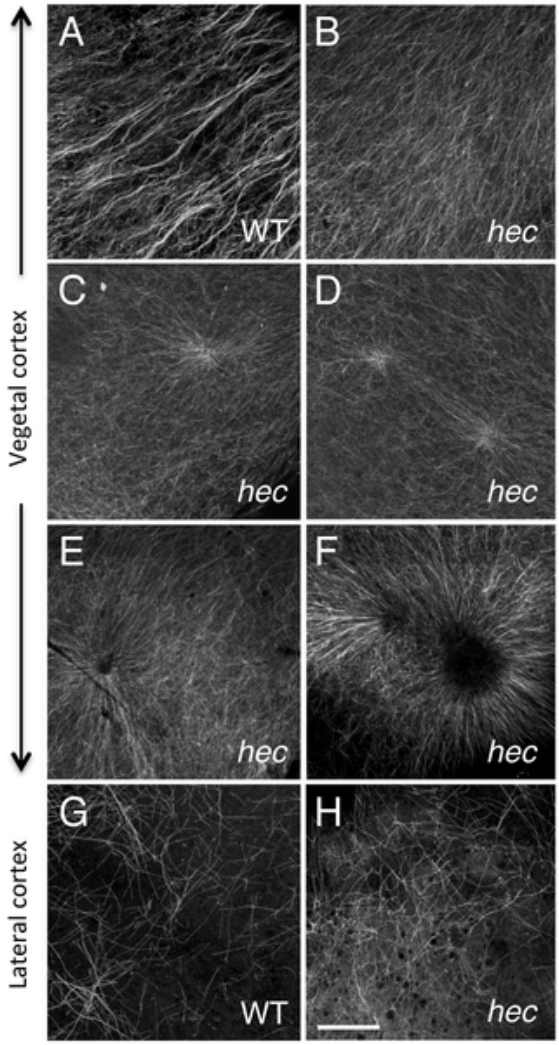

Figure 5: Microtubule reorganization at the vegetal cortex is affected in *hecate* mutants.

(A-F). Cortical microtubule network at the vegetal pole in wild-type (A) and *hec* mutant (B-F) embryos at 40 mpf. Microtubules appear oriented in the same direction and bundled in wild-type embryos (A). The extent of co-orientation and bundling is greatly reduced in *hec* mutant embryos (B), where microtubules form multiple aster-like structures which can have a well focused-center (C,D) or can exhibit a central microtubule-free zone (E,F) and often overlap (F) or interdigitate (D). The relatively unbundled microtubule arrangement shown in (B) also corresponds to a sector of a large aster-like structure emanating from a not shown central core. Up to 6 aster-like structures were observed in the vegetal cortex of a single embryo. (G,H) Cortex in mediolateral regions shows a loose and apparently random network of microtubules which appears similar in both wild-type (G) and *hec* mutant (H) embryos (n=8 for wild-type and mutants). All images are z-axis projections of confocal image stages. The phenotype was fully (100%) penetrant according to the two main categories (wild-type, aligned and bundled microtubules; mutant, radialy oriented and unbundled microtubules, with 10 wt and 25 *hec* mutant embryos imaged. Magnification bar in (H) corresponds to 40 μm for all panels.

2.3.6. Short-range symmetry breaking and anchoring of vegetally localized factors are affected in *hec* mutant embryos

Since vegetal cortical microtubules have been proposed to mediate the off-center shift of factors involved in axis induction that are initially localized to the vegetal pole, such as *grip2a*mRNA (this report), *wnt8a* mRNA ([7]; Figure 6A, 6C) and Sybu protein ([6]; Figure 6E, 6G), we tested whether these shifts were affected in *hec* mutant embryos. As noted above the *grip2a*mRNA localization domain in *hec* mutants, when still detectable, fails to undergo an off-center shift (Figure 3G). In situ hybridization analysis to detect *wnt8a* mRNA shows this mRNA also fails to undergo a noticeable off-center shift in one-cell (30 mpf) *hec* mutant embryos (Figure 6B). At the 4-cell stage (60 mpf), *wnt8a* mRNA localization at the vegetal pole is significantly reduced or undetectable (Figure 6D), although this defect is associated with an overall decrease in the relative expression of *wnt8a* mRNA (Figure S8). In the case of Sybu protein, wild-type embryos show localization centered at the vegetal pole until 20 mpf (Figure 6E) and an off-center shift of protein localization by 30 mpf (Figure 6G), as previously reported [6]. In *hec* mutants, the Sybu protein localization domain can be initially detected centered at the vegetal pole of *hec* mutants (Figure 6F). However, Sybu protein is no longer detectable by 30 mpf (Figure 6H), precluding testing an effect on Sybu protein off-center movement. These data indicate that *hec/grip2a* is essential for the short-range, symmetry-breaking transport of vegetally-localized factors, and are consistent with *hec* function being essential for microtubule reorganization in this region. The reduction in vegetally localized *wnt8a* mRNA and Sybu protein *in hec* mutants contrasts with the perduring

vegetal localization of these factors in embryos with a perturbed microtubule network ([6], [7]; Figure 3I, 6I).

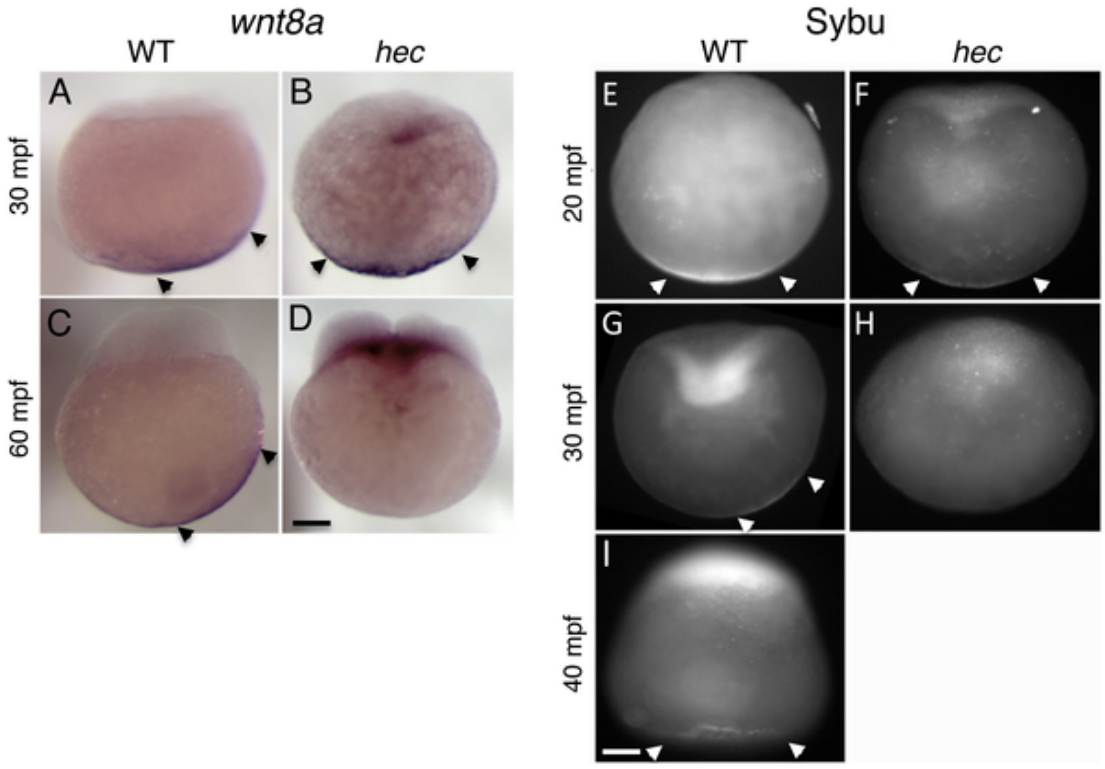

Figure 6: Defects in the vegetal localization of *wnt8a* mRNA and Sybu protein.

(A-D) Off-center shift of *wnt8a* mRNA is affected in *hec* mutants. Whole mount in situ hybridization of wild-type embryos (A,C) and embryos from mothers mutant for the *hec*^{p06ucal} allele (B,D) at the 1- (A,B, 30 mpf) and 4- (C,D, 60 mpf) cell stages. *wnt8a* mRNA does not undergo an off center shift (A,B) and becomes undetectable at the vegetal cortex (C,D). Images show representative embryos. A majority of wild-type embryos showed a clear off-center shift (85%, n=27 at 30 mpf and 74%, n= 47 at 60 mpf). A majority of *hec* mutant embryos showed vegetal localization without a shift at 30 mpf (79%, n=33, remaining embryos show no localization) and absence of localization at 60 mpf (89%, n=38, remaining embryos show reduced vegetal localization without a shift). The apparent label at the base of blastodisc is observed in a majority of embryos (71%, n=38) but not in wild-type (C) or control embryos labeled with other probes (not shown) and may reflect remaining *wnt8a* mRNA that has lost anchoring at the vegetal pole and has moved animally through the action of axial streamers {Fuentes, 2010 #5799}. (E-I) Localization of Sybu protein is affected in *hec* mutants. Whole mount immunofluorescence to detect Sybu protein of untreated wild-type embryos (E,G), untreated embryos from mothers homozygous for the *hec*^{p06ucal} allele (F,H,) and nocodazole-treated wild-type embryos (I) at the indicated stages. In wild-type embryos, an off-center shift in Sybu protein can be observed starting at 30 mpf (G). In *hec* mutants, Sybu protein becomes undetectable levels by this same time point (H). Patterns of localization of Sybu protein at 10 mpf and 20 mpf time points (combined n: 32 WT, 19 mutant for 10-20 mpf), and 30 mpf and 40 mpf time points were similar and have been combined. 59% (n=32) of wild-type and 63% (n=19) of *hec* mutant embryos showed centered vegetal localization during 10-20 mpf. At 30-40 mpf, the percent of embryos that showed vegetal localization, now with an off-center shift, was reduced to 25% (n=28) in wild-type and 0% (n=25) of *hec* mutants showed any localization at these time points. Treatment of wild-type embryos with nocodazole inhibits the shift but does not result in delocalization from the vegetal cortex (I, embryo at 40 mpf), as previously shown {Nojima, 2010 #6429}. Magnification bars in (D) and (I) correspond to 100 μm for panels sets (A-D) and (E-I), respectively.

2.3.7. Long-range animally-directed transport is independent of *hecate/grip2a* function and not restricted to the prospective dorsal region

The short-range off-center shift observed in the case of Sybu protein and *grip2a* mRNA, which occurs within the confines of the vegetal region, contrasts with the long-range transport thought to be involved in transporting a putative dorsal signal to blastomeres at the animal region [2]. *wnt8a* mRNA has been observed to reach the base of the blastomeres by the 16-cell stage (1.5 hpf; [7]), although in our experiments this RNA exhibits a relatively static off-center shift throughout the first 60 mpf (Figure 6A, 6C), similar to the short-range movement of Sybu protein and *grip2a* mRNA. The animally-directed translocation of a putative dorsal signal is thought to be reflected in the microtubule-dependent, animally-oriented movement of small (0.2 μm) polystyrene fluorescent beads during the first several cell cycles. When injected into the vegetal region, these beads reach the base of the blastomeres at the animal region by traveling through cortical paths [2].

Using the transport of microinjected fluorescent beads as an assay for this long-range transport mechanism, we tested whether long-range vegetal-to-animal movement along the cortex might be affected in *hec* mutant embryos. As previously reported [2], in wild-type embryos bead movement from the vegetal region is observed along a meridional arc along the cortex reaching the base of the blastomeres at the animal pole (41% (n=87); Figure 7A,A′). In *hec* mutant embryos, beads appear to be transported to a similar extent as in wild-type, also reaching the base of the blastodisc (Figure 7B,B′) and at a similar observed frequency (39% (n=51)). Thus, *hec* function does not appear to be required for long-range animally-directed transport along the lateral cortex. The

apparently normal movement of animally-directed beads in *hec* mutants appears to conflict with the role of this gene in early microtubule reorganization but is consistent with the observed presence of multiple microtubule populations [2], [8]: aligned bundles of short microtubules at the vegetal region, which we find to be dependent on *hec* function, and a more dispersed and randomly oriented network in more medial regions, which appears unaffected in *hec* mutants (Figure 5G, 5H and data not shown).

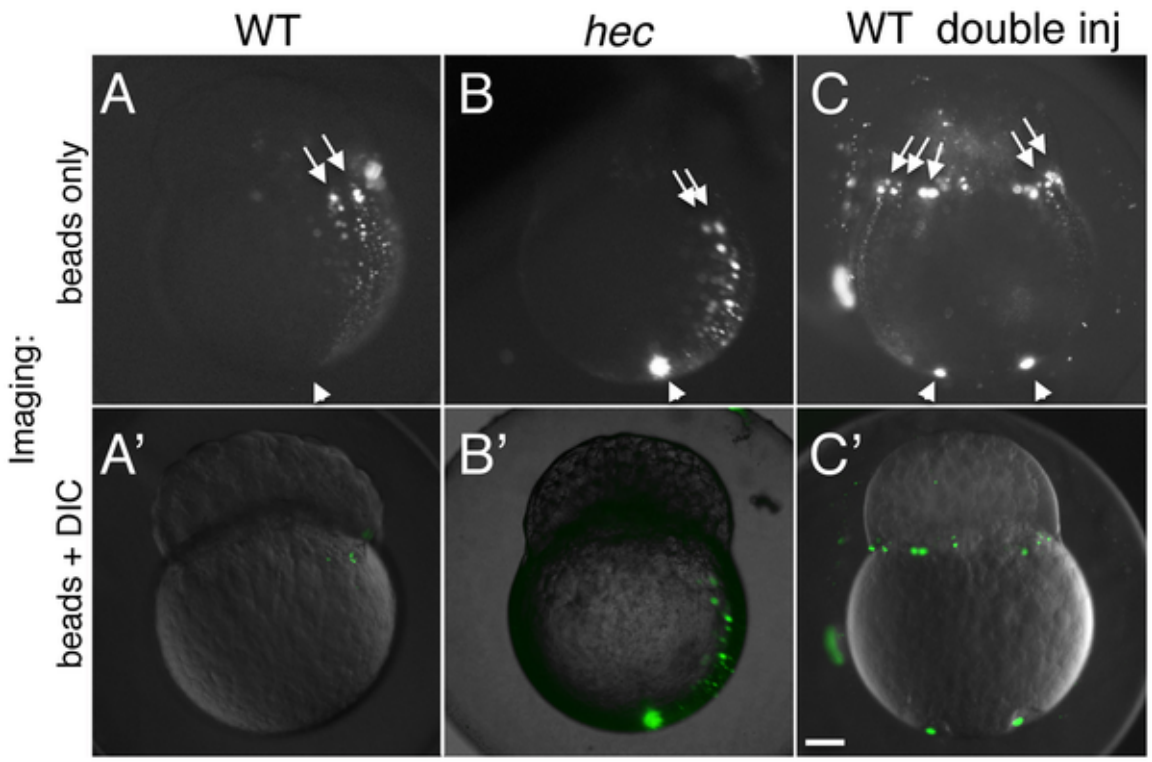

Figure 7: Long-range animally-directed transport is not affected in *hecate* mutants.

(A-C) Paths of injected 0.2um fluorescent beads after injection into the vegetal pole with a single (A,B) or double (C) injection in wild-type embryos (A,C) or embryos from mothers mutant for the *hec*^{p06ucal} allele (B). (A'-C') show merged imaged including the fluorescent channel (shown in A-C) and corresponding DIC optics at low intensity. The extent and frequency of bead transport appeared similar in wild-type and mutant embryos (A,B, see text). Injections into two opposite sides of the vegetal pole results in multiple animally-directed paths, indicating that the entirety of the mediolateral cortex is competent for bead movement. Arrowheads and arrows in (A-C) indicate site of injection in the vegetal region and animally-directed paths along mediolateral regions, respectively. Magnification bar in (C') corresponds to 100 μm for all panels.

The direction of aligned short microtubule bundles at the vegetal pole has been shown to correlate with the dorsal axis but only occurs in a limited area within the vegetal half of the early embryo [8]. Given that directionality of a long-range movement might depend on an earlier oriented symmetry-breaking event, we wondered whether the long-range animally directed movement was specific to the putative dorsal region, or whether the entirety of the cortex was competent to support such transport. To test whether long-range animally-directed transport was specific to the prospective dorsal region of the embryo or was a general property of the lateral cortex, we carried out two slightly off-center fluorescent bead injections on opposite sides of wild-type embryos. Such doubly-injected embryos show animally-directed bead transport along meridional arches in opposite regions of the embryo (Figure 7C,C′), an observation inconsistent with only the prospective dorsal region mediating long range vegetal-to-animal cortical transport. Instead, our data suggest that the entirety of the cortex can mediate long-range animally-directed movement.

The apparently normal long-range transport of beads in *hec* mutant embryos, in the presumed absence of an early short-range symmetry-breaking process, may reflect asymmetries in the location of the beads during injection, followed by the action of this *hec*-independent long-range transport mechanism. Our data suggest that the transport of dorsal determinants to the prospective site of dorsal induction depends on two sequential processes: (i) an initial short-range transport dependent on *hec*-mediated formation of short aligned microtubule bundles that results in determinant asymmetry at the vegetal region of the embryo, and (ii) a subsequent long-range transport through lateral cortical

regions, which is independent of *hec* function and not specific to the prospective dorsal region.

2.3.8. Divergence of *grip* function in zebrafish and *Xenopus*

In *Xenopus*, the homologous gene *grip2* (previously referred to as *grip2.1*), like zebrafish *hec/grip2a*, is expressed maternally and its mRNA is localized to the vegetal pole of the egg and early embryo [32]. Following this vegetal localization, *Xenopus grip2* mRNA becomes incorporated into primordial germ cells (PGCs) where it plays a role in their migration and survival [32]. In contrast, although localized to the vegetal pole, zebrafish *grip2a* mRNA does not localize to the zebrafish germ plasm or PGCs (Figure 3 and data not shown). We used whole mount in situ hybridization to test whether germ plasm localization or PGC development may be affected in *hec* mutant embryos (Figure 8). The localization patterns of *dazl* mRNA, a germ plasm component initially localized to the vegetal pole of the egg ([36], [46], [47]; Figure 8A), is not affected in these mutants (Figure 8D). During the first two cell cycles, *dazl* mRNA localizes normally to the furrows in *hec* mutants (Figure 8B, 8E), as does *vasa* mRNA (Figure 8C, 8F), an animal germ plasm component already present in the animal cortical region during egg activation [33], [36], [38], [48]. During embryonic development, although PGC migration is abnormal in strong *hec* mutants due to their radially symmetric, ventroposteriorized morphology, the average number of induced PGCs (as determined by cells expressing *vasa* in the 10.5 hpf embryo [33], [38], [48]) is similar to that in wild-type embryos (Figure 8G, 8H; Figure S9). Thus, as opposed to the case of *Xenopus grip2*, our observations do not support a role for zebrafish *hec/grip2a* in PGC development.

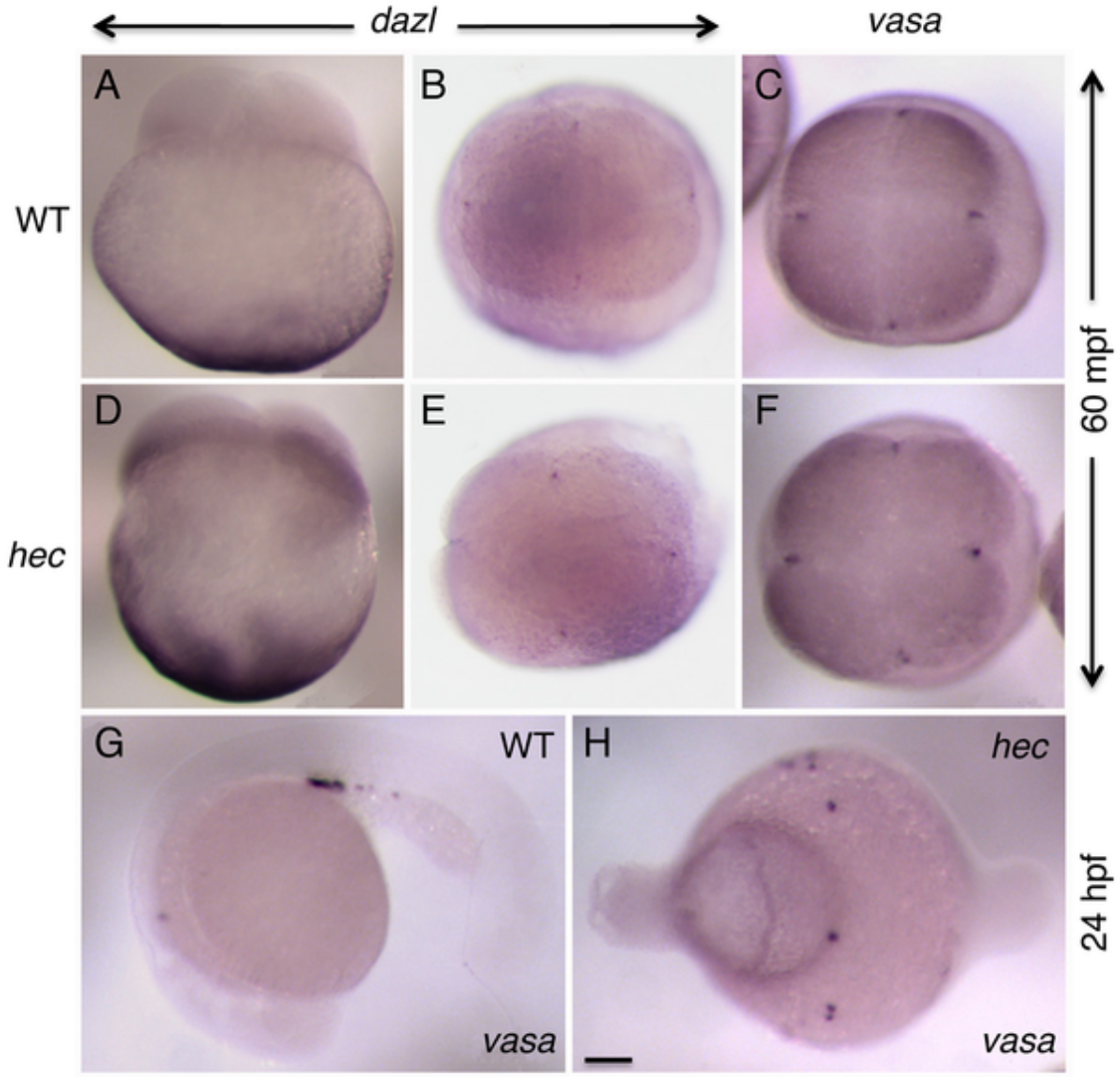

Figure 8: Germ plasm recruitment and PCG determination appears unaffected in *hecate* mutants.

Whole mount in situ hybridization of 4-cell stage (60 mpf) embryos to label the germ line-specific genes *dazl1* (A,B,D,E), and *vasa* (E,F,G,H) in wild-type embryos (A-C,G) and embryos mutant for the *hec*^{p06ucal} allele (D-F,H). Early localization of *dazl* mRNA to the vegetal pole (A,D, side views), and *dazl* mRNA and *vasa* mRNA to the germ plasm as it becomes recruited to the furrows of the first and second cleavage cycles (B,C,E,F, animal views). Localization of dazl domains of recruitment at the furrow is not detected in the side views as the levels of mRNA in these domains are relatively low and the focal plane is not optimal for their visualization. (G,H) PGC determination, as determined by *vasa* expression in 24-hour embryos, appears unaffected in *hec* mutants, although the PGCs in mutant embryos do not become clustered as in wild-type due to the aberrant cell specification in these mutants. Quantification of the number of *vasa*-expressing cells is presented in Figure S8. Magnification bar in (H) corresponds to 100 μm for all panels.

Two other zebrafish *grip*-related genes, *grip1* and *grip2b*, exhibit maternal expression as assayed by RT-PCR of RNA from 1–4 cell embryos but do not show localization to the vegetal pole or germ plasm at these early stages, or in PGCs in the 24-hour embryo ([28]; our own data). Together, these data indicate that, in spite of similar mRNA localization patterns at the vegetal pole of the egg, *grip* homologues in *Xenopus* and zebrafish have divergent roles in PGC development and axis induction, respectively.

2.4. Discussion

A gynogenesis-based forward genetic screen in the zebrafish led to the isolation of a mutation in *hec*, which results in axis induction defects [17], [20], [23]. Here, we report the isolation of two additional alleles of *hec*, identified through an F3 inbreeding screen, and the molecular identification of this gene as encoding Glutamate receptor interacting protein 2a. This molecular assignment, as well as the localization pattern of its products, suggests that vegetally localized *grip2a* mRNA in zebrafish acts at the vegetal pole in the early events of dorsal axis induction. Accordingly, we find that *hec* functions to reorganize and align microtubule bundles that are involved in the symmetry-breaking transport of factors localized to the vegetal cortex, which is essential for axis induction.

2.4.1. Role of *hecate*/*grip2a* in cortical microtubule rearrangements and axis induction

In both teleosts and amphibians, dorsal determinants are initially localized at the vegetal pole and then translocate to the prospective dorsal side in a microtubule-dependent manner to initiate the dorsal cell fate program (reviewed in [1], [49], [50]). Genetic and molecular searches have identified factors localized to the vegetal cortex with a role in axis induction in the zebrafish, such as the kinesin-1 linker Syntabulin [5], [6] and

the *wnt8a* mRNA [7]. We show that the mRNA product for zebrafish *hec/grip2a* is another zebrafish maternal factor involved in axis induction, whose product is also localized to the vegetal pole of the oocyte and early embryo.

Zebrafish *hec/grip2a* is expressed solely during oogenesis as a maternal transcript, which is consistent with the identification of multiple maternal-effect mutant alleles of this gene, all of which lack associated zygotic defects. In particular, fish homozygous for hec the *hecp*^{06ucal} allele, predicted to lack all four PDZ domains present in the wild-type protein and therefore likely a null, exhibit a highly penetrant maternal-effect phenotype yet are themselves viable. These observations indicate that *hec/grip2a* has a dedicated function in early axis determination. While we cannot rule out that *hec/grip2a* is expressed in older embryos or adults at levels below the sensitivity of our assays, other related genes such as *grip1* or *grip2b* are expressed at later stages of development ([28]; our own data) when they may provide essential zygotic functions.

Mechanisms inducing microtubule bundling and alignment, essential for the establishment of the primary body axis, remain incompletely understood. In *Xenopus*, cortical rotation and microtubule reorganization are dependent on both kinesin and dynein motor activity [51], [52]and other factors such as Trim36, a ubiquitin ligase whose mRNA is localized to the vegetal egg cortex [53], Dead end, an RNA binding factor needed for *trim36* mRNA vegetal cortex localization [54] and the lipid droplet component Perilipin 2, whose mRNA is also localized to the *Xenopus* vegetal pole [55], [56]. We find that zebrafish *hec/grip2a* function is required for the reorganization of vegetal cortex microtubules into bundles normally directed towards the prospective dorsal axis [2], [8].

The lack of microtubule network alignment in *hec* mutants and associated defects in the transport of putative dorsal determinants such as *wnt8a* mRNA likely result in the axis induction defects observed in these mutants.

Grip was originally identified as a factor interacting with AMPA-type glutamate receptors [57]and its multiple PDZ domains are thought to facilitate protein-protein interactions within large macromolecular complexes, including the surface presentation and trafficking of transmembrane proteins [58]–[60]. *grip* genes have been implicated in epithelial development in both mouse and zebrafish embryos ([28], [61], reviewed in [62]). Other studies have implicated Drosophila Grip as a mediator of Wnt ligand activity in the postsynaptic terminal of the neuromuscular junction [21], [22].

Our findings suggest parallels between subcellular transport at the vegetal pole of the zebrafish zygote and transport of neurotransmitter receptors in neurons. In the zebrafish zygote, transport of *wnt8a* mRNA depends on microtubules and occurs concomitantly with the movement of the kinesin adaptor Syntabulin [6], [7]. Similarly, in dendrites Glutamate receptors associated with mammalian GRIP1 are driven by kinesin along microtubules [63], and Syntabulin has been shown to be required for axonal transport [64]–[66]. In neurons, glutamate receptors and GRIP associate with membrane vesicles [67], [68]. Although membrane vesicles have not been reported to be associated with dorsal determinants in zebrafish, studies in *Xenopus* implicate membrane vesicles in the transport of dorsal determinants [69]–[72]. Further studies will be required to determine mechanisms driving the reorganization of vegetal cortex microtubules, the

precise role of Grip2a in this process and whether Grip factors have an analogous cytoskeletal restructuring function in other systems.

2.4.2. Is Grip2a required for downstream events in Wnt signaling involved in axis induction?

Our previous studies have shown that manipulations to activate Wnt signaling, including the overexpression of *wnt8* mRNA, can rescue the *hec* mutant phenotype, which suggests that *hec*acts in an upstream event required for Wnt signaling activation during axis induction [20]. Our identification of a role for Grip2a on cytoskeletal events needed for the relocation of dorsal determinants is consistent with such an upstream role. However, our studies do not rule out a more direct role for Grip2a as a regulator of Wnt pathway components. We note that the off-center shift of vegetally localized *grip2a* mRNA upon egg activation could provide an asymmetric source of Grip2a protein to influence Wnt signaling activity at the prospective dorsal region. Drosophila Grip is known to interact with the Wnt receptor Frizzled-2, promoting the trafficking of a Frizzled-2 C-terminal fragment to the nucleus to activate target genes [21], [22], [73], [74], and it is possible that some of these interactions are conserved in the zebrafish embryo. It is also possible that Grip2a regulates non-canonical Wnt signaling, such as Wnt/calcium signaling, which in turn influences axis induction. *hec* mutants exhibit an increased frequency of intracellular calcium transients in blastula stage embryos (2.00–3.33 hpf; [20]), and the resulting intracellular calcium increase has been proposed to attenuate Wnt/β-catenin signaling pathway activity [75]–[79]. Further studies will be necessary to determine whether *hec/grip2a*, in addition to functioning in cytoskeletal organization in the early zebrafish embryo, has a direct role in the regulation of Wnt/β-catenin signaling and axis induction.

Multiple studies in *Xenopus* have indicated the formation of long tracks of cortical microtubules associated with the cortical rotation [80]–[82]. While in this organism the cortical rotation involves the concerted movement of the cortex along a distance corresponding to a 30° arc, microtubule tracks and so-called fast transport of subcellular components, such as membrane organelles and specific factors, encompass a longer distance corresponding to a 60–90° arc (reviewed in [1]). Thus, in *Xenopus* both the cortical rotation and fast transport may participate in the relocation of dorsal determinants. In zebrafish embryos, a cortical rotation-like process results in the displacement of granules along a 20° arc from the vegetal pole of the embryo [8], with mediolateral regions of the cortex exhibiting a loose meshwork of microtubules independent of dorsoventral position [2], [8]. The restriction of microtubule bundling and alignment to the vegetal region of the zebrafish embryo raises the question of how long-range transport of dorsal determinants to the animal pole is achieved.

We found that injected beads reach the base of blastomeres in *hec* mutant embryos, which lack a cortical rotation-like movement, with a frequency similar to that observed in wild-type embryos. This suggests that transport of beads along the mediolateral cortex is independent of *hec/grip2a* function and aligned vegetal microtubules. Our finding that beads are able to move animally along opposite sides in multiply injected embryos, further suggests that the entirety of the mediolateral cortex, not just the prospective dorsal region, is competent for long-range vegetal-to-animal transport. Previous studies have identified animally-directed transport movement of cytoplasmic particles along cortical “meridional” streamers, hypothesized to mediate transport of vegetally-injected fluorescent beads [83]. This meridional transport along the mediolateral cortex may depend on various possible

structures or processes, such as perpendicular bundles aligned along the animal-vegetal axis in deep regions of the cortex [8], incipient yolk cytoplasmic layer (YCL) microtubules emanating from marginal blastomeres into the yolk [84], an emerging property of the loose network of cortical microtubules found in this region of the embryo [2], [8], or other insofar unidentified cytoskeletal networks. Further analysis of the dynamic aspects of cytoskeletal networks in this region will be required to understand the mechanistic basis of this meridional transport system and its role in axis induction. In addition, our results do not exclude the possibility that diffusion of a translated protein such as Wnt8a may also contribute to long-range transport, as previously suggested [8].

Together, these data indicate that the transport of the putative dorsal determinant in the early zebrafish embryo involves at least two separate mechanisms: a short-range transport dependent on *hec/grip2a* function and aligned microtubule bundles, and a subsequent long range transport relying on the mediolateral cytoskeletal network (Figure 9A). We hypothesize that the former generates an off-center, symmetry-breaking shift in initially symmetrically localized putative dorsal determinants, while the latter acts as a more general conduit that amplifies the early asymmetry. In *hec* mutants, the initial symmetry-breaking event is affected, so that even with a functional long-range animal transport mechanism, in most embryos an insufficient amount of dorsal determinants reaches the blastomeres at the animal pole (Figure 9B). A dual mechanism of dorsal determinant transport may also explain how a fraction of embryos from females homozygous for the presumptive null allele, hec^{06ucal}, which lacks all 4 conserved PDZ domains, can develop a normal dorsal axis. In such embryos small fluctuations may occur in the position of the vegetally localized dorsal determinant, which could be amplified by

the mediolateral transport system that is unaffected in these mutants. The presence of an embryo-wide pathway directing long-range transport towards the animal pole may also explain the appearance of double-axis embryos observed only in the weakest *hec* mutant clutches. In these cases, an aberrantly organized vegetal microtubule network may result in the off-center vegetal shift of dorsal determinants in more than one direction, leading to their animally-directed transport along multiple paths and resulting in supernumerary or expanded regions of axis induction. A wider distribution of dorsal determinants in weak *hec* mutants would result in their reduced concentration in animal regions and reduced Wnt pathway activation, consistent with the observed lack of anterior-most structures in the resulting double-axis embryos. This dual transport model suggests mechanisms by which small, directed changes, like the specific early short range symmetry-breaking event, can be amplified during early development by an embryo-wide mechanism to result in large differences in cell fate specification.

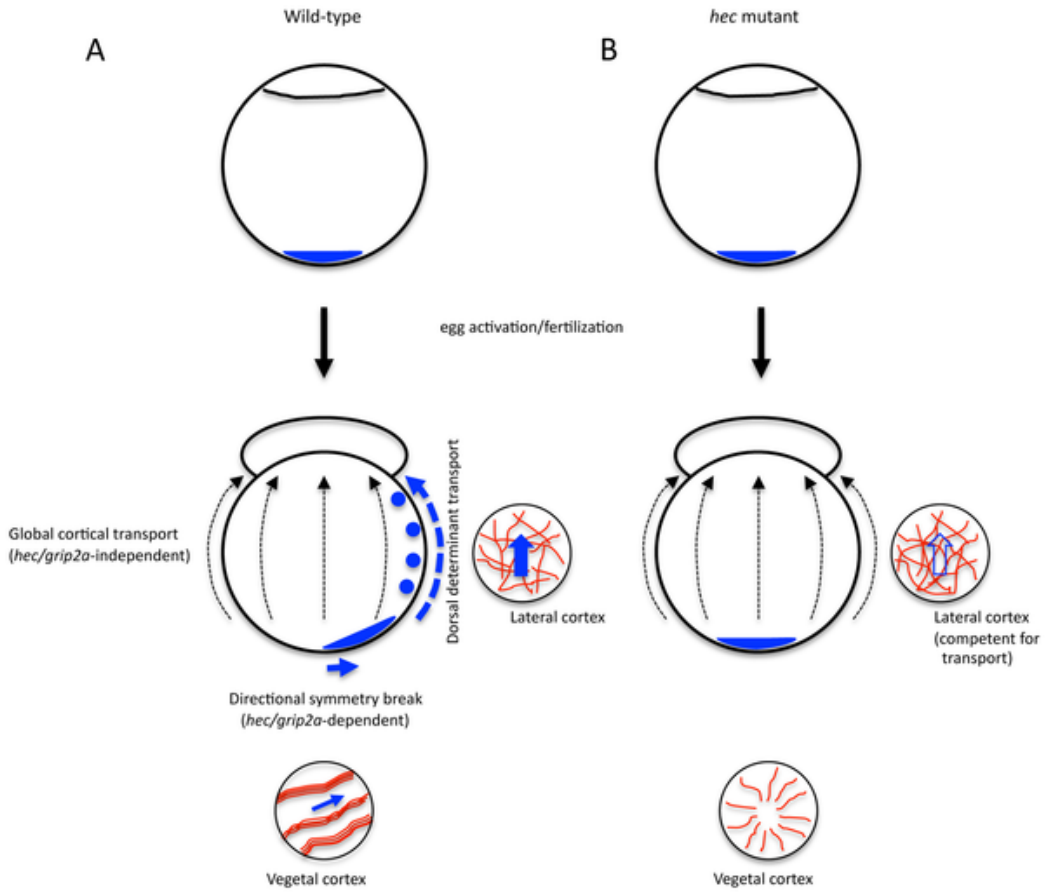

Figure 9: Amplification of *hecate/grip2a*-dependent symmetry breaking event by a general animal-directed long-range transport system.

(A) Cortical shifts of various vegetally localized components, including *wnt8a* mRNA, Sybu protein and *grip2a* mRNA {Nojima, 2010 #6429}{Lu, 2011 #6428}{Tran, 2012 #6796}; this report) are short-range and dependent on microtubule bundling and alignment, itself dependent on *hec* function. In wild-type embryos, such a short-range shift generates a symmetry breaking event that is subsequently amplified by long-range, animally-directed transport mechanism independent of *hec* function and not restricted to the prospective dorsal axis. (B) In *hec* mutant embryos, neither reorganization of vegetal microtubules into aligned bundles nor a short-range shift occur, so that, even though long-range transport remains intact, vegetal determinant transport to the animal pole is affected. The mechanistic basis for the long-range transport, occurring in the region of a loosely organized mediolateral microtubule cortical network remains to be determined (see Discussion).

Table 1: Phenotypic strength of *hecate* alleles

Genotype	V4 [1] (%)	V3 [2] (%)	V2 [3] (%)	V1 [4] (%)	Double axis [5] (%)	Normal (%)	n
WT [5]	0.2	0.2	0.0	0.1	0.0	99.5	1259
hec^{p06ucal}	76.3	7.7	6.5	8.7	0.0	0.9	1812
hec^{t2800}	46.7	13.1	9.5	15.0	0.3	15.4	655
hec^{p08ajug}	10.9	18.9	15.4	28.8	3.1	22.8	1516

Embryos from females homozygous for *hec* mutant alleles were scored at 24 hpf for ventralization phenotypes according to [24]. Results were pooled from clutches from 15 different females for each allele.

1) Severe radial ventralization and lack of all dorsoanterior structures.
2) Absence of anterior structures, including posterior head structures such as the otoliths, lack of notochord, and expanded posterior somites.
3) Absence of anterior head structures including the eyes, lack of notochord, and expanded posterior somites.
4) Reduced anterior head structures such as the eyes but otherwise normal.
5) In weak mutant clutches, a small fraction of embryos exhibit a duplicated axes, each of which often exhibits deletions of the anterior-most structures.
6) Clutches from wild-type female can produce rare ventralized embryos.

2.4.3. *hecate* may represent a gene duplication adapted for axis induction

Using BLAST searches on Ensembl and NCBI genome databases, homologous *grip1* and *grip2*genes were found for all vertebrate species. In Drosophila, there is an ancient single *Grip* gene. All other species containing recognizable *grip* genes are vertebrates. In amphibians, birds and mammals, there is one *grip1* gene and one *grip2* gene. On the other hand, zebrafish have one *grip1* gene and two *grip2* genes, likely due to an ancestral genome duplication in the teleost lineage [30], [31]. Following published nomenclature [28], we refer to the *grip2* gene corresponding to *hec*, located in chromosome 8, as *grip2a*, and the copy located in chromosome 22, as *grip2b*. Phylogenetic analysis indicates that zebrafish *grip2a* is only present in fish species (zebrafish, fugu and medaka). *Drosophila* Grip and all vertebrate Grip1 and Grip2 proteins (including zebrafish Grip2b) contain seven conserved PDZ domains, while zebrafish Grip2a contains only 4 PDZ domains.

The amphibian *grip2* homolog was identified as a novel vegetally-localized mRNA in *Xenopus*oocytes that is present in the mitochondrial cloud (Balbiani body) and subsequently in the germ plasm throughout oogenesis and early embryogenesis [32], [85], [86]. In *Xenopus grip2*morphants, PGC numbers are significantly reduced, and PGCs are also present at ectopic locations along the anteroposterior axis in tailbud stage embryos [32], [86]. However, unlike the case of *Xenopus grip2*, zebrafish *grip2a* mRNA does not localize to the germ plasm or PGCs, and the number of PGCs is unaffected in strongly ventralized mutants (i.e. radially symmetric ventralized embryos). These observations suggest that in zebrafish PGCs are determined

independently of *hec/grip2a* function. Therefore, it appears that *Xenopus grip2* and zebrafish *grip2a* mRNA, in spite of a similar localization at the vegetal pole of the oocyte, have distinct functions in early embryogenesis: *Xenopus grip2* is involved in PGC development, while zebrafish *grip2a* appears to be devoted to dorsal axis formation.

Despite this divergent function, the fact that zebrafish *hec/grip2a* and *Xenopus grip2* are maternally expressed and localized to the vegetal pole during oogenesis, the site of localization of both germ plasm components and dorsal determinants in these two lineages, suggests that an ancestral *grip* gene may have functioned in both axis induction and PGC development. There is precedent for a relationship between these two processes, notably in Drosophila [87]but also in systems as basal as planaria [88], [89] and annelids [90]. This relationship is also supported by the recent finding that the germ cell-specific factor Dead end is required for microtubule rearrangements and cortical rotation in *Xenopus* [54]. The presence of a single localization system involved in both the induction of the primary embryonic axis and the separation between germ cell and soma may constitute a simple mechanism for the species patterning and propagation. Studies of the role of *grip* genes in other organisms may shed light on the relationship between axis induction and PGC determination during evolution.

2.5. Materials & Methods

2.5.1. Fish maintenance and genetic lines

Fish stocks were raised and maintained under standard conditions at 28.5° [91]. The

hec^{t2800} allele was originally isolated in an early-pressure-based screen for recessive maternal-effect mutations [14], [17], while the *hec*^{p06ucal} and *hec*^{p08ajug} alleles were found in a four-generation scheme based on natural crosses ([16], [18], see also [92]). The *hec*^{t2800} allele was induced in an AB/Tübingen hybrid background [14], [17], which was further hybridized with the WIK line during linkage mapping. The *hec*^{p08ajug} and *hec*^{p06ucal} alleles were induced in a Tübingen background, which was hybridized to an AB line in an F4 genetic screen coordinated with linkage mapping [16], [18]. Homozygous mutant *hec* fish were identified by genotyping the flanking SSLP markers z59658 and z24511, which are 1.2 cM apart on linkage group 8 and both of which were polymorphic for all three alleles. Mutant embryos were obtained by crossing homozygous *hec* females to AB males. Embryos from females homozygous mutant for the *hec*^{p06ucal} allele were used unless otherwise specified. Wild-type control embryos were derived from either the AB line or heterozygous sibling females. Clutches were synchronized through 5-minute collections during natural spawning. Oocytes were collected from wild-type, *bucky ball*^{p106re} [39], [43] and *magellan*^{p6cv} [40] mutants. Embryos were collected and developed in E3 embryonic medium [14] and were staged according to the age and morphological standards described in [93].

For complementation tests of *hec*^{t2800}, *hec*^{p08ajug} and *hec*^{p06ucal} mutants, homozygous mutant males of one allele were crossed with heterozygous females of another allele to produce offspring, which were raised to adulthood. Female adult fish were crossed with wild-type males and phenotyped as wild-type or ventralized mutant by examining the resulting clutches at 24 hpf. Only those clutches producing more than 50 embryos were scored and non-complementation was indicated by the presence of ventralization phenotypes similar

in expressivity and penetrance to those in clutches from mutant females from the original three mutant alleles on their own.

2.5.2. Isolation and genotyping of genomic DNA

Fish were anesthetized with MESAB (0.014%) and the tail fin was clipped using a razor blade and placed into 100 ul DNA lysis buffer (10 mM Tris, pH 8.0; 10 mM EDTA, pH 8.0; 200 mM NaCl; 1% Triton X-100) containing 5 µg 10 mg/ml Proteinase K. Tissue lysates were incubated overnight at 55°C, and were incubated at 94°C for 10 minutes to inactivate Proteinase K. Lysates were diluted 1:6 with water, and 2.5 µl of this genomic DNA diluted lysate was used per 10 µl PCR reaction. For a 10 µl PCR reaction, 2 µl of GoTaq green Buffer, 0.2 µl of dNTPs, 0.05 µl of GoTaq DNA polymerase (Promega), 2.5 ul genomic DNA diluted lysate, and 1 µl each of 10 µM forward and reverse primers were used. For SSLP markers, PCR products were analyzed on a 2% high-resolution agarose gel right after the PCR reaction. For RFLP markers, PCR products were used for FastDigest Restriction Enzyme (Fermentas) digestion for 30 min, and then analyzed on a 1.5% regular agarose gel.

2.5.3. Positional cloning and sequence analysis

Initial linkage was identified by bulk segregant analysis with SSLP markers. Once initial linkage of the mutation was obtained, genotypically identified homozygous mutant males were crossed to heterozygous females to generate large numbers of fish for fine mapping [92]. Chromosome walking was conducted by screening the CHORI-211 BAC library using marker z67047 and zC150E8z (0 recombination/1762 genomes). PCR-based screening of the primary pool and secondary pools identified 2 positive BAC clones. Individual BAC clones were ordered from BACPAC resources center (http://bacpac.chori.org). To find the

mutation in *hec/grip2a*, 5 fragments of *hec/grip2a* cDNA from mutant and wild-type 1-cell embryo cDNA were amplified by RT-PCR with 5 primer pairs, which cover the entire *hec/grip2a* coding region:

1. 5′-ATGTCCTGCATCTTGCTTCCAGAG-3′ and 5′-CCTCAGTGGGAATCCCATTAATGG-3′
2. 5′-TGGAGTGTTACAAGTTGGCGACAG-3′ and 5′-TGAATGGCTTCGCTCAGAGGTTTG-3′
3. 5′-TTCATATCGGTGACCGAGTTTTGG-3′ and 5′-GACATTATTGTAGCCTCAAGCTCG-3′
4. 5′-GAGACCTGCGGTCAGTCAGAAATC-3′ and 5′-GTGCTCTGTGTTTCTCATTTGTGG-3′
5. 5′-AGGACACTTCCCAACAGTCTGCAC-3′ and 5′-ACCTGATCACTTCTAACCCAACAG-3′

All PCR products were cloned into pGEM-T easy vector and sequenced.

For Phylogenetic analysis, homologous *grip1* and *grip2* genes were found using BLAST searches on Ensembl and NCBI genome databases. A phylogenetic tree was constructed and drawn using ClustalW in the MegAlign program from Lasergen. PDZ domains were identified using CD-search in the Conserved Domain Database (CDD) in NCBI [29]. Schematic diagram of the protein domain structures for each gene were drawn using DomainDraw [94].

2.5.4. RT-PCR and quantitative RT-PCR

Total RNA was isolated from whole embryos using TRIzol reagent (Invitrogen). cDNA was synthesized using random primers (Invitrogen) and AMV Reverse Transcriptase (Promega). RT-PCR reactions were performed with primer pairs derived from *hec/grip2a* and *ef1α*, using 30 cycles at an annealing temperature of 58°C (in the semi-quantitative range). Absence of genomic contamination was verified by a negative control RT reaction without the Reverse Transcriptase. The following primers were used for the amplifications: *hec/grip2a*, 5′-GAGACCTGCGGTCAGTCAGAAATC-3′ and 5′-

TATGAAGCTCTAGAGGCACTGACG-3′,

wnt8a, 5′-CGGAAAAATGGGTGGTCGTG-3′ and 5′-AGTCGACCAGCTTCGTTGTT-3′,

ef1α, 5′-ACCGGCCATCTGATCTACAA-3′ and 5′-CAATGGTGATACCACGCTCA-3′.

Quantitative (q) RT-PCR was performed on an iCycler machine (Bio-Rad) using iQ SYBR Green Supermix (Bio-Rad). The thermal profile used for amplification is: 95°C for 3 min, 40 cycles of 94°C for 30 s, 58°C for 30 s and 72°C for 30 s. The relative mRNA level was quantified and normalized to *ef1α*.

2.5.5. *In situ* hybridizations and antibody labeling

In situ hybridizations of embryos were carried out as described previously [95]. Probes for in situ included *goosecoid* [96], *chordin* [97], *even skipped 1* [98], *vasa* [33], *dazl* [46] and *wnt8a* [7], [99]. For the *grip2a in situ* probe, a fragment of *grip2a* cDNA was cloned into pGEM-T easy vector as described in the positional cloning section. Five different probes were tested against 5 different cDNA sequences, all of which showed the same expression pattern. Subsequently, all the expression data was acquired using one of the probes. Antisense digoxygenin probe was generated by linearizing and transcribing with SacII and SP6 RNA polymerase, while sense probe control was generated by linearization with SpeI and transcription with T7 RNA polymerase. Images were acquired with a Leica-FLIII microscope and a color camera (Diagnostic Instruments Spot Insight).

Ovaries were dissected from euthanized females and fixed overnight at 4°C in 4% paraformaldehyde. Fixed ovaries were then dehydrated in MeOH.

Whole mount in situ hybridization of oocytes was performed as previously described [100]. Following staining, oocytes were embedded in JB-4 Plus Plastic resin and 7 micron sections were cut using a microtome. Stained sections were coated with Permount (Fisher) prior to

addition of a coverslip.

Antibody labeling of microtubules was as previously described [36]. Prior to the labeling procedure, embryos were dissected using fine dissecting forceps to generate two halves. To image cortical microtubules, bisections were carried out along an equatorial plane, the vegetal halves were labeled and mounted in 50% glycerol with DABCO reagent to prevent bleaching, with the vegetal cortex facing the coverslip. For imaging of mediolateral microtubules, bisections were carried out along a meridional plane and each mediolateral halves were labeled and mounted as above with the mediolateral cortex facing the coverslip. Images were acquired using an upright Zeiss LSM510 confocal microscope using an oil immersion 63× objective and collected as single 1.5 μm optical sections with a pinhole diameter of about 1 Airy unit, a low scan speed (preset 6) and noise filtering through a 4-pass line mode average. The resulting images were analyzed with Fiji software.

Antibody labeling of embryos to detect Sybu protein was carried in whole mount embryos using whole embryos as described previously [6], and images were acquired using a Zeiss Axioplan2 fluorescent microscope and OpenLab software.

Nocodazole treatment was carried out through exposure by 10 mpf of dechorionated embryos to a final concentration of 4 μg/ml nocodazole in E3 (diluted from a 5 mg/ml solution in DMSO), followed by fixation at the indicated periods.

Phalloidin labeling was carried out as in [36], with the exception that dechorionated embryos were labeled whole and equatorially bisected prior to mounting with the vegetal pole facing the coverslip.

2.5.6. Fluorescent beads injection

Fluorescent beads injection experiments were carried as previously described [2]. A suspension of 0.2 mm fluorescent polystyrene beads (1 ul; Polysciences) was diluted in 23 *m*l water and colored with trace amounts of phenol red (0.05%). The injection solution is microinjected into the embryos near the vegetal pole using a Phemtojet microinjector (Eppendorf). Embryos had been injected at the 2-cell stage and imaged at 2 hours later. Embryos were mounted in methyl cellulose and imaged with an upright fluorescence microscope (Zeiss, Axioplan II) and a black and white digital camera (Zeiss, Axiocam).

2.6. Acknowledgements

We thank all members of the Pelegri Lab for critical comments during various stages of this work. We also thank Drs. Arne Lekven (Texas A & M University) and Masahiko Hibi (Nagoya University) and other members of the zebrafish research community for generously providing reagents.

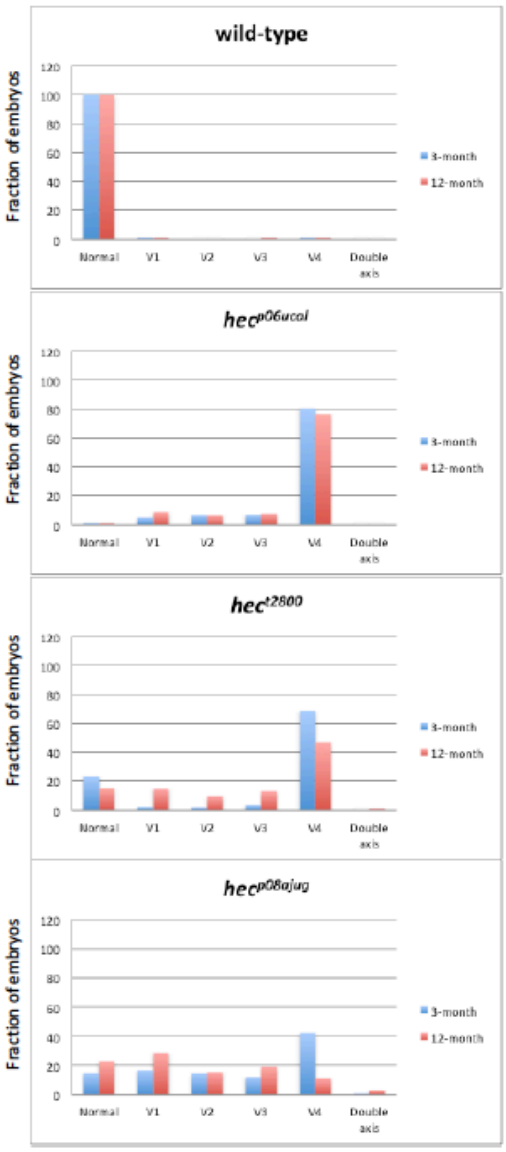

Figure S 1: Age-dependency of the *hec* mutant phenotype

The *hecate* mutant phenotype is stronger in younger females. Also note that at both ages the strength of the alleles is $hec^{p06ucal}$>hec^{t2800}>$hec^{p08ajug}$. Homozygous mutant females at 3 and 12 months after birth were crossed against wild-type males to produce clutches of mutant embryos. Phenotypes were classified at 24 hpf as in [24] and Table 1. Results were pooled from clutches from 15 different females for each allele. Number of embryos is as follows: 3-month females: WT, 1440; $hec^{p06ucal}$, 1178; hec^{t2800}, 575; $hec^{p08ajug}$, 1399; 12-month females: WT, 1259; $hec^{p06ucal}$, 1812; hec^{t2800} 655; $hec^{p08ajug}$, 1516. Pearson's Chi-squared test shows statistical significant differences between 3-month and 12-month females for all alleles (p-values: $hec^{p06ucal}$, 0.002477; hec^{t2800}, <2.2e-16; $hec^{p08ajug}$, <2.2e-16) but not for wild-type females (p-value 0.3421). Pair-wise comparisons between all three alleles are also significantly different using the same analysis (p-values: $hec^{p06ucal}$ vs. hec^{t2800}<2.2e-16; $hec^{p06ucal}$ vs. $hec^{p08ajug}$<2.2e-16; hec^{t2800} vs. $hec^{p08ajug}$<2.2e-16).

Figure S 2: Phylogenetic tree of Grip1 and Grip2 proteins among Drosophila and vertebrate species and number of PDZ domains in the predicted protein

Left: phylogenetic tree using ClustalW. Gene-ID from NCBI or Ensembl-genome databases: GRIP2 rat: NP_612544.2; GRIP2 mouse: NP_001152979.1; GRIP2 human: NP_001073892.1; Grip2 *Xenopus*: NP_001091382.1; GRIP2 chicken: ENSGALP00000010397; Grip2b zebrafish: XP_001922281.1; Grip2b medaka: ENSORLP00000012064; Grip2b fugu: ENSTRUP00000040982; Grip2a fugu: ENSTRUP00000024040; Grip2a medaka: ENSORLP00000012637; Grip2a zebrafish: NP_001116760.1; GRIP1 mouse: NP_083012.1; GRIP1 rat: ENSRNOP00000061369; GRIP1 human: ENSP00000352780; GRIP1 chicken: ENSGALP00000016069; Grip1 *Xenopus*: ENSXETP00000015955; Grip1 fugu: ENSTRUP00000012549; Grip1 medaka: ENSORLP00000021825; Grip1 zebrafish: NP_001038316.1; Grip fruitfly: NP_572285.2. Right: Diagrams of the overall structure of the respective proteins (gray) highlighting the number of PDZ domains (orange), based on Ensembl annotation.

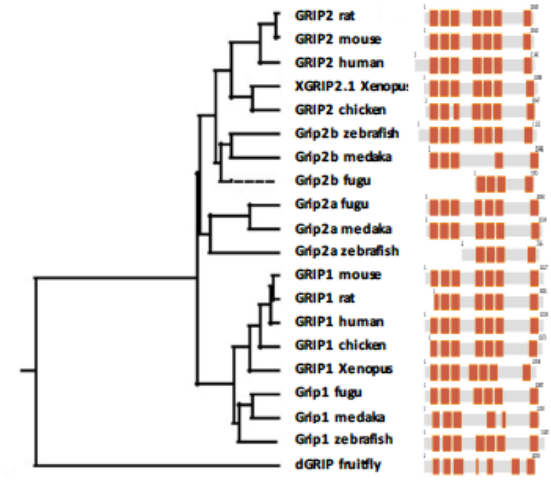

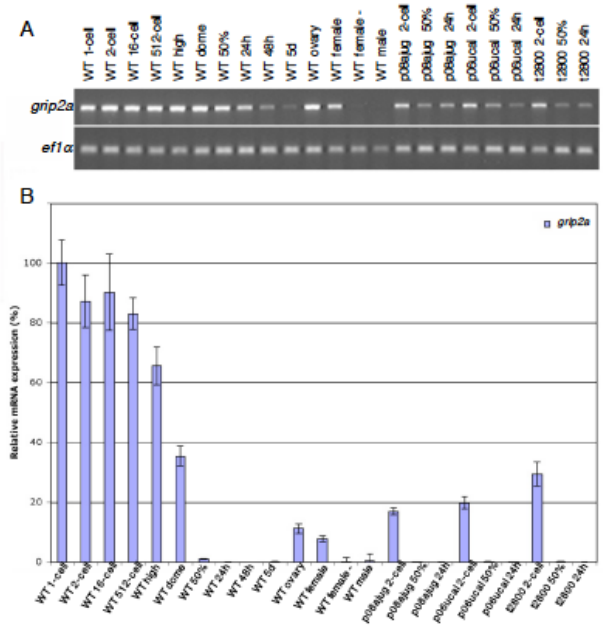

Figure S 3: Expression of zebrafish grip2a mRNA in wild-type and hecate mutant.

A) RT-PCR analysis of *grip2a* mRNA and ef1α control expression in wild-type and *hec* mutant embryos, as well as wild-type ovaries and wild-type adults (male, female, female with removed ovaries). B) Quantitative RT-PCR analysis shows *grip2a* mRNA expression levels, relative to ef1α expression at the same stages. Maternal *grip2a* mRNA levels are reduced in embryos mutant for all *hec* alleles.

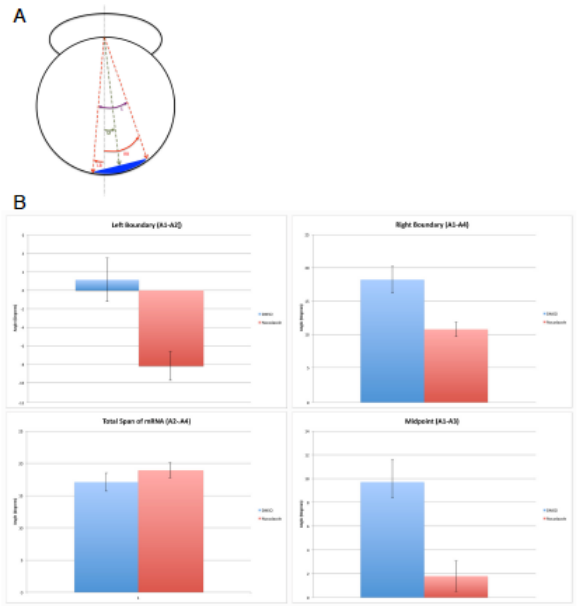

Figure S 4: Quantification of the off-center shift of *grip2a* mRNA localization domain in control (DMSO-treated) and nocodazole-treated embryos fixed at 40 mpf.

A) Diagram indicating angles of the *grip2a* mRNA localization domain landmarks with respect to the vegetal pole of the embryo. LB: left boundary; RB: right boundary; S: total span of domain; M: midpoint of domain. B) Quantification parameters, with brackets indicating standard deviation. In control embryos, but not in nocodazole-treated embryos, left and right boundaries and midpoint of the *grip2a* mRNA localization domain experience a similar off-center shift, while the span of the domain appears unchanged. Blind analysis of 38 and 41 DMSO- and nocodazole-treated embryos, respectively. Similar changes were observed in embryos fixed at 30 mpf, although differences at this time point were less pronounced than at 40 mpf (data not shown).

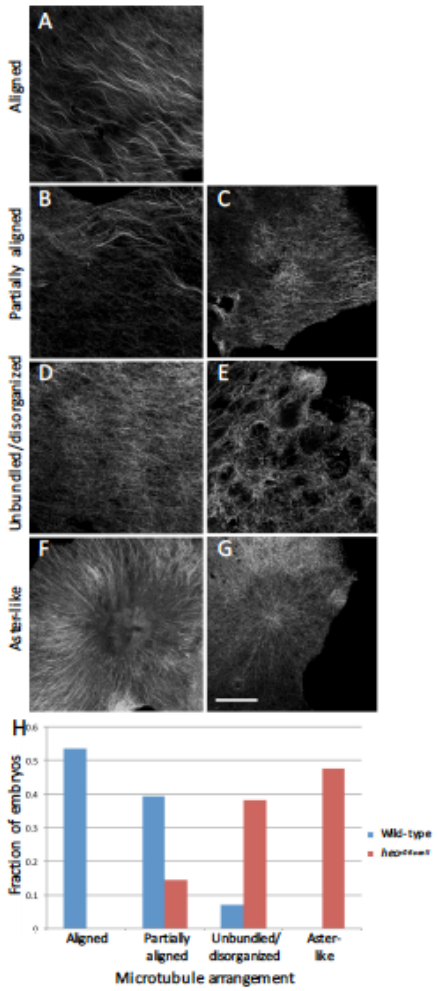

Figure S 5: Distribution of microtubule organization phenotypes at the vegetal cortex of wild-type and *hecate*

A–G) Examples of various vegetal cortex microtubule arrangements at 20 mpf: normally aligned (A), partially aligned (B, C), unbundled and lacking organization (D, E) and exhibiting aster-like structures (F, G). (A) is from a wild-type embryo and (B–G) from *hec*mutants. Magnification bar in (G) corresponds to 40 µm for panels (A–G). H) Distribution of phenotypes. Wild-type embryos exhibit highly aligned microtubule network while *hec* mutants show disorganization, lack of bundling and aster-like structures. The two distributions are significantly different (Fisher's Exact Test, p-value=5.335e-09).

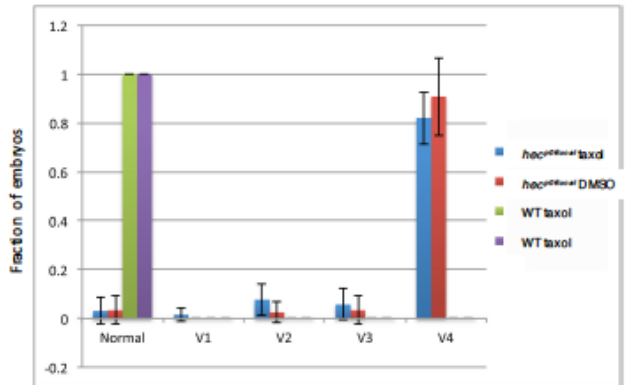

Figure S 6: Treatment with taxol does not affect the *hec* mutant phenotype.
Phenotypic distribution of axial defects (classification as in [24]) of taxol- and solvent (DMSO)-treated wild-type and *hec* mutant embryos. Data is derived from two to three different experiments after a 30 minute exposure to 10 µM taxol starting at 10 mpf. There are no statistically significant phenotypic differences between taxol-treated and control embryos (student t-test, 2-tailed, unpaired).

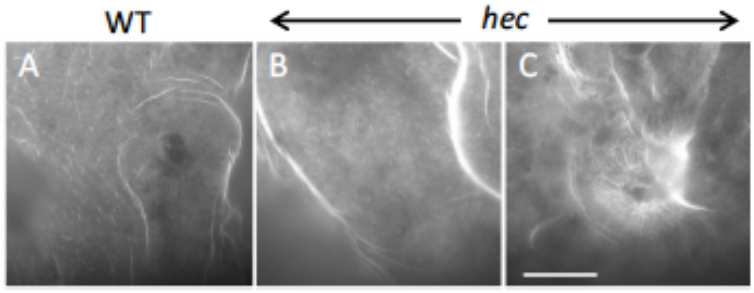

Figure S 7: F-actin cortex at the vegetal pole is similar in wild-type
At 20 mpf, both wild-type (A) and mutant (B) eggs show F-actin rich folds and villi-like structures, which may correspond to previously described microplicae [45]. Number of embryos tested: 18 wt (from a pool of four females) and 24 mutants (from two different mutant females). A fraction (21%, n=24) of *hec* mutant embryos show radial F-actin enrichments (C), correlating with aster-like microtubule structures in these embryos (Figure S5). Magnification bar in (C) corresponds to 40 µm in all panels.

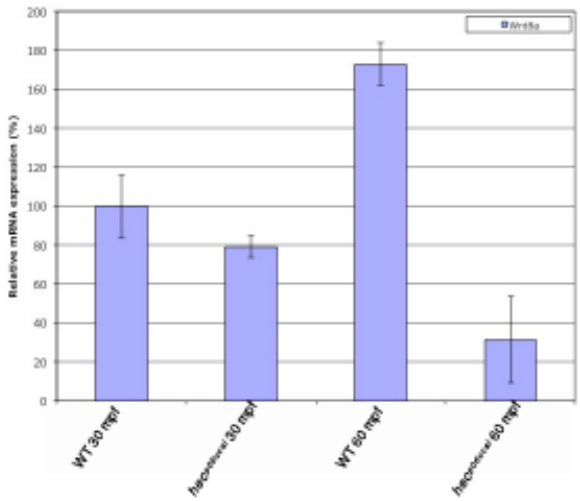

Figure S 8: Expression of *wnt8a* mRNA in *hec* mutant embryos.
Quantitative RT-PCR analysis of *wnt8a*mRNA levels relative to *ef1α* mRNA. *wnt8a* relative expression in *hec* mutants is close to wild-type at 30 mpf but becomes reduced at 60 mpf.

Figure S 9: PGC determination is not adversely affected in *hecate* mutant embryos.

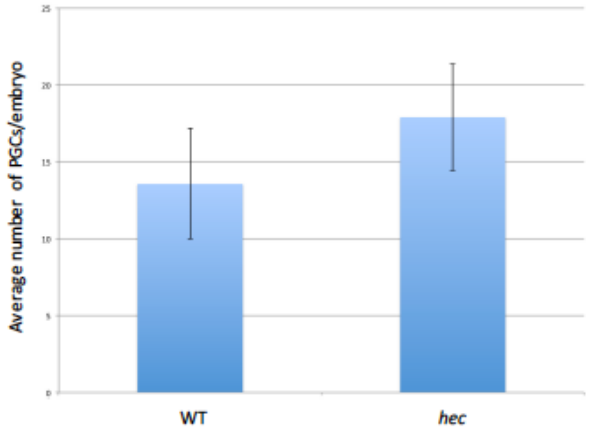

The number of PGCs (as identified by *vasa* expression through whole mount in situ hybridization) was determined in wild-type and *hec* mutant embryos at the 3- through 5-somite stages (ca. 10.5 hpf). At these stages, PGCs have not yet reached the prospective gonad location and appear relatively scattered, which facilitated quantification analysis. The average number of PGCs was 17.9 +/− 3.5 in *hec* mutant embryos (n embryos=158), compared to 13.6 +/− 3.6 in wild-type embryos (n embryos=214). The slightly higher number of PGCs in mutants was statistically significant (Student's t-test, p-value=0.02). It is possible, however, that this difference reflects a bias in our ability to count individual PGCs in *hec* mutants, where PGCs are dispersed throughout the span of the embryos, compared to wild-type embryos, where PGCs are concentrated along the dorsal axis. Regardless of this uncertainty, the data indicate that *hec* function is not essential for PGCs determination.

Table S 1: Complementation analysis of hec^{t2800}, $hec^{p06ucal}$ and $hec^{p08ajug}$ alleles.

	wild-type	mutant
*p06ucal / p06ucal * p08ajug / +*	4	8
*p06ucal / p06ucal * t2800 / +*	11	10
*t2800 / t2800 * p08ajug / +*	8	11
*t2800 / t2800 * p06ucal / +*	1	4
*p08ajug / p08ajug * t2800 / +*	8	11
*p08ajug / p08ajug * p06ucal / +*	22	14

	$hecate^{p06ucal}$	$hecate^{t2800}$	$hecate^{p08ajug}$
$hecate^{p06ucal}$	mutant	mutant	mutant
$hecate^{t2800}$		mutant	mutant
$hecate^{p08ajug}$			mutant

Top: Homozygous mutant males of one allele were crossed with heterozygous females of another allele to produce off springs, which are raised to adulthood. Female adult F_1 progeny were tested for *hec*-associated maternal effects by crossing them against wild-type males and scoring the resulting F_2 clutches as wild-type or mutant. Only test crosses with more than 50 embryos were scored, and were scored as mutant when the fraction of V1–V4 categories was ≥50%. F_2 clutches

scored as wild-type exhibited ≤2% of embryos with V1–V4 phenotypes. If mutations are allelic, crosses are expected to yield F1 females exhibiting wild-type (from heterozygote females) or mutant (from transheterozygote females) F_2 phenotypes in a 1:1 ratio. Bottom: Summary of analysis showing non-complementation of three *hec* alleles.

2.7. References

1. Houston DW (2012) Cortical rotation and messenger RNA localization in Xenopus axis formation. WIREs Dev Biol 1: 371–388.
2. Jesuthasan S, Stra¨hle U (1997) Dynamic microtubules and specification of the zebrafish embryonic axis. Curr Biol 7: 31–42.
3. Mizuno T, Yamaha E, Kuroiwa A, Takeda H (1999) Removal of vegetal yolk causes dorsal deficiencies and impairs dorsal-inducing ability of the yolk cell in zebrafish. Mech Dev 81: 51–63.
4. Ober EA, Schulte-Merker S (1999) Signals from the yolk cell induce mesoderm, neuroectoderm, the trunk organizer, and the notochord in zebrafish. Dev Biol 215: 167–181.
5. Nojima H, Shimizu T, Kim C-H, Yabe T, Bae Y-K, et al. (2004) Genetic evidence for involvement of maternally derived Wnt canonical signaling in dorsal determination in zebrafish. Mech Dev 121: 371–386.
6. Nojima H, Rothha¨mel S, Shimizu T, Kim C-H, Yonemura S, et al. (2010) Syntabulin, a motor protein linker, controls dorsal determination. Development137: 923–933.
7. Lu F-I, Thisse C, Thisse B (2011) Identification and mechanism of regulation of the zebrafish dorsal determinant. Proc Natl Acad Sci USA 108: 15876–15880.
5. Nojima H, Shimizu T, Kim C-H, Yabe T, Bae Y-K, et al. (2004) Genetic evidence for involvement of maternally derived Wnt canonical signaling in dorsal determination in zebrafish. Mech Dev 121: 371–386.
6. Nojima H, Rothha¨mel S, Shimizu T, Kim C-H, Yonemura S, et al. (2010) Syntabulin, a motor protein linker, controls dorsal determination. Development 137: 923–933.
7. Lu F-I, Thisse C, Thisse B (2011) Identification and mechanism of regulation of the zebrafish dorsal determinant. Proc Natl Acad Sci USA 108: 15876–15880.
8. Tran LD, Hino H, Quach H, Lim S, Shindo A, et al. (2012) Dynamic microtubules at the vegetal cortex predict the embryonic axis in zebrafish. Development 139: 3644–3652.
9. Gordon MD, Nusse R (2006) Wnt signaling: multiple pathways, multiple receptors, and multiple transcription factors. J Biol Chem 281: 22429–22433.
10. Petersen CP, Reddien PW (2009) Wnt signaling and the polarity of the primary body axis. Cell 139: 1056–1058.
11. Tao Q, Yokota C, Puck H, Kofron M, Birsoy B, et al. (2005) Maternal Wnt11

activates the canonical Wnt signaling pathway required for axis formation in Xenopus embryos. Cell 120: 857–871.
12. Cha S-W, Tadjuidje E, Tao Q, Wylie C, Heasman J (2008) Wnt5a and Wnt11 interact in a maternal Dkk1-regulated fashion to activate both canonical and non-canonical signaling in Xenopus axis formation. Development 135: 3719–3729.
13. Cha S-W, Tadjuidje E, White JG, Wells J, Mayhew C, et al. (2009) Wnt11/5a complex formation caused by tyrosine sulfation increases canonical signaling activity. Curr Biol 19: 1573–1580.
14. Pelegri F, Schulte-Merker S (1999) A gynogenesis-based screen for maternal effect genes in the zebrafish, Meth Cell Biol 60: 1–20.
15. Kelly C, Chin AJ, Leatherman JL, Kozlowski DJ, Weinberg ES (2000) Maternally controlled b-catenin-mediated signaling is required for organizer formation in the zebrafish. Development 127: 3899–3911.
16. Dosch R, Wagner DS, Mintzer KA, Runke G, Wiemelt AP, et al. (2004) Maternal control of vertebrate development before the midblastula transition: mutants from the zebrafish I. Dev Cell 6: 771–780.
17. Pelegri F, Dekens MPS, Schulte-Merker S, Maischein H-M, Weiler C, et al. (2004) Identification of recessive maternal-effect mutations in the zebrafish using a gynogenesis-based method. Dev Dyn 231: 325–336.
18. Wagner DS, Dosch R, Mintzer KA, Wiemelt AP, Mullins MC (2004) Maternal control of development at the midblastula transition and beyond: mutants from the zebrafish II. Dev Cell 6: 781–790.
19. Bellipanni G, Varga M, Maegawa S, Imai Y, Kelly C, et al. (2006) Essential and opposing roles of zebrafish b-catenins in the formation of dorsal axial structures and neuroectoderm. Development 133: 1299–1309.
20. Lyman-Gingerich J, Westfall TA, Slusarski DC, Pelegri F (2005) hecate, a zebrafish maternal effect gene, affects dorsal organizer induction and intracellular calcium transient frequency. Dev Biol 286: 427–439.
21. Ataman B, Ashley J, Gorczyca D, Gorczyca M, Mathew D, et al. (2006) Nuclear trafficking of Drosophila Frizzled-2 during synapse development requires the PDZ protein dGRIP. Proc Natl Acad Sci USA 103: 7841–7846.
22. Korkut C, Ataman B, Ramachandran P, Ashley J, Barria R, et al. (2009) Trans synaptic transmission of vesicular Wnt signals through Evi/Wntless. Cell 139:393–404.
23. Lyman-Gingerich J, Lindeman R, Putiri E, Stolzmann K, Pelegri F (2006) The analysis of axis induction mutant embryos reveals morphogenetic events associated with zebrafish yolk extension formation. Dev Dyn 235: 2749–2760.
24. Kishimoto Y, Lee K-H, Zon L, Hammerschmidt M, Schulte-Merker S (1997) The molecular nature of zebrafish swirl: BMP2 function is essential during early dorsoventral patterning. Development 124: 4457–4466.
25. Mohler J, Wieschaus EF (1986) Dominant maternal effect mutations of Drosophila melanogaster causing the production of double-abdomen embryos. Genetics 112: 808–822.
26. Lehmann R, Nu¨sslein-Volhard C (1991) The maternal gene nanos has a central role in posterior pattern formation of the Drosophila embryo. Development 112:679–691.

27. Mei W, Lee KW, Marlow FL, Miler AL, Mullins MC (2009) hnRNP I is required to generate the Ca2+ signal that causes egg activation in zebrafish. Development 136: 3007–3017.
28. Carney TJ, Feitosa NM, Sonntag C, Slanchev K, Kluger J, et al. (2010) Genetic analysis of fin development in zebrafish identifies Furin and Hemicentin1 as potential novel Fraser Syndrome disease genes. PLoS Genet 6: e1000907.
29. Marchler-Bauer A, Bryant SH (2004) CD-Search: protein domain annotations on the fly. Nuc Acids Res 32: W327–331.
30. Christoffels A, Koh EG, Chia JM, Brenner S, Aparicio S, et al. (2004) Fugu genome analysis provides evidence for a whole-genome duplication early during the evolution of ray-finned fishes. Mol Biol Evol 21: 1146–1151.
31. Se´mon M, Wolfe KH (2007) Reciprocal gene loss between Tetraodon and zebrafish after whole genome duplication in their ancestor. Trends Genet 23: 108–112.
32. Tarbashevich K, Koebernick K, Pieler T (2007) XGRIP2.1 is encoded by a vegetally localizing, maternal mRNA and functions in germ cell development and anteroposterior PGC positioning in Xenopus laevis. Dev Biol 311: 554–565.
33. Yoon C, Kawakami K, Hopkins N (1997) Zebrafish vasa homologue RNA is localized to the cleavage planes of 2- and 4-cell-stage embryos and is expressed in the primordial germ cells. Development 124: 3157–3165.
34. Pelegri F, Knaut H, Maischein H-M, Schulte-Merker S, Nu¨ sslein-Volhard C (1999) A mutation in the zebrafish maternal-effect gene nebel affects furrow formation and vasa RNA localization. Curr Biol 9: 1431–1440.
35. Knaut H, Pelegri F, Bohmann K, Schwarz H, Nu¨sslein-Volhard C (2000) Zebrafish vasa RNA but not its protein is a component of the germ plasm and segregates asymmetrically prior to germ line specification. J Cell Biol 149: 875–888.
36. Theusch EV, Brown KJ, Pelegri F (2006) Separate pathways of RNA recruitment lead to the compartmentalization of the zebrafish germ plasm. Dev Biol 292: 129–141.
37. Eno C, Pelegri F (2013) Gradual recruitment and selective clearing generate germ plasm aggregates in the zebrafish embryo. Bioarchitecture 3: 125–132.
38. Braat AK, Zandbergen T, van de Water S, Goos HJT, Zivkovic D (1999) Characterization of zebrafish primordial germ cells: morphology and early distribution of vasa RNA. Dev Dyn 216: 153–167.
39. Bontems F, Stein A, Marlow F, Lyautey J, Gupta T, et al. (2009) Bucky ball organizes germ plasm assembly in zebrafish. Curr Biol 19: 414–422.
40. Gupta T, Marlow FL, Ferriola D, Mackiewicz K, Dapprich J, et al. (2010) Microtubule actin crosslinking factor 1 regulates the balbiani body and animal vegetal
polarity of the zebrafish oocyte. PLoS Genet 6: e1001073.
41. Cox RT, Spradling AC (2003) A Balbiani body and the fusome mediate mitochondrial inheritance during Drosophila oogenesis. Development 130: 1579–1590.
42. Pepling ME, Wilhelm JE, O'Hara AL, Gephart GW, Spradling AC (2007) Mouse oocytes within germ cell cysts and primordial follicles contain a Balbiani body. Proc Natl Acad Sci USA 104: 187–192.

43. Marlow FL, Mullins MC (2008) Bucky ball functions in Balbiani body assembly and animal-vegetal polarity in the oocyte and follicle cell layer in zebrafish. Dev Biol 321: 40–50.
44. De Brabander M, Geuens G, Nuydens R, Willebrords R, De Mey J (1961) Taxol induces the assembly of free microtubules in living cells and blocks the organizing capacity of the centrosomes and kinetochores. Proc Natl Acad Sci USA 78: 5608–5612.
45. Donovan MJ, Hart NH (1986) Cortical granule exocytosis is coupled with membrane retrieval in the egg of Brachydanio. J Exp Zool 237: 391–405.
46. Maegawa S, Yasuda K, Inoue K (1999) Maternal mRNA localization of zebrafish DAZ-like gene. Mech Dev 81: 223–226.
47. Hashimoto Y, Maegawa S, Nagai T, Yamaha E, Suzuki H, et al. (2004) Localized maternal factors are required for zebrafish germ cell formation. Dev Biol 268: 152–161.
48. Olsen LC, Aasland R, Fjose A (1997) A vasa-like gene in zebrafish identifies putative primordial germ cells. Mech Dev 66: 95–105.
49. De Robertis EM, Kuroda H (2004) Dorsal-ventral patterning and neural induction in Xenopus embryos. Annu Rev Cell Dev Biol 20: 285–308.
50. Pelegri F (2003) Maternal factors in zebrafish development. Dev Dyn 228: 535–554.
51. Marrari Y, Terasaki M, Arrowsmith V, Houliston E (2000) Local inhibition of cortical rotation in Xenopus eggs by an anti-KRP antibody. Dev Biol 224: 250–262.
52. Marrari Y, Rouviere C, Houliston E (2004) Complementary roles for dynein and kinesins in the Xenopus egg cortical rotation. Dev Biol 271: 38–48.
53. Cuykendall TN, Houston DW (2009) Vegetally localized Xenopus trim36 regulates cortical rotation and dorsal axis formation. Development 136: 3057–3065.
54. Mei W, Jin Z, Lai F, Schwend T, Houston DW, et al. (2013) Maternal Dead-End1 is required for vegetal cortical microtubule assembly during Xenopus axis specification. Development 140: 2334–2344.
55. Chan AP, Kloc M, Etkin LD (1999) fatvg encodes a new localized RNA that uses a 25-nucleotide element (FVLE1) to localize to the vegetal cortex of Xenopus oocytes. Development 126: 4943–4953.
56. Chan AP, Kloc M, Larabell CA, LeGross M, Etkin LD (2007) The maternally localized RNA fatvg is required for cortical rotation and germ cell formation. Mech Dev 124: 350–363.
57. Dong H, Zhang P, Song I, Petralia RS, Liao D, et al. (1999) Characterization of the Glutamate receptor-interacting proteins GRIP1 and GRIP2. J Neurosci 19: 6930–6941.
58. Lee HJ, Zheng JJ (2010) PDZ domains and their binding partners: structure, specificity, and modification. Cell Commun Signal 8: 8.
59. Bard L, Groc L (2011) Glutamate receptor dynamics and protein interaction: lessons from the NMDA receptor. Mol Cell Neurosci 48: 298–307.
60. Ivarsson Y (2012) Plasticity of PDZ domains in ligand recognition and signaling. FEBS Lett 586: 2638–2647.
61. Takamiya K, Kostourou V, Adams S, Jadeja S, Chalepakis G, et al. (2004) A direct functional link betwen the multi-PDZ domain protein GRIP1 and the Fraser sydrome protein Fras1. Nat Genet 36: 172–177.

62. Sugiura T, Shimizu T, Kijima A, Minakata S, Kato Y (2011) PDZ adaptors: their regulation of epithelial transporters and involvement in human diseases. J Pharm Sci 100: 3620–3635.
63. Setou M, Seog DH, Tanaka Y, Kanai Y, Takei Y, et al. (2002) Glutamate receptor-interacting protein GRIP1 directly steers kinesin to dendrites. Nature 417: 83–87.
64. Su Q, Cai Q, Gerwin C, Smith CL, Sheng ZH (2004) Syntabulin is a microtubule-associated protein implicated in syntaxin transport in neurons. Nat Cell Biol 6: 941–953.
65. Cai Q, Gerwin C, Sheng ZH (2005) Syntabulin-mediated anterograde transport of mitochondria along neuronal processes. J Cell Biol 170: 959–969.
66. Cai Q, Pen PY, Sheng ZH (2007) Syntabulin-kinesin-1 family member 5B mediated axonal transport contributes to activity-dependent presynaptic assembly. J Neurosci 27: 7284–7296.
67. Fagni L, Ango F, Peroy J, Bockaert J (2004) Identification and functional roles of metabotropic glutamate receptor-interacting proteins. Sem Cell Dev Biol 15:289–298.
68. Furukawa J (2012) Structure and function of glutamate receptor amino terminal domains. J Physiol 590: 63–72.
69. Larabell CA, Torres M, Rowning BA, Yost C, Miller JR, et al. (1997) Establishment of the dorsoventral axis in Xenopus embryos is presaged by early asymmetries in b-catenin that are modulated by the Wnt signalling pathway. J Cell Biol 136: 1123–1134.
70. Rowning BA, Wells J, Wu M, Gerhart JC, Moon RT, et al. (1997) Microtubule-mediated transport of organelles and localization of b–catenin to the future dorsal side of Xenopus eggs. Proc Natl Acad Sci USA 94: 1224–1229.
71. Miller JR, Rowning BA, Larabell CA, Yang-Snyder JA, Bates R, et al. (1999) Establishment of the dorsal-ventral axis in Xenopus embryos coincides with the dorsal enrichment of dishevelled that is dependent on cortical rotation. J Cell Biol 146: 427–437.
72. Weaver C, Far III GH, Pan W, Rowning BA, Wang J, et al. (2003) GBP binds kinesin light chain and translocates during cortical rotation in Xenopus eggs. Development 130: 5425–5436.
73. Swan LE, Wichmann C, Prange U, Schmid A, Schmidt M, et al. (2004) A glutamate receptor-interacting protein homolog organizes muscle guidance in Drosophila. Genes Dev 18: 223–237.
74. Swan LE, Schmidt M, Schwarz T, Ponimaskin E, Prange U, et al. (2006) Complex interaction of Drosophila GRIP PDZ domains and Echinoid during muscle morphogenesis. EMBO J 25: 3640–3651.
75. Kume S, Inoue T, Mikoshiba K (2000) Gas family G proteins activate IP3-Ca2+ signaling via Gbc and transduce ventralizing signals in Xenopus. Dev Biol 226:88–103.
76. Saneyoshi T, Kume S, Amasaki Y, Mikoshiba K (2002) The Wnt/calcium pathway activates NF-AT and promotes ventral cell fate in Xenopus embryos. Nature 417: 295–299.
77. Westfall TA, Brimeyer R, Twedt J, Gladon J, Olberding A, et al. (2003) Wnt5/

pipetail functions in vertebrate axis formation as a negative regulator of Wnt/B-catenin activity. J Cell Biol 162: 889–898.
78. Westfall TA, Hjertos B, Slusarski DC (2003) Requirement for intracellular calcium modulation in zebrafish dorsal-ventral patterning. Dev Biol 259: 380–391.
79. Wu S-Y, Shin J, Sepich DS, Solnica-Krezel L (2012) Chemokine GPCR signaling inhibits b-catenin during zebrafish axis formation. PLoS Biol 10: e1001403.
80. Elinson RP, Rowning B (1988) Transient array of parallel microtubules in frog eggs: potential tracks for a cytoplasmic rotation that specifies the dorso-ventral axis. Dev Biol 128: 185–197.
81. Houliston E, Elinson RP (1991) Patterns of microtubule polymerization relating to cortical rotation in Xenopus laevis eggs. Development 112: 107–117.
82. Schroeder MM, Gard DL (1992) Organization and regulation of cortical microtubules during the first cell cycle of Xenopus eggs. Development 114: 699–709.
83. Fuentes R, Ferna´ndez J (2010) Ooplasmic segregation in the zebrafish zygote and early embryo: pattern of ooplasmic movements and transport pathways. Dev Dyn 239: 2172–2189.
84. Solnica-Krezel L, Driever W (1994) Microtubule arrays of the zebrafish yolk cell: organization and function during epiboly. Development 120: 2443–2455.
85. Kaneshiro K, Miyauchi M, Tanigawa Y, Ikenishi K, Komiya T (2007) The mRNA coding for Xenopus glutamate receptor interacting protein 2 (XGRIP2) is maternally transcribed, transported through the late pathway and localized to the germ plasm. Biochem Biophys Res Commun 355: 902–906.
86. Kirilenko P, Weierud FK, Zorn AM, Woodland HR (2008) The efficiency of Xenopus primordial germ cell migration depends on the germplasm mRNA encoding the PDZ domain protein Grip2. Differentiation 76: 392–403.
87. St. Johnston D, Nu¨sslein-Volhard C (1992) The origin of pattern and polarity in the Drosophila embryo. Cell 68: 201–219.
88. Rebscher N, Zelada-Gonza´lez F, Banisch TU, Raible F, Arendt D (2007) Vasa unveils a common origin of germ cells and of somatic stem cells from the posterior growth zone in the polychaete Platynereis dumerilii. Dev Biol 306: 599–611.
89. Wang Y, Zayas RM, Guo T, Newmark PA (2007) nanos function is essential for development and regeneration of planarian germ cells. Proc Natl Acad Sci USA 104: 5901–5906.
90. Gazave E, Be´hague J, Laplane L, Guillou A, Pre´au L, et al. (2013) Posterior elongation in the annelid Platynereis dumerilii involves stem cells molecularely related to primordial germ cells. Dev Biol 382: 246–267.
91. Brand M, Granato M, Nu¨sslein-Volhard C (2002) Keeping and raising zebrafish. In: Nu¨ sslein-Volhard C, Dahm R, editors. Zebrafish - A Practical Approach. Oxford: Oxford University Press. 7–37 p.
92. Pelegri F, Mullins M (2011) Genetic screens for mutations affecting adult traits and parental-effect genes. Meth Cell Biol 104: 83–120.
93. Kimmel C, Ballard WW, Kimmel SR, Ullmann B, Schilling TF (1995) Stages of embryonic development in the zebrafish. Dev Dyn 203: 253–310.

94. Fink JL, Hamilton N (2007) DomainDraw: a macromolecular feature drawing program. In Silico Biol 7: 145–150.
95. Pelegri F, Maischein H-M (1998) Function of zebrafish b-catenin and TCF-3 in dorsoventral patterning. Mech Dev 77: 63–74.
96. Schulte-Merker S, Hammerschmidt M, Beuchle D, Cho K, DeRobertis EM, et al. (1994) Expression of the zebrafish goosecoid and no tail gene products in wildtype and mutant ntl embryos. Development 120: 843–852.
97. Schulte-Merker S, Lee KJ, McMahon AP, Hammerschmidt M (1997) The zebrafish organizer requires chordino. Nature 387: 862–863.
98. Joly J-S, Joly C, Schulte-Merker S, Boulkebache H, Condamine H (1993) The ventral and posterior expression of the homeobox gene eve1 is perturbed in dorsalized and mutant embryos. Development 119: 1261–1275.
99. Lekven AC, Thorpe CJ, Waxman JS, Moon RT (2001) Zebrafish wnt8 encodes two wnt8 proteins on a bicistronic transcript and is required for mesoderm and neuroectoderm pattterning. Dev Cell 1: 103–114.
100. Thisse C, Thisse B, Schilling TF, Postlethwait JH (1993) Structure of the zebrafish snail1 gene and its expression in wild-type, spadetail and no tail mutant embryos. Development 119: 1203–1215.
101. Selman K, Wallace RA, Sarka A, Qi X (1993) Stages of oocyte development in the zebrafish, Brachydanio rerio. J Morphol 218: 203–224.

Chapter 3: Cortical depth and differential transport of vegetally localized dorsal and germ line determinants in the zebrafish embryo

Elaine Welch and Francisco Pelegri*

Laboratory of Genetics
University of Wisconsin – Madison
425-G Henry Mall
Madison, WI 53706, USA

* Author for correspondence: fjpelegri@wisc.edu

Author contribution: Elaine Welch performed the experiments and wrote the manuscript. FP edited before publication.

Welch, E. and Pelegri, F. (2015). Cortical depth and differential transport of vegetally localized dorsal and germ line determinants in the zebrafish embryo. BioArchitecture, 5:1-2, 13-26, DOI: 10.1080/19490992.2015.1080891

3.1. Abstract

In zebrafish embryos, factors involved in both axis induction and primordial germ cell (PGC) development are localized to the vegetal pole of the egg. However, upon egg activation axis induction factors experience an asymmetric off-center shift whereas PGC factors undergo symmetric animally-directed movement. We examined the spatial relationship between the proposed dorsal genes *wnt8a* and *grip2a* and the PGC factor *dazl* at the vegetal cortex. We find that RNAs for these genes localize to different cortical depths, with the RNA for the PGC factor *dazl* at a deeper cortical level than those for axis-inducing factors. In addition, and in contrast to the role of microtubules in the long-range transport of dorsal determinants, we find that germ line determinant transport depends on the actin cytoskeleton. Our results support a model in which vegetal cortex differential RNA transport behavior is facilitated by RNA localization along cortical depth and differential coupling to cortical transport.

Keywords

Axis induction, germ cell determination, germ plasm, RNA localization, cortical rotation, vegetal cortex, embryo, zebrafish

3.2. Introduction

One of the main processes that take place during vertebrate embryogenesis is the establishment of the dorsoventral axis. This process has been extensively studied in amphibians through classic experiments involving embryological manipulations [1,2]. In *Xenopus laevis*, these manipulations indicated that shortly after fertilization, dorsal determinants are transported to the future dorsal side of the embryo coincident with the shift of the outer cortex, the "cortical rotation", relative to the entire cytoplasm [2,3]. Subsequent studies have indicated that this process depends on the microtubule cytoskeleton at the vegetal cortex, and in particular the reorganization of vegetal microtubules as long tracks of aligned, parallel bundles. It has been argued that microtubule alignment coupled to motor function causes the relative shift of the cortex, which feeds back to reinforce further microtubule alignment. In *Xenopus*, these tracks of aligned microtubule bundles extend the relatively long span from the vegetal pole to the prospective dorsal region near the animal pole, and visualization of particles, vesicles and fluorescently labeled factors suggest that these tracks may be acting as a substrate for long range transport. This has led to a model in which cortical rotation and microtubule-dependent transport are interdependent processes that together mediate the transport of dorsal determinants [2]. These determinants, through mechanisms that have not been fully determined, result in the activation of the canonical Wnt/β-catenin signaling pathway [4,5], leading to dorsal gene expression and the induction of the dorsal organizer [6].

Similar to *Xenopus*, manipulations of the zebrafish embryo have demonstrated that dorsal determinants are maternally supplied and initially localized at the vegetal pole of the unfertilized egg and the one cell embryo, and subsequently translocate to the prospective dorsal side via a microtubule dependent process [7-9]. Early imaging studies in the zebrafish embryo showed that fluorescent polystyrene beads injected at the vegetal cortex of the embryo move animally along a cortical arc in a microtubule-dependent manner [7]. Moreover, this and subsequent studies showed that zebrafish vegetal cortex microtubules, as in *Xenopus*, become reorganized into parallel bundles [7,10]. Visualization of microtubules in live embryos further showed that the direction of these tracks and cytoplasmic granule movement corresponds to the site of dorsal induction [10]. This led to the idea that, as in *Xenopus*, tracks of aligned cortical microtubules mediate the transport of dorsal determinants from the vegetal pole to the prospective site of dorsal induction in blastomeres at the animal pole. These studies painted a picture of translocation of dorsal axis determinants that was remarkably similar to that in *Xenopus*, with dorsal determinant transport dependent on aligned microtubule tracks and an associated cortical shift.

In spite of similarities between *Xenopus* and zebrafish, previous studies have also highlighted potential differences with regards to the contribution of microtubule alignment to the overall dorsal determinant transport process. In particular, the range of product transport and region covered by aligned microtubules is significantly less in zebrafish, where it is confined only to the vegetal-most 30^{o} arc [10]. Moreover, localized products encoded by genes required for axis induction, such as RNAs coding for the Wnt8a ligand and the intracellular protein Hecate/Grip2a, as well as the protein for the kinesin 1 linker Tokkaebi/Syntabulin, experience a similar restricted shift upon egg activation [11-13],

which roughly coincides with the region of microtubule alignment. *hecate/grip2a* function was shown to be required for the reorganization of vegetal cortex microtubules into aligned bundles, as well as the associated movement of these localized factors [13]. These observations indicated the presence of a short range, off-center shift dependent on *hecate/grip2a* function and vegetal microtubule reorganization, which contrasts with the long-range process based on this system as described in *Xenopus*.

Previous studies had shown extensive movement of ooplasm in the zebrafish one-cell embryo, including in cortical mediolateral regions [14,15]; could it be possible that zebrafish embryos rely on a general transport mechanism and a second phase of animally-oriented transport? This was directly tested in zebrafish embryos using the bead injection assay. Remarkably, beads injected into the vegetal pole of *hecate/grip2a* mutant embryos could still travel animally along mediolateral cortical tracks even though these mutants lack an early short-range asymmetry [13]. Even more surprising, beads injected near the vegetal pole, but at opposite sides of the embryo, were equally able to undergo animally-oriented transport [13]. These observations clearly indicated a transport mechanism at the mediolateral cortex of the early zebrafish embryo that is independent of *hecate/grip2a* function and vegetal microtubule reorganization, and indicated that the entire cortex, and not just that along the prospective dorsal region, is competent for this transport.

These studies have highlighted similarities and differences between mechanisms of dorsal determinant transport in *Xenopus* and zebrafish. In both cases there appears to be a cortical rotation-like process that is associated with microtubule alignment. However, in *Xenopus* this process appears to be an integral part of the mechanism that conveys dorsal determinants to their final location in animal blastomeres, while in zebrafish the end-point

transport appears to depend on two sequential processes. In zebrafish, an initial short-range phase of transport involves a cortical rotation-like mechanism, dependent on vegetal cortex microtubule alignment, itself dependent on *hecate/grip2a* function [13]. Subsequently, a second, long-range transport phase involves animally-directed movement along the mediolateral region by a mechanism that is neither spatially restricted nor dependent on *hecate/grip2a* function or vegetal microtubule reorganization [7,13]. Thus, the zebrafish embryo constitutes a remarkable example in which a small, random change, such as the orientation of microtubule alignment leads to an off-center shift that creates an early embryonic asymmetry. This subtle difference is subsequently amplified by a less specific mechanism that generates a larger embryo-wide response.

In this two-step pathway, the off-center shift of localized factors involved in dorsal axis induction is a key determinative event. However, the zebrafish embryo contains other vegetally localized factors, in particular RNAs that eventually become associated with the zebrafish germ plasm, a cytoplasmic structure containing ribonucleoparticles (RNPs) that determines the germ cell fate. Two germ plasm-associated RNAs, for the genes *deleted in azoospermia*-like (*dazl*) and *Bruno-like*, are originally localized to the vegetal pole of the mature egg [16,17]. Upon egg activation, RNPs containing these vegetally localized RNAs are transported along cortical paths toward the animal pole, where they become incorporated into germ plasm masses [18,19]. These masses are associated with the cellular furrows corresponding to the first and second cell cycles [20] and, due to the alternate pattern of furrow orientation in the zebrafish [21], become distributed in four quadrants of the embryo. Observations indicate that both animally-directed transport of vegetal germ plasm RNPs along the mediolateral cortex and recruitment of these RNPs at

the furrows occurs evenly throughout the embryo, without a dorsoventral bias [19,20,22]. This suggests that, in contrast to the asymmetric movement of products involved in dorsal axis induction, animally-oriented translocation of vegetal germ plasm RNPs occurs symmetrically along the mediolateral cortex.

Here, we study the underlying basis of the differential behavior of these two types of determinants, namely asymmetric movement of factors involved in axis induction (*wnt8a* and *grip2a* RNAs) and the symmetric movement of vegetal germ plasm RNPs (*dazl* RNA). We use fluorescent in situ hybridization (FISH) to detect these RNAs at the subcellular level and find that they are present in non-overlapping sets of RNPs. Asymmetrically-transported RNPs containing factors involved in axis induction, are preferentially found in the outermost cortical region, whereas symmetrically-transported vegetal germ plasm RNPs are enriched in more internal regions of the embryo. In contrast to the proposed requirement for microtubules in the long-range transport of dorsal determinants [7], we find that animally-directed movement of the germ plasm factor *dazl* is dependent on F-actin function. Thus, a pre-pattern of RNP localization at different cortical depths, coupled to microtubule-based cortical rotation and subsequently implemented by different cytoskeletal systems, underlies the differential migratory behavior of axis induction and vegetal germ plasm factors.

3.3. Results

In zebrafish, parallel microtubules become aligned at the vegetal cortex beginning at approximately 14 mpf and start to dissociate at ~26 mpf [10]. Formation of an array of aligned vegetal microtubules is essential for the off-center asymmetric shift experienced by

several factors involved in axis induction, such as *wnt8a* RNA [12], *hecate/grip2a* RNA [13] and Syntabulin protein [11]. In wild type embryos at 10 and 30 mpf, RNA localization domains for *hecate/grip2a* and *wnt8a*, respectively, show an off-center movement, a shift not observed in embryos where the microtubule network is inhibited due to exposure to nocodazole. In contrast, the RNA of the vegetally localized germ plasm gene *dazl* is at this time point also localized at the base of the vegetal cortex but does not experience an asymmetric movement (Fig. 1). Instead, vegetal pole localization of *dazl* RNA remains symmetric even as it begins animally-directed transport, and this symmetry is similar regardless of the integrity of the microtubule network.

In order to understand the basis for this differential transport behavior, we examined at the subcellular level the spatial relationship between these RNAs during the first cell cycle (20 mpf, when the microtubule array is maximally aligned and RNP movement is likely occurring). We carried out double fluorescence in situ hybridization to detect pairs of RNAs for axis induction factors (*wnt8a*, *grip2a)* and vegetal germ plasm components (*dazl*) at the vegetal-most embryonic cortex (Fig. 2). Two-dimensional projections indicate the presence of transcripts as discreet punctae in the case of *wnt8a* and *dazl* RNAs and a more diffuse pattern albeit with noticeable enrichments in the case of *grip2a* RNA. Overlay of fluorescence channels shows virtually no signal overlap between the three RNA pair combinations: *wnt8a/dazl, grip2a/dazl* and *wnt8a/grip2a*. This indicates that these three vegetally localized RNAs, in spite of being present in the same general embryonic region, are present in separate RNPs. The observation that *wnt8a* and *grip2a* RNAs are present in different particles indicates that multiple types of RNPs have a role in the process of axis induction.

To better understand the localization of these RNPs at the vegetal cortex, we generated 3-D renderings of these pair-wise comparisons of doubly-labeled fluorescence in situ hybridizations (Fig. 3). Co-detection of *wnt8a* and *dazl* RNAs show that *wnt8a* RNA-containing particles tend to be present in the cortical most region, whereas *dazl* RNA-containing particles occur in more internal regions (Fig. 3A). Dual labeling of *grip2a* and *dazl* RNAs exhibit a similar pattern, with *grip2a* -containing particles in the cortical most region and *dazl* RNA-containing particles enriched in deeper regions (Fig. 3B). In contrast, co-detection of *wnt8a* and *grip2a* RNAs do not show any apparent differential distribution between these RNAs with respect to cortical depth (Fig. 3C). We quantified these distributions by binning particles in three sub-cortical regions of equal thickness, corresponding to the cortical-most (outer), intermediate, and most internal regions within a region 9 microns below the membrane surface (Fig. 3D-F; see Methods). This analysis confirms a statistically significant difference in particle distribution for both the *wnt8a*/*dazl* and *grip2a*/*dazl* comparisons, in which *wnt8a* and *grip2a* RNAs are enriched at the outer cortical region and *dazl* RNA is enriched in the inner cortical region. Together, these data indicate that the particles containing dorsal factor RNAs, which experience an asymmetric shift and act during axis induction, are preferentially localized in the outer most region of the cortex, whereas particles containing *dazl* RNA, which do not experience an asymmetric shift, are located in a more internal regions of the cortex.

Animally-directed movement of dorsal determinants towards the animal pole is thought to depend on an intact microtubule network [7]. Given the different initial cortical localization and transport behavior of the germ plasm component *dazl* RNA, we tested the cytoskeletal requirement for its animally-directed movement. Exposure of early embryos

to the microtubule inhibitor nocodazole, whose effects were confirmed by a complete inhibition of blastomere furrowing, did not have an apparent effect on *dazl* RNA animally-directed movement as judged by the presence of cortical *dazl* RNPs in mediolateral and animal cortex regions (Fig. 4A, A', B, B' and data not shown). However, *dazl* RNA fails to migrate animally toward the furrows when actin assembly is inhibited using latrunculin A (Fig. 4C, C'). These results suggest that the actin cytoskeleton is important for the animally-directed transport of vegetally-localized germ plasm RNPs prior to their recruitment at the distal ends of cleavage furrows.

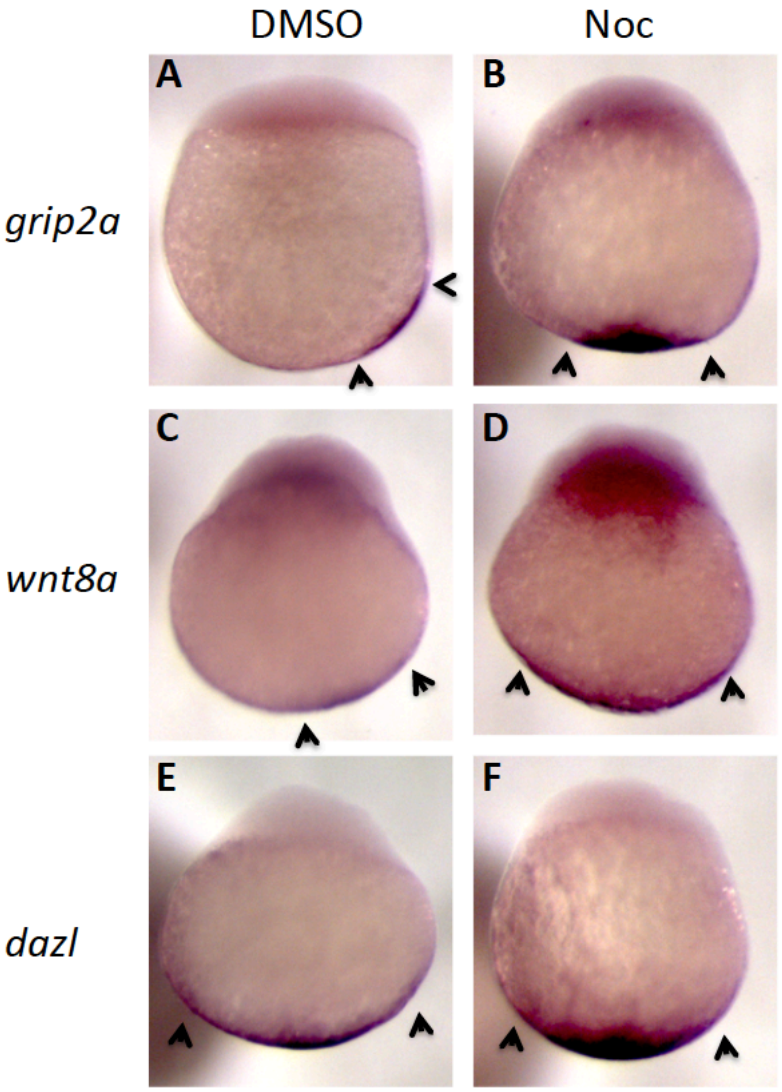

Figure 1: Differential behavior of localized determinants at the vegetal pole of the embryo.

A-D) Asymmetric movement of mRNAs for dorsal factors. Whole mount in situ hybridization shows that *grip2a* and *wnt8a* mRNA are localized at the base of the vegetal cortex and experience an off-center shift in control (DMSO-treated) embryos ((A) *grip2a:* 88%, n=27; (C) *wnt8a:* 85%, n=13). Treatment with nocodazole inhibits asymmetric movement ((B) *grip2a:* 84%, n=19, (D) *wnt8a*: 85%, n=13). E-F) Symmetric localization of the germ line *dazl* mRNA. *dazl* mRNA is also localized to the base of the vegetal cortex in control embryos ((E) 90%, n=11) and this distribution appears unaffected by nocodazole treatment ((F) 100%, n= 12). Embryos fixed at 40mpf. Animal pole up, dorsal (when known) right. Arrowheads demark RNA localization domains.

3.4. Discussion

Recent advances have provided new insights on mechanisms of axis induction in amphibians and teleosts, including the identities of primary inducing molecules [2]. In addition, studies have shown that a dramatic reorganization of the microtubule apparatus is required for the movement of these axis-induction determinants from their initial localization at the vegetal pole to the site of dorsal induction in blastomeres at the animal pole [2]. In amphibians, a long history of studies have described a so-called cortical rotation, the movement of the cortex in relation to the inner core of the early embryo, which facilitates the movement of these determinants [3,27]. The cortical rotation was originally identified by the appearance of new cytoplasmic crescent after rotation, reflective of the resulting misalignment of the pigmented animal cortex and the underlying fertilized egg inner core. Later, this cortical rotation was associated with the function of an array of parallel microtubule bundles at the vegetal cortex, which in amphibians spans the length of the arc between the vegetal pole and the prospective dorsal site [28-30]. The spatial extension of this microtubule array, coupled with the observation of movement of vegetal localizing factors to the animal pole region, has led to the postulation that this array is also involved in the long-range transport of dorsal determinants.

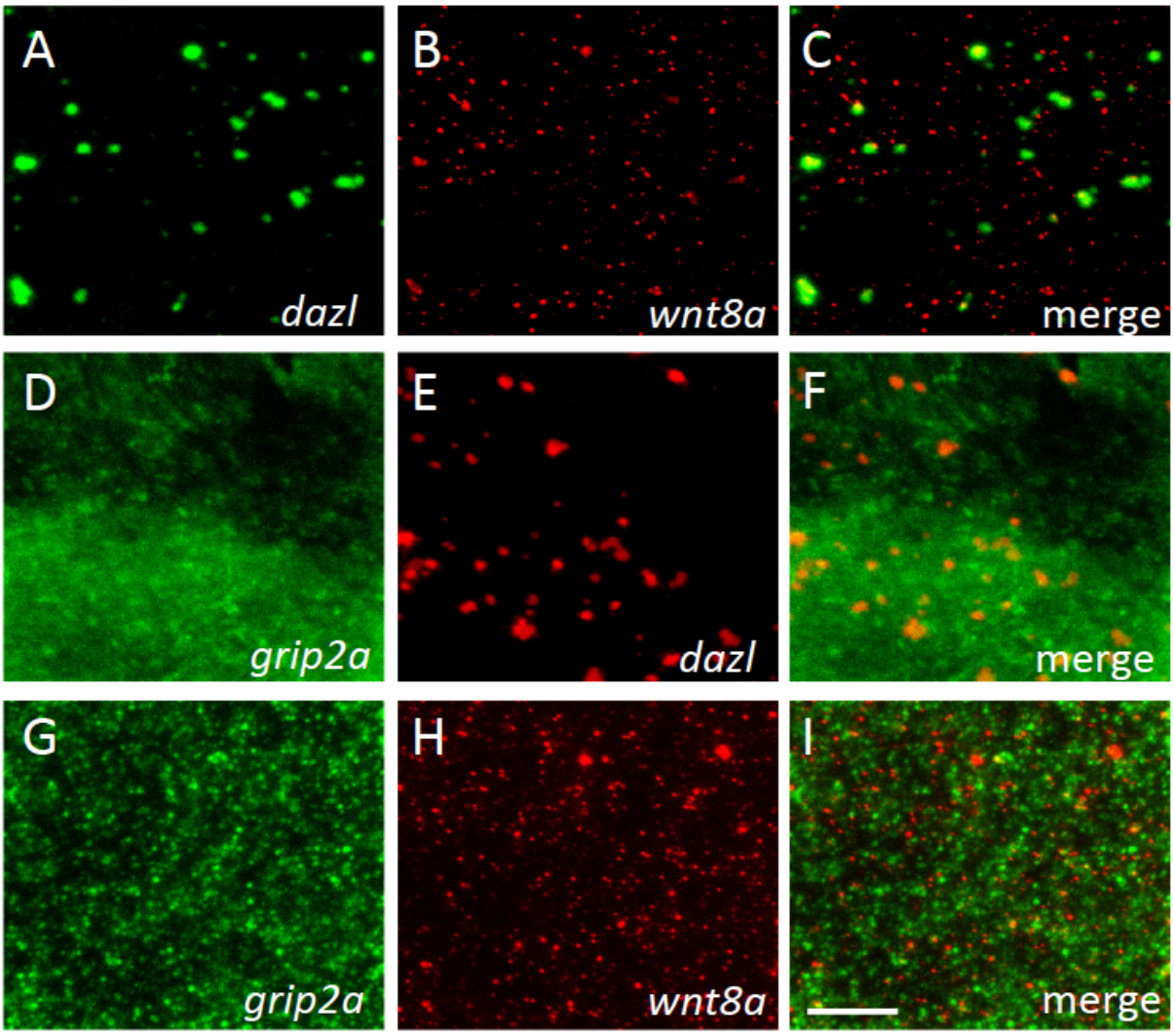

Figure 2: Dual label FISH of pairwise comparisons of *wnt8a*, *grip2a* and *dazl* mRNA localization at the vegetal cortex

A-C) *dazl* (green) and *wnt8a* (red). D-F) *grip2a* (green) and *dazl* (red). G-I) *grip2a* (green) and *wnt8a* (red). In all cases mRNAs localize to discrete units, which do not overlap between different RNAs. Embryos are wild type fixed at 20mpf. Panels are 2-D projections of imaged vegetal cortex samples. Scale bar in (I) represents 5μm for all images.

Movement of cortical granules towards the prospective dorsal site has also been observed in the early zebrafish embryo, along with the observation of parallel-arrayed microtubule bundles oriented along this movement [7,10]. However, in the zebrafish embryo these bundles span a much less extensive domain encompassing only about a 30-degree arc from the vegetal pole. The remainder of the distance to dorsal blastomeres at the animal pole appears to be dependent on a separate process independent of microtubule reorganization in the vegetal region. This is suggested by the observation that embryos mutant for the *hecate/grip2a* gene, which are defective in vegetal microtubule reorganization, appear unaffected in the animally-directed transport of injected beads along the mediolateral cortex [13].

In spite of these differences, both amphibian and teleost embryos exhibit an initial symmetry-breaking event dependent on the reorganization of vegetal cortex microtubules and associated cortical movement, which results in the asymmetric localization of dorsal factors such as *wnt8a* and *grip2a* RNAs. This asymmetric transport contrasts with the segregation pattern of a second type of cell determinant also localized to the vegetal pole region, namely germ plasm components. In the case of *Xenopus*, germ plasm RNPs are present in the vegetal pole and segregate into four large germ cell-determining masses that remain in the vegetal region of the embryo [31]. In the case of zebrafish, germ plasm components appear to be split into two types of particles [19]. One set of zebrafish germ plasm RNPs, containing RNAs for genes such as *vasa*, *nanos1* and *dead end*, is present at the animal pole [19,20,32,33]. A second set of zebrafish germ plasm RNPs, containing RNAs for genes such as *dazl* and *bruno-like*, is, as in amphibians, initially localized to the vegetal region [17,26]. Upon egg activation, vegetally-localized zebrafish germ plasm RNPs migrate

animally to join the animal germ plasm RNPs, to generate germ plasm masses in forming blastomere furrows [18,19]. In spite of species-specific differences, in both systems dorsal and germ plasm factors are initially localized to the vegetal cortex and dorsal determinants undergo an asymmetric movement. Moreover, no dorsoventral asymmetry can be detected in zebrafish *dazl* RNA localization, nor in the size of germ plasm or the number of induced PGCs in neither amphibians nor teleosts [20,22,31]. This implies that, in spite of a similar localization pattern at the vegetal pole, dorsal and PGC determinants undergo different transport mechanisms.

We examine the basis of this differential transport by visualizing at high resolution the vegetal pole localization of RNAs corresponding to dorsal and PGC factors. We find that RNAs for these three factors are found in different particles at the vegetal cortex. Moreover, the RNAs for dorsal factors, *wnt8a* and *grip2a*, are enriched in the outermost layer of the cortex, whereas the RNA for the PGC factor *dazl* is present in more internal regions. This observation supports the idea that a cortical rotation-like process is, as in amphibians, involved in generating the asymmetry of dorsal determinants in the early zebrafish. As also proposed in amphibians, in the zebrafish embryo the higher density of the yolk cell would be expected to maintain the core of the egg in a stable conformation after a cortical rotation event, so that the movement of the vegetal cortex in relation to the core would result in a shift of cortical components away from the vegetal-most pole of the embryo, as is observed for dorsal factors. Thus, a location of dorsal determinants in the outer most region of the cortex would facilitate the development of an off-center asymmetry through cortical rotation. On the other hand, an enrichment of germ plasm RNPs, such as those containing

dazl RNA, in a more internal region would facilitate their being excluded from the shifting cortex and instead allow their symmetric distribution.

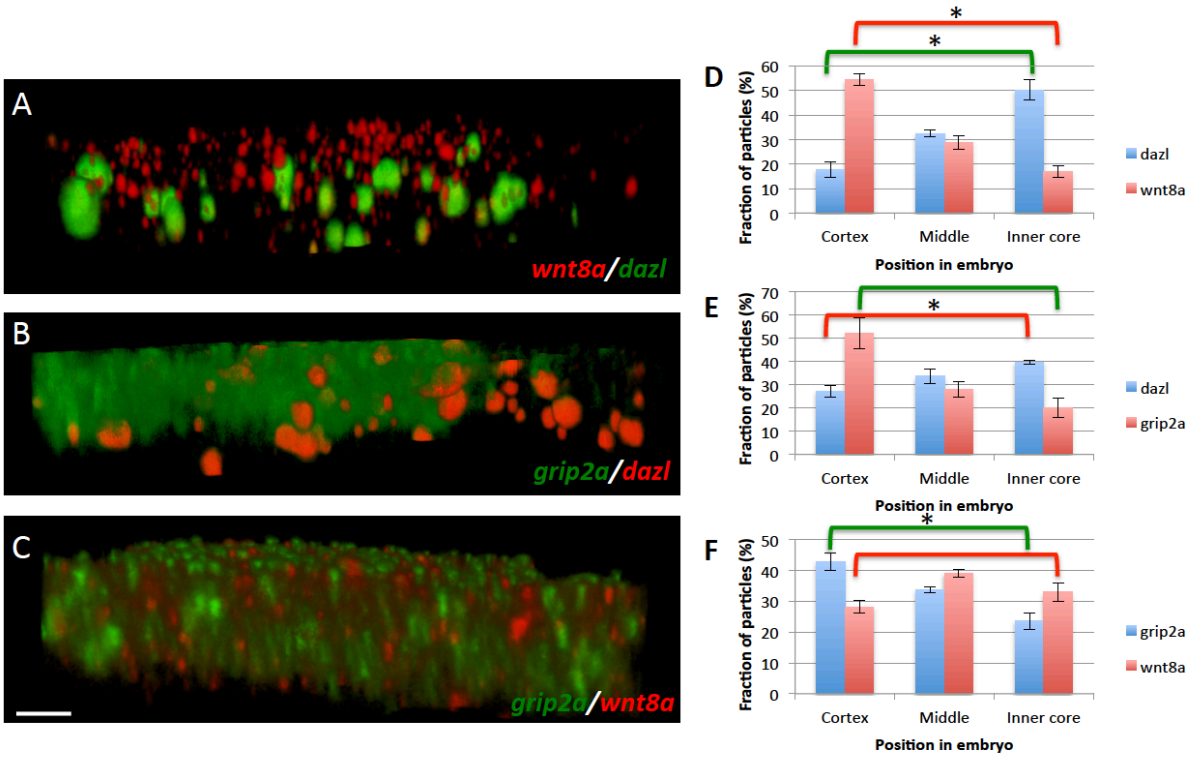

Figure 3: Colocalization analysis of *wnt8a*, *grip2a* and *dazl* mRNA localization.

A-C) 3-D rendering of dual labeled FISH for pairwise comparisons: A) *wnt8a* (red) and *dazl* (green); B) *grip2a* (green) and *dazl* (red); and C) *grip2a* (green) and *wnt8a* (red). D-F) Quantification of particles according to cortical depth within a 9µm section of the vegetal half of the embryo divided into outer (0 – 2.997µm), intermediate (3.087 – 5 µm) and most internal (6.084 – 9 µm) (see Methods). Particles containing *wnt8a* and *grip2a* mRNAs are enriched in the outer section whereas particles containing *dazl* mRNA are enriched in the inner section. Brackets indicate comparisons evaluated for statistical significance, with green and red bracket colors corresponding to FISH label. Asterisks indicate statistical significance according to a Comparing Means T-test (StatPlus), with p-values as follows: (D) p=0.02 and 0.006 for *dazl* and *wnt8a*, respectively; (E) p=0.001 and 0.07 for *dazl* and *grip2a*, respectively; (F) p=0.01 and 0.5 for *grip2a* and *wnt8a*, respectively. Scale bar in (C) represents 5µm for panels (A-C).

A more internal location for vegetal germ plasm RNPs may also facilitate their movement towards the animal pole relying on general mechanisms for the movement of ooplasm components in the early embryo. These mechanisms are currently unknown, although they may be related to those driving animally-directed ooplasmic streaming [14,15,34,35]. Consistent with this idea, our results indicate that mediolateral transport of *dazl* RNPs towards the animal pole is affected by inhibition of the actin cytoskeleton, itself known to be required for ooplasmic streaming [35]. Our results do not rule out alternative possibilities, for example that cortical actin anchors *dazl* RNPs as they are transported towards the animal pole. Our observation that the latrunculin A, known to act by making actin monomers unavailable for polymerization, suggests that dynamic F-actin changes, including filament growth, are required for this process.

In contrast to F-actin inhibition, we also find that inhibition of microtubule function, which interferes with transport of injected beads as markers for dorsal determinants,[7] does not affect animally-directed cortical transport of *dazl* RNPs. Thus, the available data show a correlation for cortical depth and long-range transport cytoskeletal requirement, with dorsal factors using microtubule-based system in the outer cortex, and PGC factors a more internal F-actin-dependent process. However, current studies lack an adequate number of endogenous factors as markers for long-range transport, which would be required to validate these conclusions.

Interestingly, even within the cortical most region we find that *wnt8a* RNA- and *grip2a* RNA-containing particles are distinct, suggesting the presence of multiple type of particles and potentially different mechanisms for asymmetric transport even within the outer cortex. The shift of the entire cortical region through a cortical rotation-like

mechanism would insure that all factors of the cortex move coordinately, even if present in different particles. Differences in the cellular anatomies of zebrafish and *Xenopus* eggs and early embryos suggest, however, that a cortical rotation-like process in these two species may not be entirely analogous. In particular, the specialized cortex at the animal pole of the teloblastically-cleaving teleost zygote, from which the blastodisc forms [36], may impose restrictions on global cortical displacement, restrictions that may not be present in the meroblastically-cleaving amphibian zygote. It is possible that a cortical rotation movement in zebrafish occurs locally, solely in the vegetal region. If this is the case, it is unclear how the embryo compensates for such a localized cortical shift, since there appears to be no observable morphological events that reflect such compensation. Alternatively, it is possible that the coordinated movement of vegetal RNAs and particles interpreted as a cortical rotation is in reality an *en mass* movement of such components along a more static cortex, with microtubule tracks providing a substrate for such transport. Further studies will be required to solve these questions. In spite of ambiguities on the precise mode of transport along the outer cortex, the localization of dorsal factor RNAs in the outermost cortical region is expected to facilitate their asymmetric movement.

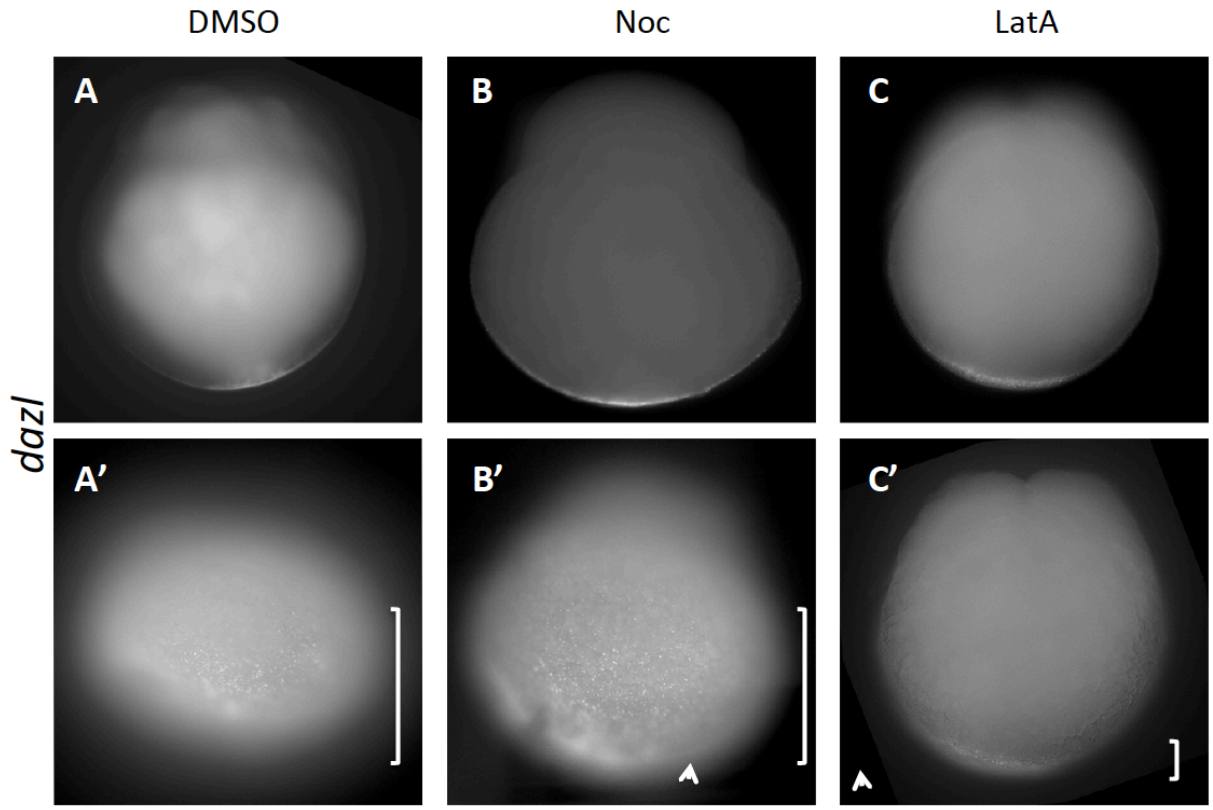

Figure 4: Fluorescent in situ hybridization to detect animally-directed movement of *dazl* RNA.

(A-A') In DMSO control embryos, *dazl* RNPs are transported toward the animal pole (67% with transport, n=12). B-B') Movement toward the animal pole appears unaffected by treatment with nocodazole (93% with transport, n=15). C-C') Injection of latrunculin A inhibits the transport of *dazl* RNPs toward the animal pole region (69% with movement inhibited, n=13; the effects of injected latrunculin A are expected to be non-uniform due to inhibition of ooplasmic movement and resulting uneven drug distribution, as has been previously observed).[19] Top and bottom panels present different focal planes of the same embryos, focusing on side edge and frontal cortex, respectively. Movement of *dazl* RNA along the cortex is best visualized in the frontal cortex (extent of RNA movement is highlighted by brackets). Nocodazole exposure was initiated at 5 mpf and latrunculin A injection was carried out at 7-12 mpf. All embryos were fixed at 60 mpf. Results are from three independent experiments, which produced similar results.

The differential localization of dorsal and germ plasm determinant RNAs with respect to cortical depth could originate during oogenesis, at a time in which RNAs become localized to the vegetal cortex. Mechanisms of RNA localization during oogenesis have been studied in greatest detail in the *Xenopus laevis* embryo [2,37,38]. In this organism, localization of vegetal RNAs in the developing oocyte occurs primarily through two sequential pathways. An early pathway mediated by the temporary association to a mitochondrial-rich structure, the mitochondrial cloud or Balbiani body, which migrates towards the vegetal pole of the forming oocyte and mediates the transport of RNAs to this region. At a later stage in oogenesis, a late pathway results in the localization of additional RNAs to the vegetal pole. Interestingly, RNAs localized via these pathways exhibit differential association to the cytoskeleton: upon egg maturation and activation RNAs localized by the early pathway remain anchored to the cytoskeleton, whereas RNAs localized via the late pathway are released into the vegetal cytoplasm [39]. In zebrafish, *wnt8a*, *grip2a* and *dazl* RNAs localize to the vegetal pole during oogenesis through a mechanism dependent on the mitochondrial cloud [12,13,40,41] and thus potentially analogous to the *Xenopus* early localization pathway. These zebrafish RNAs are temporarily localized through similar dynamics by first temporary enrichment at the mitochondrial cloud and subsequently vegetal cortex localization in the mature oocyte.

Three-dimensional ultrastructural analysis has shown that various components of the *Xenopus* vegetal cortex occupy different subdomains within a larger structure. For example, RNA for the *Xenopus* homologue of zebrafish *nanos*, *Xcat2*, is a component of germ plasm granules, whereas *Xdazl* and *wnt11* RNAs are found in the matrix between germ plasm granules [42]. In the zebrafish vegetal cortex, *wnt8a* and *dazl* RNAs exhibit

localization confined to discrete RNP units, whereas *grip2a* RNAs is more diffuse though also exhibiting spatial enrichments. Reminiscent of ultrastructural domains in *Xenopus*, we find that RNAs in the early zebrafish vegetal cortex exhibit mutually exclusive localization. It is possible that differences in the cortical depth localization of these RNAs in the early embryo are established during oogenesis and/or egg maturation via independent sets of particles and localization signals. Alternatively, cortical depth localization differences may arise after egg activation, possibly due to differential anchoring of RNPs to the outermost cortex, reminiscent of RNA release observed in *Xenopus* eggs [39]. Further studies will be required to test the origin of RNA cortical depth differences in the vegetal region of the early zebrafish embryo.

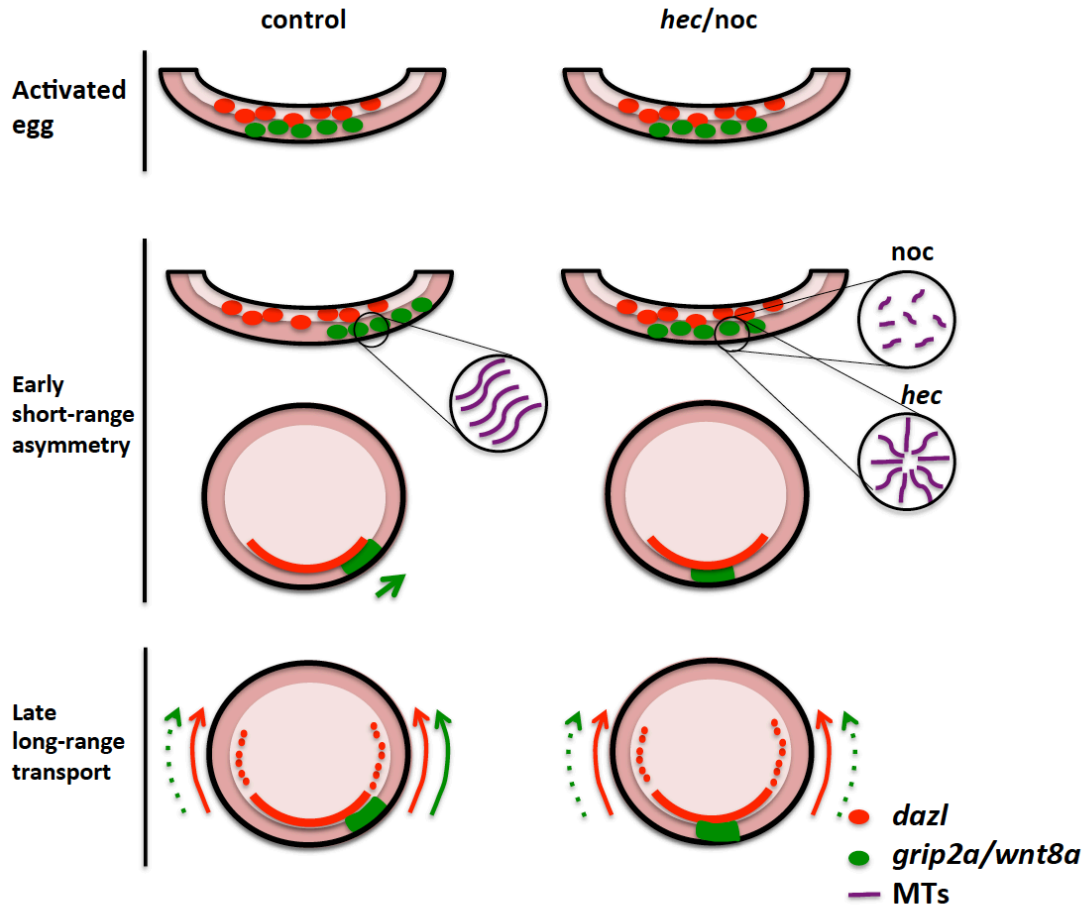

Figure 5: Cortical depth and cytoskeletal-based movements involved in axis induction and germ cell determination in the zebrafish.

Top two rows present a magnified view of the vegetal cortex, whereas the bottom two rows present embryo overviews. In the activated egg, RNAs for both dorsal-inducing factors and germ line determinants are localized to the vegetal pole at different cortical depths. Upon fertilization, microtubules become aligned into parallel bundles and mediate the off-center movement of outer cortex components with respect to the central core (green short arrow). The differential cortical depth of dorsal (*wnt8a*, *grip2a*, in the outer cortex) and germ line (*dazl*, in a more internal layer) RNAs is coupled to this cortical movement and together these processes contribute to a differential transport: dorsal factor RNAs are transported to generate an early, short-range asymmetry, whereas germ line RNAs remain in a symmetric pattern. Three situations concerning the vegetal cortex microtubule (MT) array reorganization at 20 mpf are presented: normal array formation in the left column, and abnormal reorganization (as in *hecate/grip2a* mutants) or microtubule inhibition (nocodazole-treated embryos) in the right column. Long arrows in the bottom row represent the subsequent paths of long-range factor movement by general transport mechanisms: F-actin-dependent transport of germ cell factors in more internal layers (red arrows) and microtubule-dependent transport of dorsal factors in the outermost cortex (green long arrows) [7,13]. Stippled arrows represent long-range transport system that are competent but nevertheless do not contribute to actual factor transport due to the spatial factor distribution resulting from upstream events in the pathway.

The association of germ cell and axial identity is a common occurrence in animal embryonic development, as exemplified by studies in *Drosophila* [43,44], *C. elegans* [45] and *Xenopus* [46,47]. Moreover, there appears to be functional overlap between factors involved in these processes. For example, the germ cell specification factors *Xenopus dead end* and zebrafish *grip2a* have been shown to be involved in the vegetal cortex microtubule reorganization required for axis induction [13,48]. Such shared localization pathways and functional links may be reflective of an ancestral developmental mechanism to insure the coordination of two of the most important decisions in the early embryo, patterning of the main body axis and generation of the germ line [49]. However, this coordinated process also needs to be properly regulated to allow its divergence into separate cell determination pathways in the embryo. Our studies reveal specific RNA localization sub-patterning features at the vegetal cortex, including distinct RNP composition and cortical depth localization, which together with a cortical shift transport system facilitate uncoupling two key patterning processes, dorsal induction and germ cell specification.

3.5. Materials & Methods

3.5.1. Animal husbandry and embryo collection

All zebrafish were handled in strict accordance with good animal practice as defined by the relevant national and/or local animal welfare bodies, and all animal work was approved by the appropriate committee (University of Wisconsin-Madison assurance number A3368–01). Fish stocks were raised and maintained under standard conditions at 28.5°C. Wild type fish were mated and embryos synchronized by collection within 5 minutes of fertilization, and allowed to developed in E3 embryonic medium (E3) [23].

3.5.2. Drug treatment: Nocodazole was prepared as a 5 mg/ml stock in DMSO and used at 1μg/ml after dilution in embryonic medium. For nocodazole treatment, embryos were collected and treated by immersion at approximately at 5 mpf in the drug solution. Latrunculin A was prepared as a 1 mg/ml stock in DMSO and this stock was diluted to 30μg/ml in embryonic medium immediately prior to injection, and 1 nl of diluted drug solution was injected into one-cell embryos between 7-12 mpf.

3.5.3. Whole mount in situ hybridization (WMISH) and Fluorescent in situ hybridization (FISH): WMISH labeled by the standard blue, visible substrate was performed as previously described [24], using digoxigenin-labeled antisense RNA probes against *wnt8a* [25], *dazl* [26] and *grip2a* [13]. For dual-label FISH, embryos were labeled using a digoxigenin antisense RNA probe for the genes *wnt8a* and *dazl* and detected using anti-DIG-peroxidase antibody (1:1000) and Alexa-488 Tyramid (1:50), and a fluorescein-labeled antisense RNA probe for the *grip2a* gene and detected using TSA fluorescein-POD antibody (1:5000) and tyrosine-fluorescein (1:50). The FISH procedure was carried out as described in ZFIN protocol for multiple channel fluorescent RNA in situ hybridization. Isolation of the vegetal cortex region was carried out by manually dissecting fixed embryos with fine forceps to produce vegetal cortex halves. These vegetal cortex fragments were subsequently processed using the dual label FISH procedure.

3.5.4. Imaging and quantitation

WMISH embryos were imaged using a Leica EC3 camera and analyzed with Leica Acquire software. FISH embryos were analyzed by taking vegetal Z-stack images of labeled cortical fragments using a Zeiss 510 confocal LSM by acquiring 100 slices of 0.09 micron thickness

spanning the cortical-most 9 micron section from the surface. The resulting images were analyzed using FIJI software. 2-D images were obtained by Z-projection of all slices. 3-D renderings were generated using the 3D viewer plugin in FIJI. Quantification was obtained by binning sections from the Z-stacks into three sub-regions of equivalent thickness according to the distance from the cortex, corresponding to 0 – 2.997 microns (most cortical), 3.087 – 5.994 microns (intermediate) and 6.084 - 9 microns (most internal). Z-stacks for each of these sub-regions were used to generate a partial 3-D rendering, in which particles were manually counted. Particles that spanned partial 3-D renderings for two adjacent sub-regions were counted only in the sub-region that contained the greater fraction of the particle, after side-to-side comparisons of the partial 3-D renderings.

3.6. Acknowledgements

We thank all members of the Pelegri Lab for feedback during various stages of this project. We particularly thank Andrew Hasley for help with statistical analysis. This work was supported by NIH grant RO1GM065303 to F.P with a diversity supplement to E.W.

3.7. References

1. Sive HL. The frog prince-ss: a molecular formula for dorsoventral patterning in Xenopus. Genes Dev 1993; 7:1-12.
2. Houston DW. Cortical rotation and messenger RNA localization in Xenopus axis formation. WIREs Dev Biol 2012; 1:371-388.
3. Gerhart J, Danilchik M, Doniach T, Roberts S, Rowning B, Steward R. Cortical rotation of the Xenopus egg: consequences for the anteroposterior pattern of embryonic dorsal development. Development 1989; Supplement:37-51.

4. Schneider S, Steinbeisser H, Warga RM, Hausen P. ß-catenin translocation into nuclei demarcates the dorsalizing centers in frog and fish embryos. Mech Dev 1996; 57:191-198.
5. Larabell CA, Torres M, Rowning BA, Yost C, Miller JR, Wu M, Kimelman DT, Moon RT. Establishment of the dorsoventral axis in Xenopus embryos is presaged by early asymmetries in ß-catenin that are modulated by the Wnt signalling pathway. J Cell Biol 1997; 136:1123-1134.
6. Petersen CP, Reddien PW. Wnt signaling and the polarity of the primary body axis. Cell 2009; 139:1056-1058.
7. Jesuthasan S, Strähle U. Dynamic microtubules and specification of the zebrafish embryonic axis. Curr Biol 1997; 7:31-42.
8. Mizuno T, Yamaha E, Kuroiwa A, Takeda H. Removal of vegetal yolk causes dorsal deficiencies and impairs dorsal-inducing ability of the yolk cell in zebrafish. Mech Dev 1999; 81:51-63.
9. Ober EA, Schulte-Merker S. Signals from the yolk cell induce mesoderm, neuroectoderm, the trunk organizer, and the notochord in zebrafish. Dev Biol 1999; 215:167-181.
10. Tran LD, Hino H, Quach H, Lim S, Shindo A. Mimori-Kiyosue Y, Mione M, Ueno N, Winkler C, Hibi M, Sampath K. Dynamic microtubules at the vegetal cortex predict the embryonic axis in zebrafish. Development 2012; 139:3644-3652.
11. Nojima H, Rothhämel S, Shimizu T, Kim C-H, Yonemura S, Marlow FL, Hibi M. Syntabulin, a motor protein linker, controls dorsal determination. Development 2010; 137:923-933.
12. Lu F-I, Thisse C, Thisse B. Identification and mechanism of regulation of the zebrafish dorsal determinant. Proc Natl Acad Sci USA 2011; 108:15876-15880.
13. Ge X, Grotjahn D, Welch E, Lyman-Gingerich J, Holguin C, Dimitrova E, Abrams EW, Gupta T, Marlow FL, Yabe T, Adler A, Mullins MC, Pelegri F. Hecate/Grip2a acts to reorganize the cytoskeleton in the symmetry-breaking event of embryonic axis induction. PLoS Genet 2014; 10:e1004422.
14. Fernández J, Valladares M, Fuentes R, Ubilla A. Reorganization of cytoplasm in the zebrafish oocyte and egg during early steps of ooplasmic segregation. Dev Dyn 2006; 235:656-671.
15. Fuentes R, and Fernández J. Ooplasmic segregation in the zebrafish zygote and early embryo: pattern of ooplasmic movements and transport pathways. Dev Dyn 2010; 239:2172-2189.
16. Maegawa S, Yamashita M, Yasuda K, Inoue K. Zebrafish DAZ-like protein controls translation via the sequence 'CUUC'. Genes Cells 2002; 7:971-984.
17. Suzuki H, Maegawa S, Nishibu T, Sugiyama T, Yasuda K, Inoue K. Vegetal localization of the maternal mRNA encoding an EDEN-BP/Bruno-like protein in zebrafish. Mech Dev 2000; 93:205-209.
18. Hashimoto Y, Maegawa S, Nagai T, Yamaha E, Suzuki H, Yasuda K, Inoue K. Localized maternal factors are required for zebrafish germ cell formation. Dev Biol 2004; 268:152-161.
19. Theusch EV, Brown KJ, Pelegri F. Separate pathways of RNA recruitment lead to the compartmentalization of the zebrafish germ plasm. Dev Biol 2006; 292:129-141.

20. Yoon C, Kawakami K, Hopkins N. Zebrafish vasa homologue RNA is localized to the cleavage planes of 2- and 4-cell-stage embryos and is expressed in the primordial germ cells. Development 1997; 124:3157-3165.
21. Kimmel C, Ballard WW, Kimmel SR, Ullmann B, Schilling TF. Stages of embryonic development in the zebrafish. Dev Dyn 1995; 203:253-310.
22. Eno C, Pelegri F. Gradual recruitment and selective clearing generate germ plasm aggregates in the zebrafish embryo. Bioarchitecture 2013; 3:125-132.
23. Brand M, Granato M, Nüsslein-Volhard C. Keeping and raising zebrafish, in *Zebrafish - A Practical Approach*, C. Nüsslein-Volhard and R. Dahm, Editors. 2002, Oxford University Press: Oxford. p. 7-37.
24. Thisse C, Thisse B. High-resolution in situ hybridization to whole-mount zebrafish embryos. Nature Methods 2008; 3:59-69.
25. Lekven AC, Thorpe CJ, Waxman JS, Moon RT. Zebrafish wnt8 encodes two wnt8 proteins on a bicistronic transcript and is required for mesoderm and neuroectoderm pattterning. Dev Cell 2001; 1:103-114.
26. Maegawa S, Yasuda K, Inoue K. Maternal mRNA localization of zebrafish DAZ-like gene. Mech Dev 1999; 81:223-226.
27. Gerhart JC. Mechanisms regulating pattern formation in the amphibian egg and early embryo, in *Biological Regulation and Development*, R.F. Goldberg, Editor. 1980, Plenum Press: New York. p. 133-150.
28. Elinson RP, Rowning B. Transient array of parallel microtubules in frog eggs: potential tracks for a cytoplasmic rotation that specifies the dorso-ventral axis. Dev Biol 1988; 128:185-197.
29. Houliston E, Elinson RP. Evidence for the involvement of microtubules, ER, and kinesin in the cortical rotation of fertilized frog eggs. J Cell Biol 1991; 114:1017-1028.
30. Houliston E, Elinson RP., Patterns of microtubule polymerization relating to cortical rotation in *Xenopus laevis* eggs. Development 1991; 112:107-117.
31. Ressom RE, Dixon KE. Relocation and reorganization of germ plasm in Xenopus embryos after fertilization. Development 1988; 103:507-518.
32. Köprunner M, Thisse C, Thisse B, Raz E. A zebrafish nanos-related gene is essential for the development of primordial germ cells. Genes Dev 2001; 15:2877-2885.
33. Weidinger G, Stebler J, Slanchev K, Dumstrei K, Wise C, Lovell-Badge R, Thisse C, Thisse B, Raz E. dead end, a novel vertebrate germ plasm component, is required for zebrafish primordial germ cell migration and survival. Curr Biol 2003; 13:1429-1434.
34. Leung CF, Webb SE, Miller AL. Calcium transients accompany ooplasmic segregation in zebrafish embryos. Dev Growth Differ 1998; 40:313-326.
35. Leung CF, Webb SE, Miller AL. On the mechanism of ooplasmic segregation in single-cell zebrafish embryos. Dev Growth Differ 2000; 42: 29-40.
36. Becker KA, Hart NH. The cortical actin cytoskeleton of unactivated zebrafish eggs: spatial organization and distribution of filamentous actin, nonfilamentous actin, and myosin-II. Mol Reprod Dev 1996; 43:536-547.
37. King ML, Messitt TJ, Mowry KL. Putting RNAs in the right place at the right time: RNA localization in the frog oocyte. Biol Cell 2005; 1:19-33.

38. White JA, Heasman J. Maternal control of pattern formation in *Xenopus laevis*. J Exp Zool B Mol Dev Evol 2008; 310:73-84.
39. Forristall C, Pondel M, Chen L, King ML. Patterns of localization and cytoskeletal association of two vegetally localized RNAs, Vg1 and Xcat-2*.* Development 1995; 121:201-208.
40. Howley C, Ho RK. mRNA localization patterns in zebrafish oocytes. Mech Dev 2000; 92:305-309.
41. Kosaka K, Kawakami K, Sakamoto H, Inoue K. Spatiotemporal localization of germ plasm RNAs during zebrafish oogenesis. Mech Dev 2007; 124:279-289.
42. Kloc M, Dougherety MT, Bilinski S, Chan AP, Brey E, King ML, Patrick CW Jr, ETkin LD. Three-dimensional ultrastructural analysis of RNA distribution within germinal granules of Xenopus. Dev Biol 2002; 241:79-93.
43. Lehmann R, Nüsslein-Volhard C. The maternal gene nanos has a central role in posterior pattern formation of the Drosophila embryo. Development 1991; 112:679-691.
44. Sinsimer KS, Jain RA, Chatterjee S, Gavis ER. A late phase of germ plasm accumulation during Drosophila oogenesis requires Lost and Rumpelstiltskin. Development 2011; 138:3431-3440.
45. Lyczak R, Gomes JE, Bowerman B. Heads or tails: cell polarity and axis formation in the early *Caenorhabditis elegans* embryo. Dev Cell 2002; 3:157-166.
46. Tarbashevich K, Koebernick K, and Pieler T. XGRIP2.1 is encoded by a vegetally localizing, maternal mRNA and functions in germ cell development and anteroposterior PGC positioning in *Xenopus laevis.* Dev Biol 2007; 311:554-565.
47. Colozza G, De Robertis EM. Maternal syntabulin is required for dorsal axis formation and is a germ plasm component in Xenopus. Differentiation 2014; 88:17-26.
48. Mei W, Jin Z, Lai F, Schwend T, Houston DW, King ML, Yang J. Maternal Dead-End1 is required for vegetal cortical microtubule assembly during Xenopus axis specification*.* Development 2013; 140:2334-2344.
49. Gazave E, Béhague J, Laplane L, Guillou A, Préau L, Demilly A, Balavoine G, Vervoort M. Posterior elongation in the annelid *Platynereis dumerilii* involves stem cells molecularely related to primordial germ cells. Dev Biol 2013; 382:246-267.

Chapter 4: Zebrafish *too much information*/prc1-like is required for cytokinesis during meiosis, early embryonic mitoses and for vegetal microtubule reorganization during axis induction

[2]Nair, S*, [1]Welch, E.L.*, [1]Pelegri, F.

* shared first authorship

1. Laboratory of Genetics, University of Wisconsin-Madison, Madison, WI, USA

2. Tata Institute of Fundamental Research, Department of Biological Sciences, Mumbai, India

Correspondence to: Francisco Pelegri at fjpelegri@wisc.edu 608-265-9286

Author contribution: Elaine Welch performed the experiments and wrote the first draft of the manuscript.

4.1. Abstract

In this study we identified and characterized the zebrafish maternal-effect mutation *too much information (tmi*) and show that it corresponds to Prc1-like, a zebrafish homolog of mammalian PRC1 and budding yeast Ase1, shown to be midbody-associated proteins. Embryos from Prc1l homozygous mutant mothers display a defect in cytokinesis as evident by the lack of a cleavage furrow in the early embryo and failed extrusion of the polar body during meiosis. Surprisingly, we found that *tmi* mutant embryos fail to organize microtubules at the vegetal cortex into parallel bundles. Our data suggest that *tmi/prc1l* is not only required for cytokinesis but also required for vegetal pole microtubule reorganization involved in axis induction.

4.2. Introduction

Cytokinesis involves the assembly and constriction of an actomyosin ring that gives rise to a transient intracellular bridge known as the midbody [1], [2]. The midbody forms as the cleavage furrow closes, and eventually bundles the central spindle microtubules. The midbody is home to several spindle and chromosome-derived proteins that are compacted at the center of the intercellular bridge [1], which previously corresponded to the spindle midzone. Though initially thought of only a remnant of the meiotic spindle, recent studies have shown that the midbody has active roles in cell cycling and determination, such as regulated roles in coordinating the transition from mitosis to G1 of the cell cycle [1], a novel role in primary ciliogenesis [3] and an association with the pluripotency state [4].

Midzone assembly occurs during the metaphase to anaphase transition, at the time when the cleavage furrow initiates [5]. The midzone, also referred to the central spindle, is

the site of localization to many proteins that play important roles in cell division for successful cleavage furrow positioning and membrane abscission during cytokinesis. Some of these factors include kinesin-like motors, chromosomal passenger proteins, kinases, phosphatases and the spindle midzone bundling protein PRC1 [6]–[9]. Several studies in higher eukaryotes have shown that kinesins are important for spindle assembly and function, chromosome segregation, mitotic checkpoint and cytokinesis [10]–[12]. One such kinesin, MKLP-1, was reported to play a role in regulating midzone-midbody formation and cytokinesis in various organisms [9], [13]. Another study reported that kinesin-like protein 3A (Kif4) translocates PRC1 to the plus ends of interdigitating microtubules on the spindle during the metaphase to anaphase transition, and that phosphorylation of PRC1 by Cdk controls the timing of PRC1 translocation by Kif4 [5].

Protein regulator of cytokinesis-1 (PRC1) is a part of the MAP65/Ase1/PRC1 family of microtubule-associated proteins and contains three coil-coiled domains. MAP65/Ase1/PRC1, including MAP65 (MAP65-1/2/3/4/5/6/7/8/9) from Arabidopsis, Ase1 from yeast, and PRC1 from mammals. MAP65-1 plays a role in stabilizing anti-parallel microtubules in the central spindle at anaphase to early cytokinesis, and is cell cycle regulated by phosphorylation [14]–[16]. Ase1 localizes to the midzone of the anaphase spindle [17], [18], is required for spindle assembly, elongation, stabilization, and disassembly in mitosis, and is cell cycle-regulated by the anaphase-promoting complex [19]–[21]. Mammalian PRC1 is a key regulator of cytokinesis that cross-links antiparallel microtubules at an average distance of 35 nm [22]. It is essential for controlling the spatiotemporal formation of the midzone and successful cytokinesis. PRC1 is also required

for KIF14 localization to the central spindle and midbody as well as for recruiting PLK1 to the spindle [5], [23].

The function of mammalian PRC1 is widely studied and has been shown to be important for stabilizing antiparallel microtubules at the central spindle by limiting the extent of overlap at the midzone as well as regulating spindle elongation [8], [19], [22]. It has been shown that though the mitotic spindle is not required for cytokinesis, microtubules that are assembled during anaphase are necessary for contraction of the cleavage furrow [24], [25], and PRC1 has also been identified as a CDK substrate protein essential for this transition in mammalian cells [19].

Here we describe a zebrafish maternal-effect mutation *tmi* and identify it as *prc1-like* (prc1l), a zebrafish gene with homology to mammalian PRC1. Our results indicate that Prc1l colocalizes with microtubules and has a regulatory function essential for cytokinesis during meiotic and early embryonic mitoses. Specifically, *tmi* mutants display cell division phenotypes characteristic of cytokinesis failure and meiotic and mitotic chromosome segregation defects during meiosis and early embryonic mitoses. Unexpectedly, we found that the *tmi* mutation also exhibits a haploinsufficient defect on axis induction, and that full *tmi* functional reduction results in the disruption in the parallel arrangement of vegetal microtubules required for the asymmetric segregation of dorsal determinants in the early embryo.

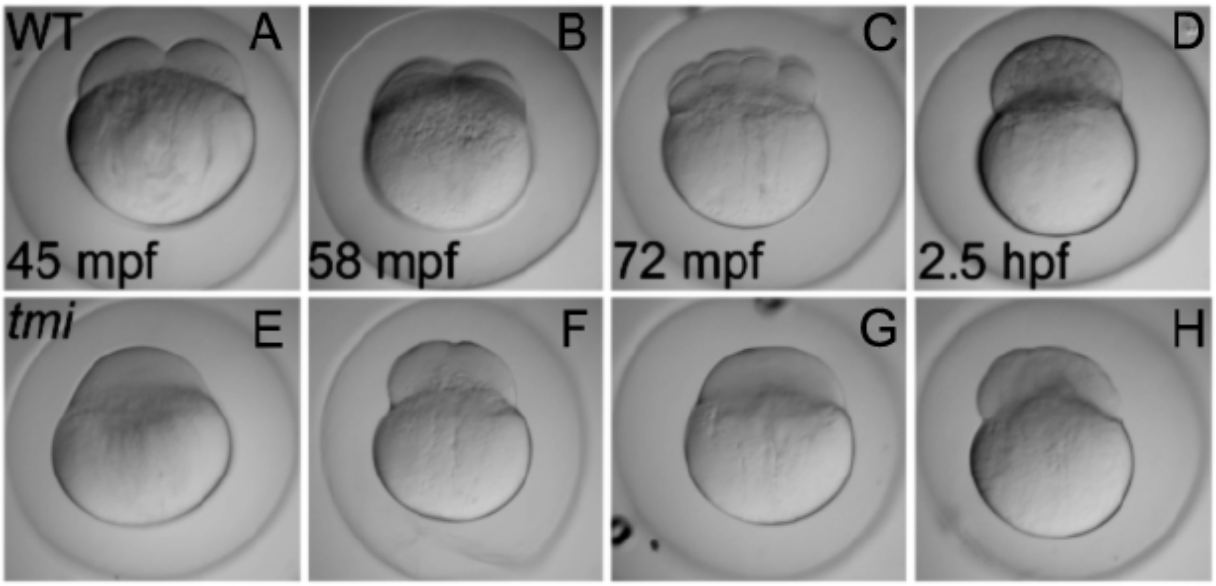

Figure 1: Phenotypic analysis of wild type and mutant embryos.

A-D) Wild type embryos at the 2, 4, 8 and 256 cell stages show proper cell division and cleavage of the blastodiscs. E-H) Similar live analysis of *tmi* mutant embryos revealed partial attempts at cytokinesis, with the cytokinesis furrows rapidly regressing, eventually resulting in an uneven blastoderm.

4.3. Results

4.3.1. A maternal effect mutation in *tmi* affects cell division and cytokinesis

The *tmi* mutation was isolated in an ENU-induced mutagenesis screen for recessive zebrafish maternal-effect genes [26], [27], and displays early cytokinesis defects in the embryo. Females that are homozygous for the *tmi* mutation mature into viable, phenotypically wild type adults; however, embryos from such females (henceforth referred to as *tmi* mutants) display cell division and cytokinesis defects that result in the formation of an acellular embryo followed by lysis around 6 hours post fertilization (hpf). Processes characteristic of egg activation, such as chorion expansion and ooplasm streaming leading to the lifting of the blastodisc, which occur during the first 30 minutes post fertilization (mpf), appear normal in *tmi* mutant embryos (data not shown). Differences between wild-type and mutant embryos begin to appear upon initiation of cell division. At approximately 45 mpf, wild type embryos have completed the first cell cycle and a furrow leading to a two cell embryo is clearly evident (figure 1A-D), and cleavage furrow corresponding to subsequent cell cycles occur every 15 minutes thereafter. In contrast, *tmi* mutant embryos show a minor indentation at the site of furrow formation but do not exhibit deepening of the furrow during cell division (figure 1F). At later stages, nuclei can be observed to accumulate, indicating the formation of an aberrant syncytium (figure 1E-H). The formation of a syncytium in *tmi* mutants is corroborated by immunolabeling of membrane markers such as ß-catenin, a component of the cell adhesion junction present in mature furrows of the early zebrafish embryo (figure 2A-D). In *tmi* mutants, localization of ß-catenin to the furrow is absent (figure 2E-H), consistent with a defect in furrow formation.

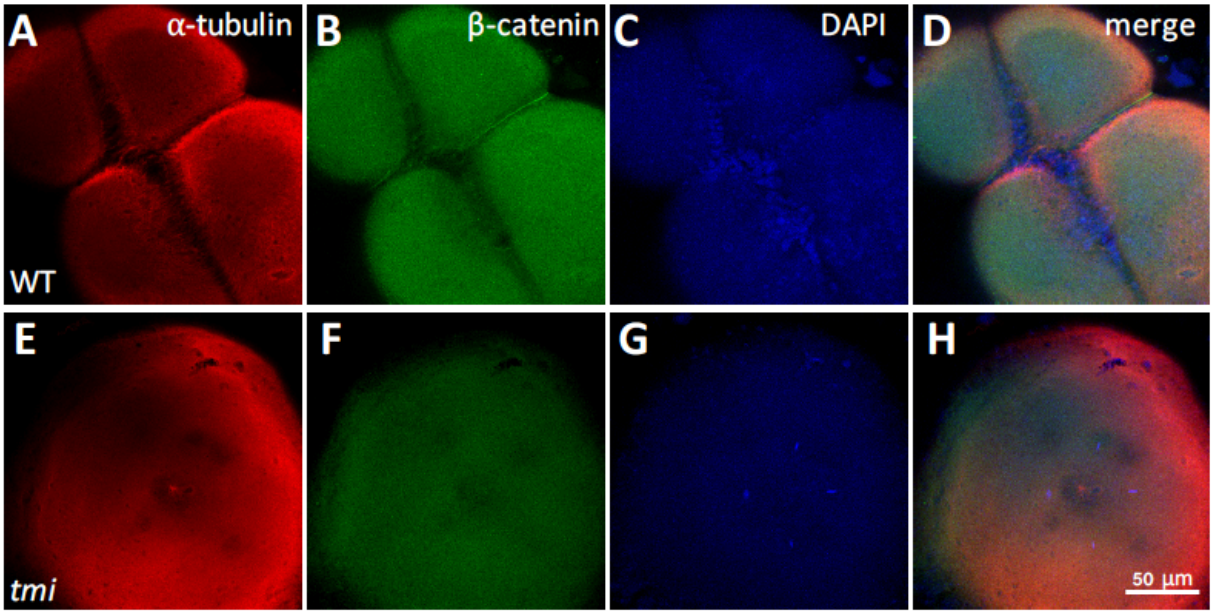

Figure 2: The membrane marker β-catenin is absent in *tmi* mutant embryos.

A-D) Embryos at the 4 cells stage show that the membrane marker β-catenin is accumulated at the cleavage furrows in wild type embryos. E-H) Acellular *tmi* mutant embryos lack the representative localization of β-catenin. Red represents microtubules labeled with alpha tubulin; Green represents β-catenin; Blue represents DAPI that labels nuclei. Scale bar in H represents 50 microns for all panels.

Immunolabeling with an antibody against alpha tubulin during the 2- to 4-cell stages revealed an array of microtubules at the furrow in wild type embryos (figure 3A-F). *tmi* mutant embryos, at the same time in development form a zone of microtubule exclusion at the site of furrow initiation (figure 3G-L), which likely corresponds to the incipient furrow observed in live embryos (figure 1F). However, these microtubules do not resolve into a fully formed furrow microtubule array (FMA), an array of microtubules parallel to each other and perpendicular to the furrow characteristic of maturing furrows [28]–[30]. Though the cells do not divide, DNA segregation appears to occur normally with the expected number of nuclei in 2- to 8-cell embryos. However, subsequent divisions show aberrant nuclei positioning, as well as nuclei exhibiting clumps of DNA (not shown).

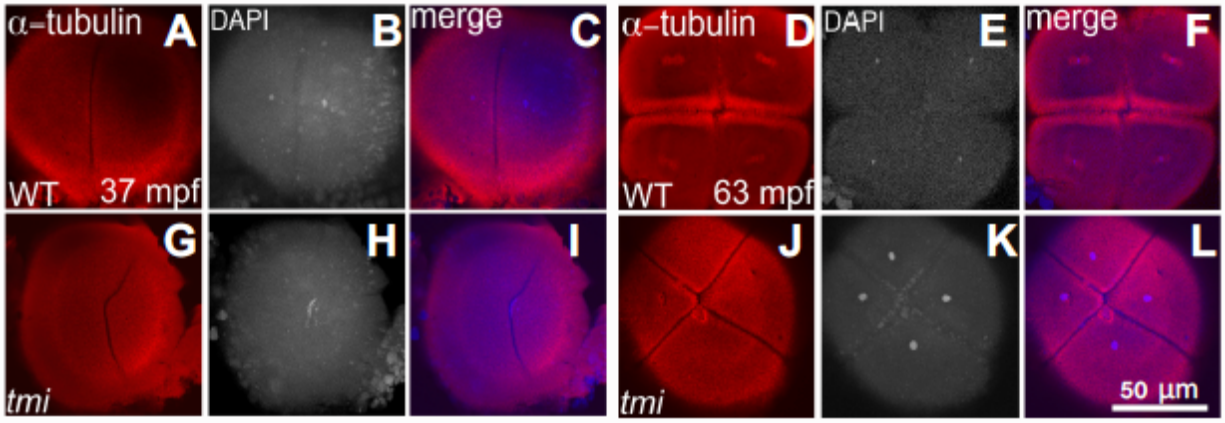

Figure 3: Furrow dynamics in wild type and *tmi* mutant embryos.

A-F) Immunolabeling for α-tubulin in 2 and 4 cell embryos revealed the presence of robust orthogonally placed cytokinetic microtubular arrays in wild type control embryos at 2 cell (A-C) and 4 cell (D-F). G-L) In *tmi* mutant embryos, cytokinetic microtubular arrays did exist as was expected from the partial cytokinesis attempts seen in live embryos. However, the microtubular arrays were positioned abnormally, bisecting each other non-othogonally in 1 cell (G-I) and 4 cell embryos (J-L). 50 micron scale bar in L is representative of fluorescent images.

4.3.2. Short spindles are characteristic of *tmi* mutant embryos

In addition to controlling the extent of overlap of antiparallel microtubules at the midzone, mammalian PRC1 has also been implicated in spindle elongation and length [31]. In addition, previous studies have shown that depletion of PRC1 by RNA interference results in two spindle halves [8]. We looked at spindle dynamics in both wild type and *tmi* embryos using antibodies against alpha-tubulin along with gamma tubulin to label centrosomes. In wild type embryos during metaphase (~45mpf), chromosomes are aligned at the metaphase plate and astral microtubules emanate from the centrosomes at each spindle pole (figure 4A-H), with kinetochore microtubules undergoing separation at anaphase when chromosomes move away from each other (figure 4I-L). In *tmi* embryos at the same time point (~45mpf), there appears to be a delay for cells to enter metaphase. At this time, mutant embryos show short and rounded monopolar spindle with one visible centrosome and decondensed DNA (figure 4A'-D'). Around 51 mpf, *tmi* mutant embryos show chromosomes aligned at the metaphase plate and two visible spindle poles as evident by the labeling of centrosomes (figure 4E'-H'). Later at around 60 mpf, chromosomes begin movement towards the poles characteristic of anaphase, spindle morphology is abnormal, with an expanded array of astral microtubules and the poles are closer to each other than wild-type (figure 4I'-L').

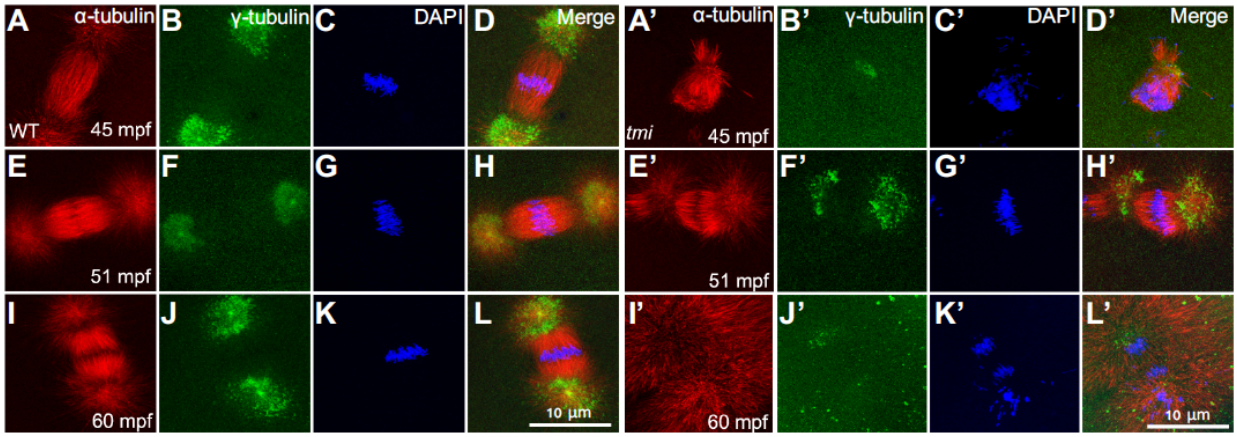

Figure 4: Mitotic spindle dynamics in wild type and *tmi* mutant embryos.

A-P) Spindles in wild type embryos at varying stages of the cell cycle are elongated and the chromosomes are properly aligned and oriented at the midzone. A'-P') Spindles in *tmi* embryos are shortened and show some missegregation of chromosomes. Centrosomes appear to be normal for the most part in *tmi* mutant embryos. Red is microtubules labeled with alpha tubulin; green in centrosome labeled with gamma tubulin; blue is DAPI labeling nuclei. 3x4 panel on the left are WT embryos and 3x4 panel on the right are *tmi* mutant embryos. Scale bar is representative of all panels.

4.3.3. *tmi* encodes Prc1-like, a maternally-expressed protein of the Microtubule-associated protein (MAP65/ASE1) family

Positional cloning of *tmi* using Simple Sequence Length Polymorphism (SSLP) mapping linked the mutation to linkage group 21 in the vicinity of three markers z25665, z65461 and z9233. Recombination frequencies for markers polymorphic in available segregation crosses were 3/268 for z25665, 0/132 for z65461 and 21/52 for z9233. The varying numbers of individual recombinants for each marker is due to the genomic region of interest being non-polymorphic in some of the mapping families that were raised. A candidate gene strategy guided by the *tmi* phenotype led to seven candidate genes: sfswap, FYN binding protein, MOZART, mitotic spindle organizing protein 2B, smarcb1b and two novel proteins zgc:193801 and zgc:86764 in a ~20Mb region spanning the three linked SSLPs. Full length cDNAs for each of the seven candidate genes were cloned from mature eggs of wild type and *tmi* homozygous females and sequenced to identify a potential lesion. Amongst the seven candidate genes sequenced, only one zgc:86764 revealed the presence of a potential causative mutation. zgc:86764, located in linkage group 21, encodes a novel protein belonging to the Microtubule Associated Protein (MAP65/ASE1) family, also known as Protein Regulator of Cytokinesis 1 (PRC1). zgc:86764 encodes a 580 amino acid protein and sequence analysis revealed the presence of a transversion mutation that changed a T to an A resulting in the conversion of a Leucine at position 221 into a stop codon (figure 5A-C). The mutated *tmi* allele codes for a truncated *tmi* protein that lacks the C-terminal-most 350 amino acids and is likely a functional null.

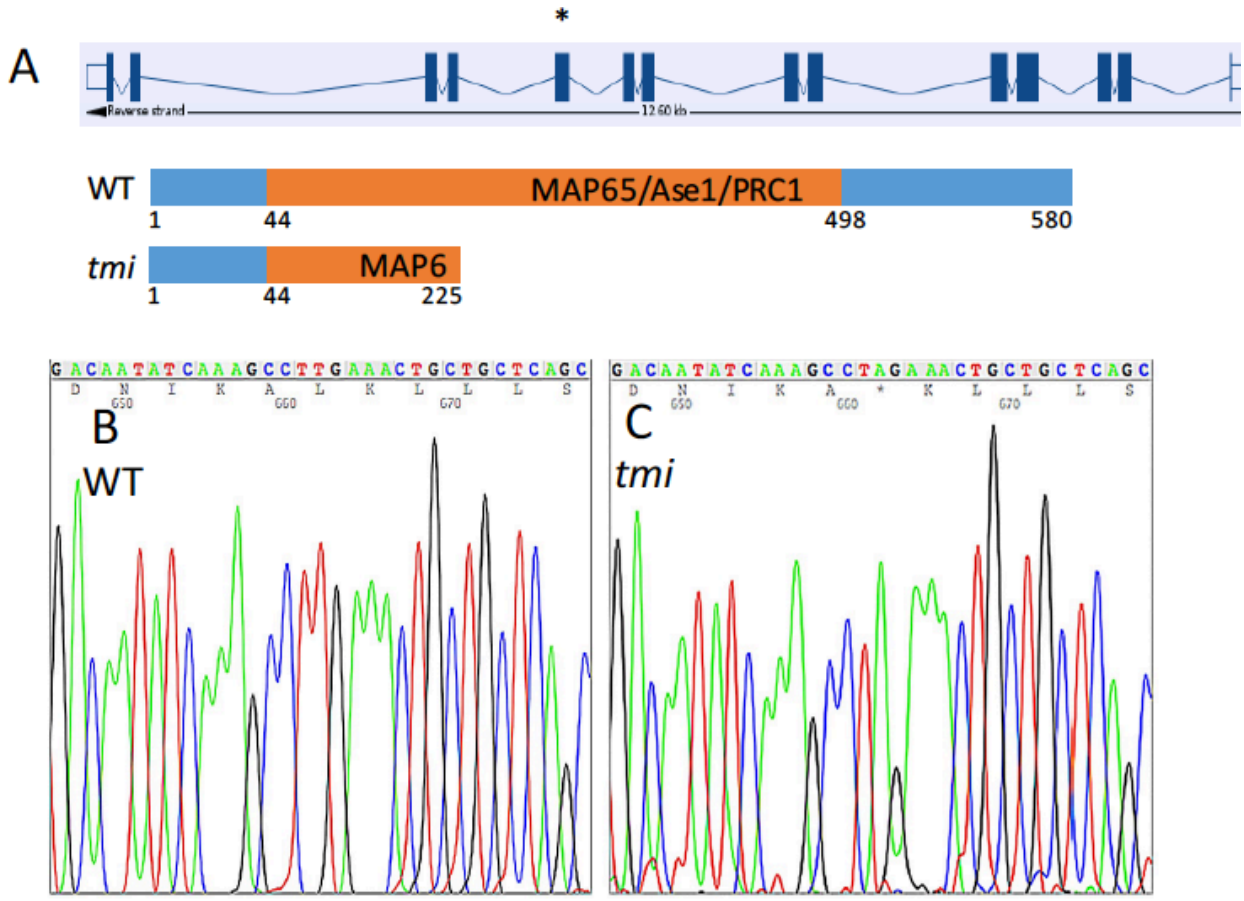

Figure 5: Genetic identity of Prc1l.

A) Diagram of the Prc1l gene containing 14 exons. The asterisk points to exon 5 where the mutation in *tmi* occurs. The schematic represents the wild type protein and the corresponding MAP/Ase1/PRC1 domain (top) and the bottom diagram shows the truncated protein affected by the nonsense mutation. Sequence chromatograms of wild type (B) and *tmi* (C) show that the leucine in wild type at position 662 has been altered in *tmi* to a stop codon (asterisk in C).

4.3.4. *tmi* is a maternal gene and mRNA is ubiquitously expressed in the blastodisc

Whole mount in situ hybridization shows prc1l RNA is evenly distributed in 1-cell to 4 cell wild-type embryos (figure 6A-D; compare to control antisense in figure 6I), with *tmi* mutant embryos exhibiting a similar pattern of expression (figure 6E-H). Quantitative real time PCR (qPCR) shows that *prc1l* is highly expressed early in development and becomes significantly reduced starting at the 64-cell stage (figure 6J). Thus *prc1l* is a maternally expressed gene.

The zebrafish genome encodes two additional paralogs of PRC1, Prc1a and Prc1b on linkage group 25 and 7 respectively. qPCR analysis revealed that both prc1a and prc1b are maternally expressed with high relative transcripts early in development and a reduction beginning at sphere stage, similar to that of prc1l and undetectable by 5 days post fertilization (Figure S1). Phylogenetic analysis comparing vertebrate species revealed that zebrafish prc1l groups with other vertebrates that have prc1l, including *Xenopus* and salmon (S 2C). Prc1a and prc1b are more closely related to human PRC1. This suggests that prc1l could be a diverged copy of prc1 that became subfunctionalized for maternal and early embryonic functions.

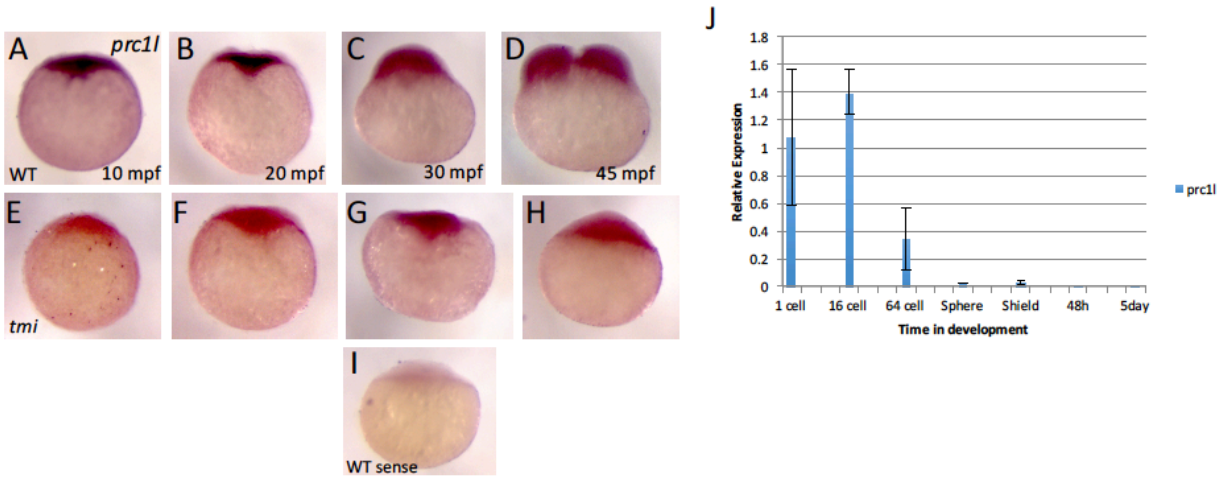

Figure 6: *prc1l* mRNA expression in wild type and *tmi* mutant embryos.

A-D) An antisense probe against *prc1l* mRNA show is being ubiquitously expressed in the blastodisc of wild type embryos beginning at 10 mpf to 45 mpf. E-H) A similar pattern is observed in *tmi* mutant embryos with ubiquitous localizaiton in the blastodisc. I) A sense probe against *prc1l* revealed no staining in the blastodisc of wild type embryos at 30 mpf. J) qRT-PCR analysis shows that *prc1l* mRNA is highly expressed in early in embryogenesis and becomes reduced later in development.

4.3.5. *tmi/prc1* mutation results in meiosis defects during zebrafish oogenesis

In addition to defects in mitotic spindle assembly, the early mitotic time course analysis consistently showed that *tmi* mutant embryos appeared to have excess DNA, which appeared as clumps of nuclei and could be derived from meiosis defects. Because *tmi* embryos do not cellularize and lack membrane partitioning components, the excess DNA might have resulted from neighboring sister blastomeres clumping together as well as the polar bodies that don't get extruded. Several factors involved in furrow formation during embryonic mitoses also play an important role in meiosis including Survivin [27] and AURKC in mammals [32]. Therefore, we assessed for potential meiosis defects in oocytes of *tmi* mutant females. Mature zebrafish eggs are arrested at metaphase of meiosis II, which can be visualized through labeling of α-tubulin and DNA. In eggs from control wild type females, at ~ 5 minutes after water activation, a robust elongated meiotic spindle with distinct sister chromatids sets can be visualized (figure 7A-C). These resolve by 20 minutes post activation (mpa) into a condensed polar body attached to a meiotic midbody and a decondensed female pronucleus which will participate in fertilization (figure 7G-O). In activated eggs from homozygous *tmi* females, a meiotic spindle was visible, but it was short and tubby, reminiscent of the mitotic spindle phenotype (figure 7D-F). By 8 mpa, this tubby spindle subsequently collapsed into a disorganized mass of α-tubulin around which the sister chromatids were unable to resolve into the polar body and pronuclear chromatin (figure 7J-L). Eventually, by 20 mpa both chromatid sets appeared to collapse into a single mass of DNA, which presumably participates in post-fertilization events resulting in the appearance of excess DNA in *tmi* mutant embryos (figure 7P-R).

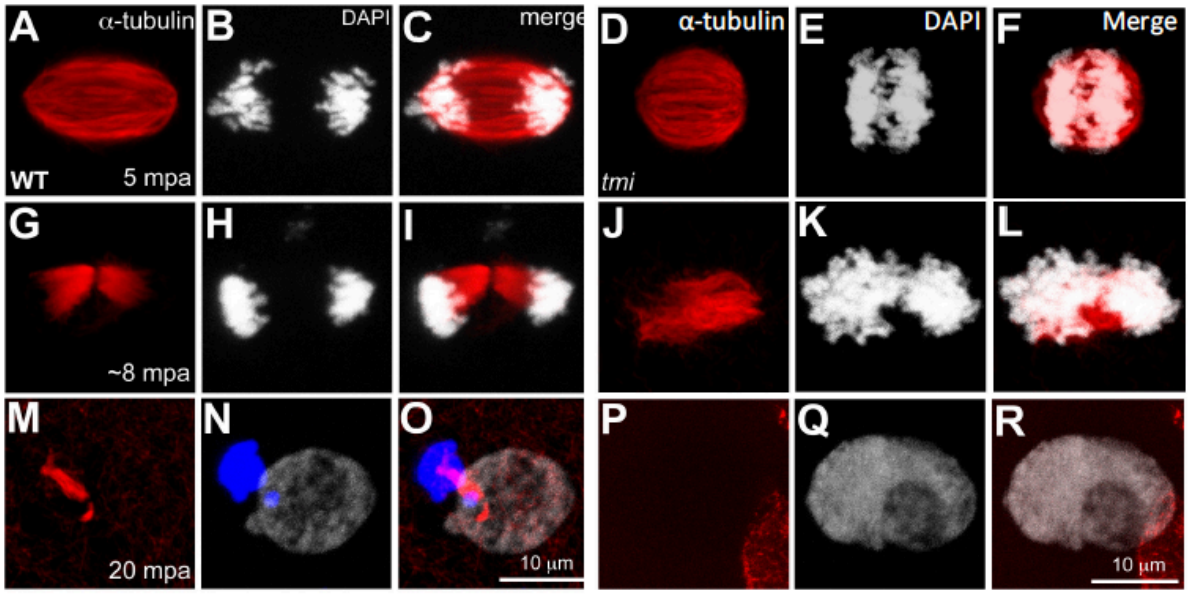

Figure 7: *tmi* mutant eggs display meiosis defects.

A-C) In water activated wild type eggs, the spindle is elongated and chromatin align at meiotic spindle poles. G-I) The meiotic spindle bundles into a nascent midbody between a set on condensing chromosomes. M-O) Chromatids resolve into a condensed polar body that is attached to the midbody and the female pronucleus. D-F) Activated eggs from *tmi* homozygous mothers show a short and tubby meiotic spindle. J-L) This tubby spindle subsequently collapsed into a disorganized mass around which chromatids are unable to form the polar body. P-R) Eventually both chromatid sets collapse into a single mass of DNA. Red labels microtubules, and white labels chromatin. The blue in N and O are polar bodies. 10 micron scale bar is representative of all panels.

4.3.6. *tmi* mutants have a disrupted furrow microtubule array

It has been shown that microtubules mediate trafficking of intracellular membranes to the furrow where they undergo exocytosis and deliver adhesion molecules to the blastomere surface [29]. Though *tmi* mutants do not form a mature furrow, the initiation of a furrow can be seen as mentioned above. During the cleavage stages in wild type embryos, a microtubule free zone appears between arrays of bundled microtubules at the incipient furrow. Since we know that microtubules are required for the localization of ß-catenin to the cleavage furrow, we wanted to examine furrow microtubule dynamics at different stages of development in both wild type and *tmi* mutant embryos. In wild type embryos antiparallel microtubules extend from both sides of the furrow and abut each other at the center of the furrow (figure 8A-P'), and these microtubules average a length of approximately 14.2 μm (figure 8S). In *tmi* mutants at the same time in development, mature furrows fail to form and these immature furrows display a disrupted furrow microtubule array as seen by a reduction in the length of microtubules at the furrow that do not make contact with each other in the center of the furrow (figure 8J-R', T). We also noticed that the zone on microtubule exclusion at the furrow is different in *tmi* mutants. In wild type embryos, the abutting microtubules at the center of the furrow forms a tight junction between the cells (figure 8A'-I'), these average approximately 1.2 μm (figure 8T); however, in *tmi* mutants, there is a much wider area between microtubules at each side of the furrow (figure 8J'-R') that averages approximately 7.8 μm in length (figure 8T). These data suggest that prc1l is important for FMA formation.

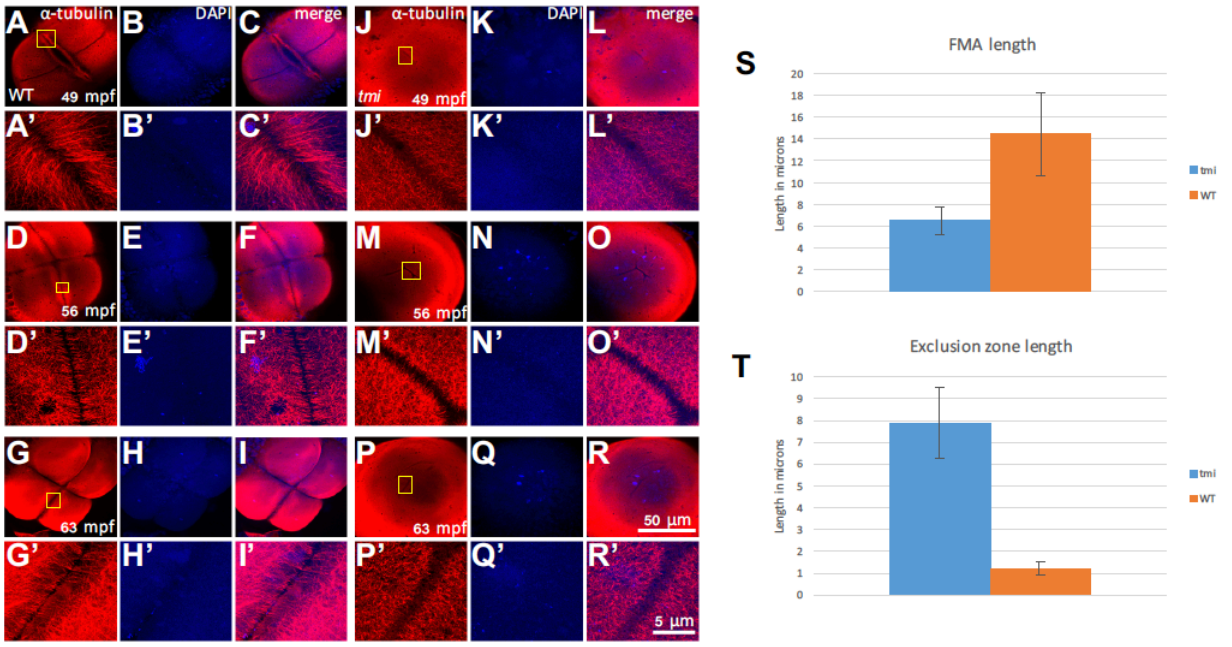

Figure 8: Dynamics of furrow microtubule array and microtubule exclusion in *tmi* and wild type embryos

A-P) Wild type embryos at 49 mpf at low magnification show a tight furrow microtubule array (FMA). Inset in A'-P' shows FMA at a higher magnification. Microtubules abut each other at the center of the furrow. J-R') *tmi* embryos do not form a proper furrow microtubule array as seen with a reduction in microtubule length (S) and the area at the center of the furrow or the microtubule exclusion zone is expanded (T). 50 micron scale bar represents all images in panels with low magnification and 5 micron scale represents all images in panels at higher magnification.

4.3.7. Localization of Prc1l protein

To determine the subcellular localization of Prc1l we raised two antibodies against parts of the Prc1l protein. One was directed against amino acids 59-102 representing the N terminus and the other was directed against amino acids 242-331 representing the middle to C terminal region. Western Blot analysis showed that both antibodies recognized a band of the expected size (67 kD) in wild type embryos that was absent in *tmi* mutant embryos (figure S2 D). For our studies, we used the antibody representing the N terminus region of Prc1l. Immunofluorescence experiments revealed that Prc1l is localized around the polar body in wild type embryos and as seen with the Western Blot and is absent in *tmi* mutant embryos. In wild type embryos at 7 mpf we can see the spindle apparatus bundling to form the meiotic midbody (figure 9A-D). By 12 mpf, the transient midbody has been fully formed and is in tight connection with the polar body, and Prc1l can be seen wrapping around the polar body (figure 9E-H). As the embryo progresses through development, the midbody becomes progressively thinner, but Prc1l remains connected to the polar body (figure 9I-P). By 27 mpf, when the midbody is no longer present, Prc1l protein is no longer detectable (figure 9Q-T). In *tmi* mutant embryos, where between 7-27 mpf the meiotic midbody is not formed and the polar bodies do not get extruded, Prc1l protein does not become localized at the animal pole (figure 9A'-T'). We have also investigated the localization of Prc1l at the cleavage furrow, at the spindle midzone and the midbody; however, Prc1l protein is only seen localized to the polar body and at the vegetal pole of the embryo with microtubules. These results suggest that Prc1l is localized at the animal pole via the polar body and is important for polar body extrusion.

4.3.8. *tmi*/Prc1l is important for vegetal microtubule reorganization

Unexpectedly, we noticed during stock propagation that a significant proportion of embryos from mothers heterozygous for the *tmi* mutant allele display a range of ventralized phenotypes (figure 10Q) similar to those described for maternal-effect mutations causing axis induction defects, such as *ichabod* [33], [34], *tokkaibi* [35] and *hecate/grip2a* [36], suggesting a role for Prc1l function in dorsoventral patterning. We reasoned that the observed defects in embryos from heterozygous *tmi* mutant mothers may be caused by haploinsufficiency for maternal Prc1l product, and that embryos with fully reduced Prc1l function, i.e. embryos from females homozygous mutant for the *tmi* allele, would exhibit strong axis induction defects. However, because the cell division defect of embryos from homozygous *tmi* mutant females precludes the development of live embryos, precluding assessing axis induction through morphological observation, we assayed instead in these embryos molecular events within the pathway of axis induction.

The process of cortical rotation is an early key process in embryo patterning and axis specification, which has long been described in the amphibian *Xenopus laevis* [37] and also more recently suggested to occur in zebrafish [36], [38], [39]. The cortical rotation takes place minutes after fertilization and depends on a parallel array of microtubules at the vegetal pole of the embryo that are required for transporting dorsal determinants from the vegetal pole to the prospective dorsal region. In wild type zebrafish embryos, these microtubules initiate alignment around 14 mpf (not shown), become fully aligned by 20 mpf (figure 10A), and start to dissociate at approximately 26 mpf (data not shown). In *tmi* mutant embryos at 20 mpf, we find that microtubules at the vegetal cortex do not become aligned into parallel bundles, but instead appear as a disorganized branched meshwork

that extends the vegetal cortex (figure 10D). Vegetal microtubules lacking parallel bundling have also been observed in *hecate/grip2a* mutants [36] (figure 10G), which also often exhibit radial arrangements [36].

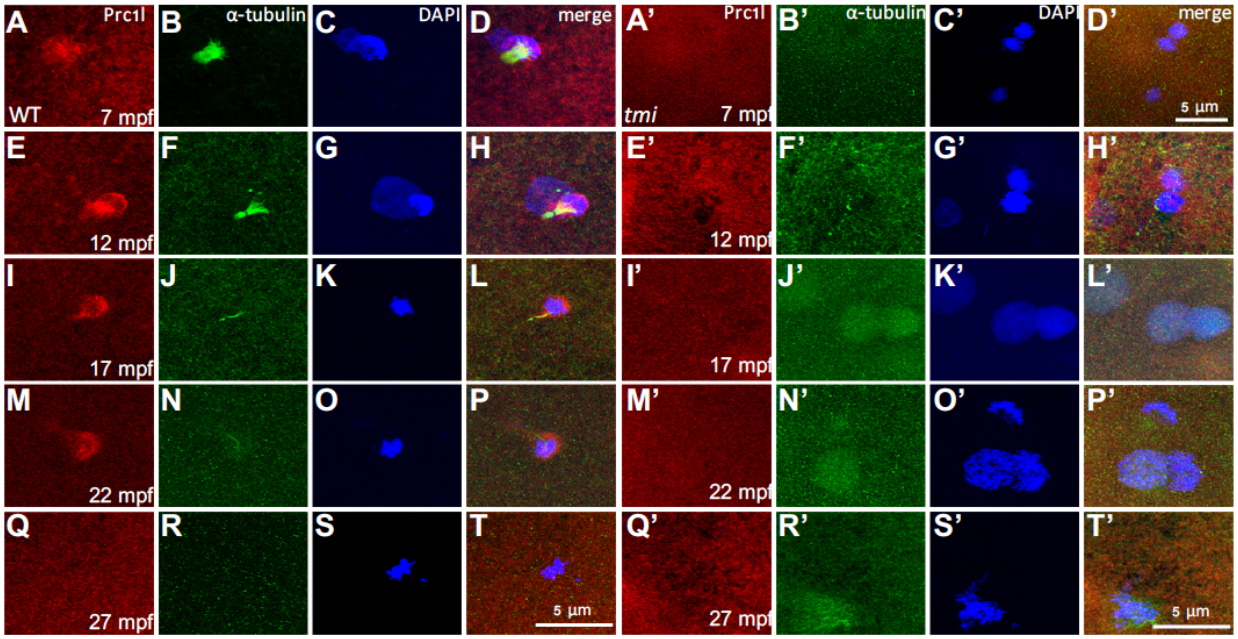

Figure 9: Subcellular localization of Prc1l in wild type and *tmi* embryos.

A-D) Prc1 is seen localized to the polar body connected to the forming midbody. E-H) At 12 mpf Prc1l is seen localized even stronger to the polar body and the midbody is fully formed. I-P) At 17 and 22 mpf Prc1l is still localized to the polar body as the midbody is becoming thinner (J). Q-T) At 27 mpf Prc1l is no longer localized (Q), the midbody has disappeared (R), and the polar body is becoming fragmented for extrusion (S). A'-T') In *tmi* embryos, Prc1l is not localized at any time, there is no midbody present and the polar bodies are not extruded. 5 micron scale bar represents all panels.

4.3.9. Short range movement of vegetally localized factors are affected in *tmi* mutant embryos

Previous studies in zebrafish has identified *wnt8a* as a vegetally localized axis-inducing determinant important for patterning the zebrafish embryo axis [40]. The mRNA for this gene is initially localized to the base of the vegetal pole and, after fertilization, undergoes a lateral shift, presumably along parallel tracks of vegetal microtubules directed towards the dorsal region. We tested whether the lateral shift of *wnt8a* RNA was affected in *tmi* mutant embryos, using whole mount in situ hybridization. Wild type embryos experience the expected asymmetric shift of *wnt8a* mRNA at 30 and 60 mpf toward the dorsal region (figure 10B-C). However, *tmi* mutant embryos fail to exhibit off-center movement *wnt8a*, which remains instead anchored to the base of the vegetal pole in embryos at 30 and 60 mpf (figure 10E-F). This lack of lateral shift upon egg activation is similar to that observed in *hecate/grip2a* mutants [36] (figure 10H-I). Thus Prc1l function is essential for the lateral displacement of dorsal determinants likely through a role in the reorganization of microtubules into parallel bundles.

4.3.10. Prc1l is localized along vegetal microtubule tracks

Given the unexpected role for Prc1 function in axis induction we investigated Prc1l protein localization in microtubules at the vegetal cortex. Immunolocalization studies within this region revealed that Prc1l protein is localized along parallel tracks of microtubules in a distinct repeated pattern (figure 10J-P). Together these data indicate that

Prc1l binds microtubules at the vegetal pole cortex, consistent with a function in their reorganization leading to the movement of dorsal determinants.

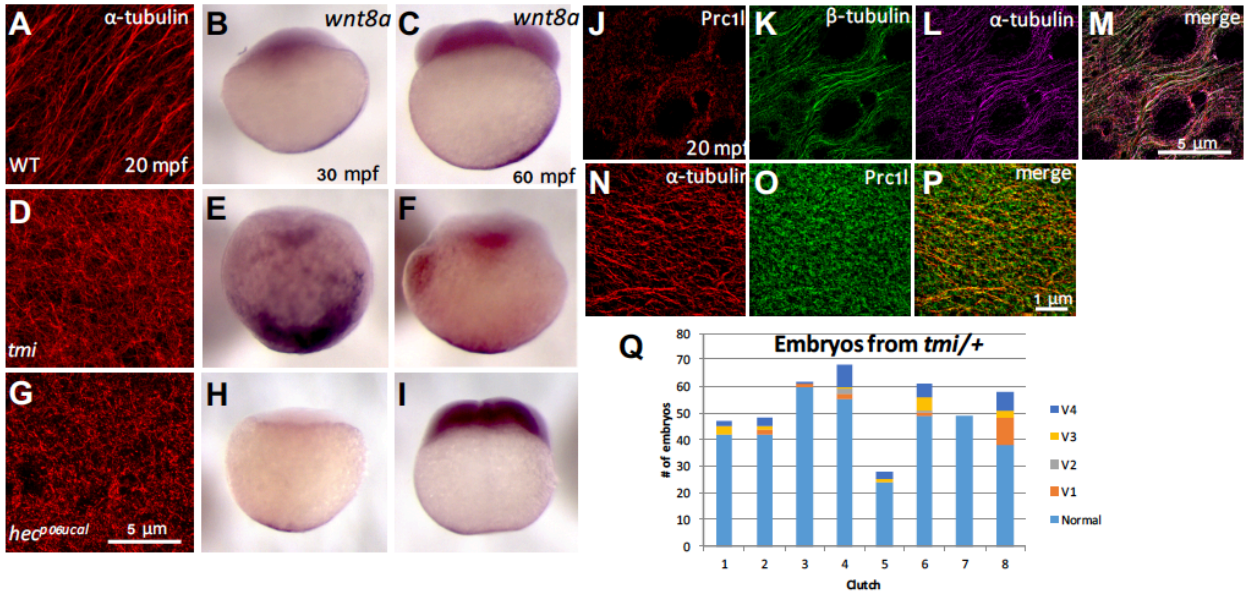

Figure 10: Vegetal microtubule reorganization, Prc1l localization and *wnt8a* movement is disrupted in *tmi* mutant embryos.

A-C) Immunostaining with alpha tubulin in wild type embryos show that microtubules are arranged in parallel bundles spanning the vegetal cortex at 20 mpf (A), and the corresponding off-center movement of *wnt8a* mRNA in embryos at 30 mpf (B) and 60 mpf (C). D-F) *tmi* mutant embryos do not display the parallel arrangement of vegetal microtubules, but instead show a branched, disorganized meshwork (D), and the off-center movement of the dorsal determinant *wnt8a* is inhibited and remains at the base of the vegetal pole at 30 mpf (E) and 60 mpf (F). G-I) *hec*^{p06ucal} mutant embryos also is defective in the parallel arrangement of vegetal cortex microtubules (G), as well as the off-center movement of *wnt8a* mRNA at 30 mpf (H) and 60 mpf at which time is becomes reduced (I) [36]. The 5 micron scale bar in G is representative of all panels on the left. J-M) Wild type embryos at 20 mpf show that Prc1l is localized along tracks of parallel microtubules at the vegetal cortex, and between alpha and beta tubulin dimers. N-P) Super resolution imaging shows Prc1l localization with microtubules. Q) Graph showing the number of embryos from *tmi* heterozygous mothers whose embryos display a variation of ventralized phenotypes.

4.4. Discussion

We have shown that prc1l is a maternally expressed gene and that the maternal effect mutation *tmi* corresponds to Prc1-like, a homolog of mammalian PRC1. Our studies indicate that Prc1l is important for meiosis, mitosis and cytokinesis in the early zebrafish embryo, and surprisingly, plays a role in vegetal microtubule reorganization and bundling necessary for dorsal axis induction. The requirement of Prc1l for the bundling and alignment of vegetal microtubules lead us to believe that Prc1l has dual functions in the embryo, at both the animal and vegetal poles. Our observations suggest that the prc1l gene may have been a result gene duplication which subsequently underwent neofunctionalization to carry out a set of specialized maternal functions. PRC1 is known to localize and bind microtubules by localizing to the spindle midzone, where it mediates antiparallel microtubule overlap, and later to the transient midbody [5], [8]. Zebrafish prc1l appears to have a similar function yet it is likely specialized for meiosis and the early mitotic divisions. The observed phenotypes in spindles structure and cytokinesis for the early embryonic mitoses indicates that Prc1l functions in spindle formation and cytokinesis, although we have insofar been unable to visualize Prc1l to the mitotic spindle midzone. We do observe Prc1l protein wrapping around the polar body, consistent with a function in polar body extrusion. Unexpectedly and contrary to PRC1's known localization with antiparallel microtubules, we also see Prc1l at the vegetal pole along parallel microtubules.

4.4.1. Domain structure

Prc1l is a member of the family of microtubule-associated proteins. It contains two coiled

coil domains toward the N terminus of the protein. Coiled coil domains have been shown to play important roles in protein-protein interactions [41] in various organisms, but their function in Prc1l is unknown. Human PRC1 has 3 coiled coil domains as well as a dimerization, spectrin and an unstructured domain [8], [42]. Research has shown that microtubule binding during mitosis correlates with the presence of the conserved central region of the protein. It was also shown that the N terminus confers midzone association and localization at the cleavage furrow, and that the nuclear localization consensus sequence is responsible for the nuclear localization during interphase [8]. Prc1l shares 40% sequence homology to PRC1. It would be worth investigating the roles of the known and other possible domains contained in Prc1in various early cellular functions.

4.4.2. Mitotic and meiotic defects of Prc1l

Meiosis and mitosis are critical steps in the cell division process and as well as cytokinesis. Successful cell division is evident in the zebrafish by the presence of a cleaving blastodisc. Cleavage has two distinct stages, the first involving an initial cortical contraction and the second involves the final separation of the cells [1], and with the loss of Prc1l as shown with *tmi* mutant embryos, all these processes are disrupted. It is possible that Prc1l may play a role in each of these events. Protein comparison across vertebrate species indicate that the mutated lysine in *tmi* homozygous mutants is highly conserved (figure S2 A) and that mutating this lysine residue has a suspected high incidence for disease (figure S2 B).

4.4.3. Role of Prc1l in microtubule reorganization and axis induction

In addition to *prc1l*, the zebrafish genome contains two other copies, namely *prc1a* and *prc1b*, potentially due to a tandem gene duplication and an additional teleost-specific duplication. Based on qPCR analysis, all three paralogs appear to be maternally enriched, becoming reduced later in embryogenesis (figure S1). The observations for prc1l are consistent with the observed phenotype of *tmi.* Prc1l is not believed to contain a microtubule-based motor domain, and its localization and potential movement along parallel microtubules is mediated by motor proteins. In mammalian cells, PRC1 is translocated by the motor protein Kif4 along the mitotic spindle to the plus ends of interdigitating microtubules [5]. We suspect that a similar mechanism occurs at the vegetal pole of the zebrafish embryo. It would also be interesting to see what role, if any, other midbody/midzone-associated proteins play in the function of Prc1l at the vegetal pole. During cell division, we know that other proteins play a role in assembling the central spindle including mitotic kinesin like protein 1 (Mklp1), which is phosphorylated by Aurora B kinase [43], [44]. Aurora B kinase also phosphorylates MgRacGAP, which serves as a critical regulator of RhoA activation and contractile ring assembly [31], [45]. Further work will determine the association of Prc1l with other proteins, as well as its specific role in bundling parallel microtubules.

4.5. Materials and methods

Ethics Statement: All animals were handled in strict accordance with good animal practice as defined by the relevant national and/or local animal welfare bodies, and all animal work

was approved by the appropriate committee (University of Wisconsin – Madison assurance number A3368-01).

Fish maintenance and genetic lines

Fish stocks were raised and maintained under standard conditions at 26.5°C. *tmi* was originally isolated from an ENU induced mutagenesis screen. Homozygous *tmi* mutant fish were identified phenotyping, or by using Locked Nucleic Acid (LNA) Endpoint genotyping method that employs 2 fluorescent probes; HEX for identification of the WT allele, and FAM for identification of the mutant allele. Mutant embryos were obtained by pairing homozygous mutant females with male siblings. Wild type controls were obtained from the AB line. Embryos were collected and allowed to develop in E3 embryonic medium until the desired stage, at which point they were fixed using 4% paraformaldehyde.

Genotyping

Fish were anesthetized with 0.014% tricaine and the tail fin was clipped using a razor blade and placed in 100µl of 50mM NaOH. Tissue lysates were incubated at 95°C for 20 minutes then cooled to 4°C for approximately 5 minutes. $1/10^{th}$ the volume of Tris HCl pH 8.0 was added to the lysate to neutralize, and centrifuged at 13k rpm for 2 minutes. A typical 10µl endpoint genotyping reaction contains 5µl primetime gene expression master mix (IDT), 1µl of 10µM forward and reverse primer mix, 0.5µl, FAM, 0.5µl HEX, DNA between 10 -25ng of genomic DNA and ddH_2O up to 10µl.

Antibody labeling

Embryos were dechorionated and fixed in paraformaldehyde and glutaraldehyde, and antibody labeling was carried out as previously described [46]. Primary antibodies used are as follows: mouse anti-Prc1l, derived from three separate peptides at the N terminus of

Prc1l, 1:400 (Abmart), mouse anti-a-Tubulin, 1:2500 (Sigma T5168), rat anti-a-Tubulin, 1:1000 (Abcam ab6161), rabbit anti B-Tubulin, 1:1000 (Abcam ab15568). Confocal microscopy images were obtained using a Zeiss LSM 510 for fixed images or Zeiss LSM 780 (for high magnification) and processed with Fiji.

in situ hybridization

Whole mount in situ hybridization, labeled by a standard blue visible substrate was carried out as described previously [47], using digoxygenin labeled antisense RNA probes against *wnt8a* and *prc1l* RNAs. To generate the *prc1l* antisense probe, the T7 promoter sequence was attached to a 20bp antisense sequence of *prc1l* cDNA via PCR; then was in vitro transcribed with the PCR product as a template using T7 polymerase and labeled with digoxygenin. A sense control probe was also designed by attaching the T7 promoter sequence to the 20bp sense cDNA sequence. These sequences were also used as primers for RT-PCR and qRT-PCR. The *wnt8a* probe was a gift from the Lekven lab, and generated by linearizing with Ap1I.

Western Blot

Approximately 200-500 embryos were collected from wild type and *tmi* mutant fish. Embryos were lysed in RIPA buffer using a 22G syringe. Lysates were centrifuges at 13K rpm for 5 minutes at 4°C to collect debris. Protein concentration was determined and 150 or 300 µg was loaded onto precast 4-15% TGX gels (BioRad) and blotted onto PVDF membranes for 1 hour at 100V at 4°C. Membranes were blocked in 5% milk and blotted

with 1:200 mouse-anti Prc1l (Abmart) and 1:5000 anti-mouse HRP (ThermoScientific). Membranes were developed using SuperSignal West Pico (ThermoScientific).

RT-PCR and qRT-PCR

Total RNA was extracted from both wild type and *tmi* embryos using TRIZOL reagent (Invitrogen). cDNA was synthesized using an oligodT primer and AMV reverse transcriptase (Promega). RT and qPCR reactions were performed with primer pairs derived from *prc1l* cDNA, 5'-CTGCCAAGAGGACCAAGACC-3' 5'-CACCGTTTGCTTTCCTGGAG-3' and using 18S as the endogenous control. Absence of genomic contamination was verified by running a no template control without cDNA. qPCR was performed in a light cycler 480 (Roche).

Prc1L cloning and rescue – fusion protein

Total RNA was extracted from both wild type and *tmi* embryos, and cDNA synthesized as mentioned above. prc1l alleles were amplified from cDNA with primers 5'-ATGATGACTTGTCGAAAAAGTGAAGCTTTGGC and 5'-GTTCTCAATTCCACTGTTAAAGATGTCCTC using Q5 high fidelity polymerase. pCS2+ containing eGFP N1 was linearized with XmaI and NcoI. Prc1l was cloned into pCS2+ containing eGFP N1 using In-Fusion HD Cloning Kit (Takara). Sense mRNA for the rescue experiment was synthesized from the Sp6 promoter using the mMessage mMachine kit (Ambion).

Prc1l cloning and rescue - CRISPR

sgRNA was designed using https://chopchop.rc.fas.harvard.edu and PCR amplified using universal primers [48], and in vitro transcribed using the MEGAscript T7 transcription Kit (Invitrogen). Plasmid #46757 pT3TS::nCas9n [49], [50] was digested with XbaI, purified and transcribed using the T3 Mmessage Mmachine kit (Ambion). Cas9 RNA and sgRNAs were injected at 100 ng/µl and 30ng/µl, respectively. Injected fish were raised and mated with wild type fish to produce the F1 generation. F1 was raised, sequenced and mated for detection of any phenotypic anomalies.

Phylogenetic Analysis

Phylogenetic tree, sequence alignment and phenotypic prediction were carried out using Phylogeny.fr [51], [52], PRALINE (CIBVU) and SuSPect [53], respectively.

4.6. Acknowledgements

We would like to thank members of the Pelegri lab for advice on this project and writing of the manuscript. This work was supported by NIH grant RO1GM065303 to F.P and NIH training grant to EW.

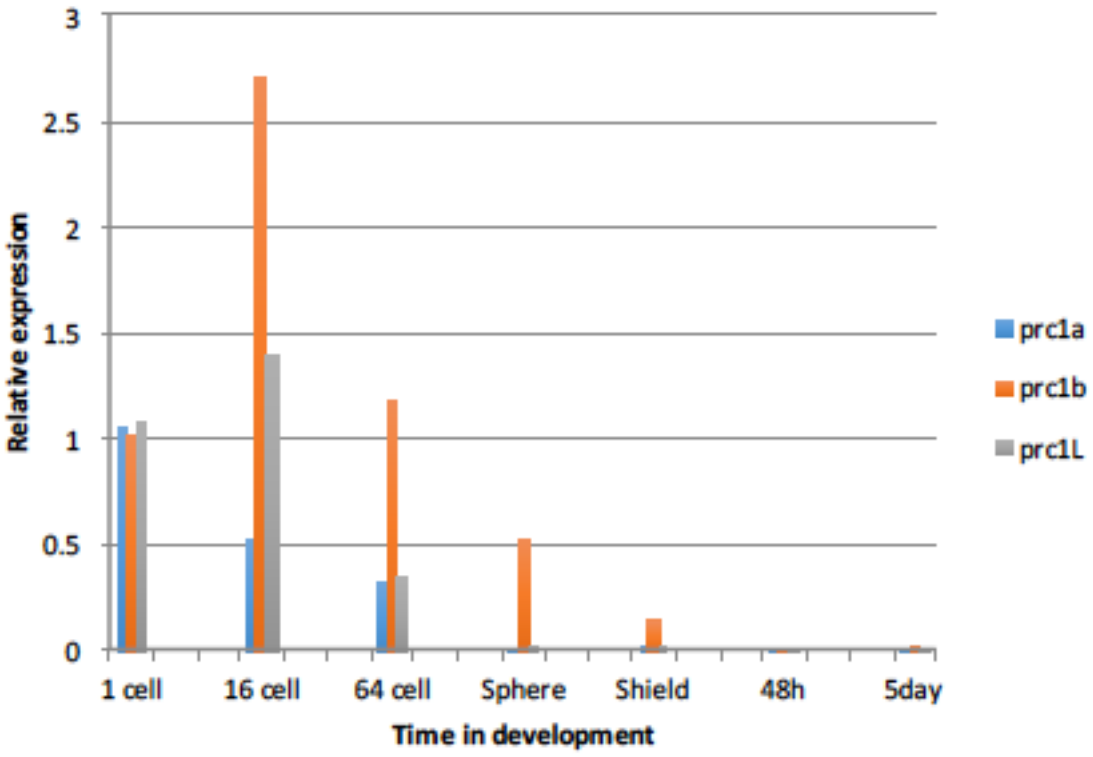

Figure S1: mRNA expression of zebrafish prc1 genes.

qPCR analysis show that all three paralogs are enriched maternally and become reduced later in development.

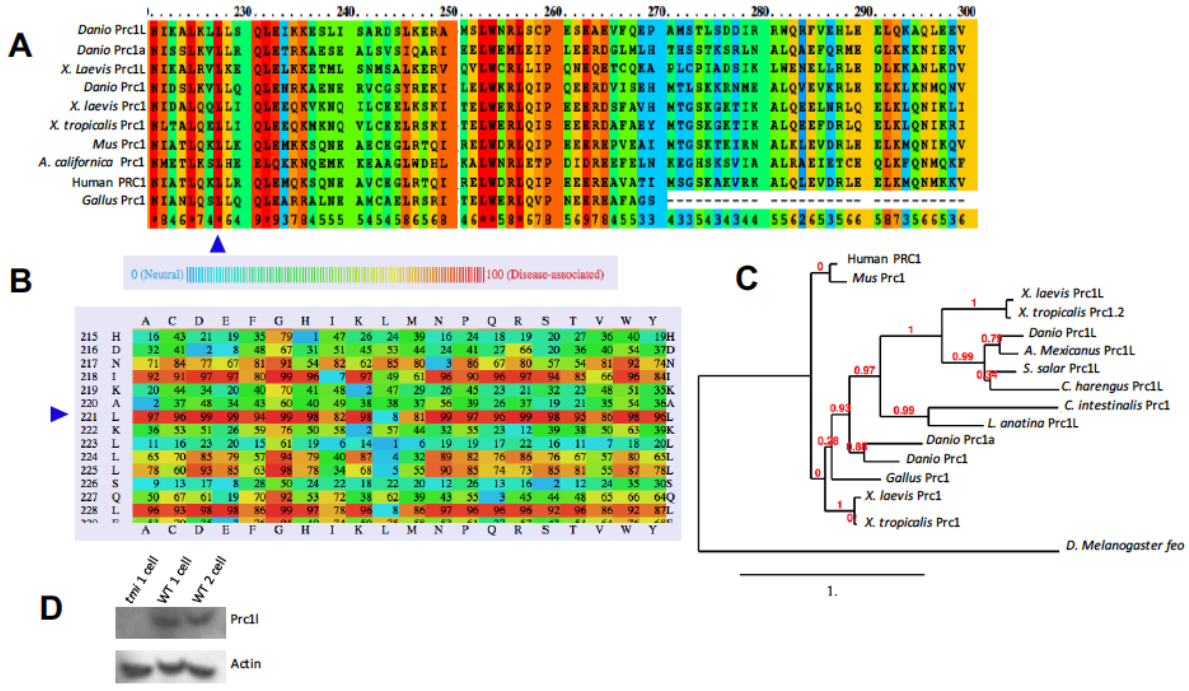

Figure S2: Sequence comparison.

A) Protein comparison across vertebrate species reveal that the leucine is a highly conserved residue. B) SusPect analysis suggest that there is a high prevalence of disease when this leucine is mutated. Blue arrowheads points to the mutated leucine residue in *tmi*. C) Phylogenetic analysis show that zebrafish prc1l clusters with other vertebrates with this gene. And prc1a and prc1b are more closely related to human PRC1. D) Western Blot analysis showed a band in wild type 1 and 3 cell embryo, which is absent in *tmi* mutant embryos.

4.7. References

[1] S. G. Zeitlin and K. F. Sullivan, “Animal cytokinesis : Breaking up is hard to do,” pp. 514–516, 2001.

[2] K. Verbrugghe and J. White, “SPD-1 Is Required for the Formation of the Spindle Midzone but Is Not Essential for the Completion of Cytokinesis in C. elegans Embryos,” *Curr. Biol.*, vol. 14, pp. 1755–1760, 2004.

[3] M. Bernabé-Rubio, G. Andrés, J. Casares-Arias, J. Fernández-Barrera, L. Rangel, N. Reglero-Real, D. C. Gershlick, J. J. Fernández, J. Millán, I. Correas, D. G. Miguez, and M. A. Alonso, “Novel role for the midbody in primary ciliogenesis by polarized epithelial cells,” *J. Cell Biol.*, vol. 214, no. 3, pp. 259–273, 2016.

[4] K. O. Schink and H. Stenmark, “Cell differentiation: Midbody remnants - Junk or fate factors?,” *Curr. Biol.*, vol. 21, no. 23, pp. R958–R960, 2011.

[5] C. Zhu and W. Jiang, “Cell cycle-dependent translocation of PRC1 on the spindle by Kif4 is essential for midzone formation and cytokinesis,” *Proc. Natl. Acad. Sci.*, vol. 102, no. 2, pp. 343–348, 2004.

[6] S. P. Wheatley, E. H. Hinchcliffe, M. Glotzer, A. A. Hyman, G. Sluder, and Y. L. Wang, “CDK1 inactivation regulates anaphase spindle dynamics and cytokinesis in vivo,” *J. Cell Biol.*, vol. 138, no. 2, pp. 385–393, 1997.

[7] R. R. Adams, M. Carmena, and W. C. Earnshaw, “Chromosomal passengers and the (aurora) ABCs of mitosis,” *Trends Cell Biol.*, vol. 11, no. 2, pp. 49–54, 2001.

[8] C. Mollinari, J. P. Kleman, W. Jiang, G. Schoehn, T. Hunter, and R. L. Margolis, “PRC1 is a microtubule binding and bundling protein essential to maintain the mitotic spindle midzone,” *J. Cell Biol.*, vol. 157, no. 7, pp. 1175–1186, 2002.

[9] M. Mishima, V. Pavicic, U. Gruneberg, E. a Nigg, and M. Glotzer, “Cell cycle regulation of central spindle assembly,” *Nature*, vol. 430, no. 7002, pp. 908–913, 2004.

[10] C. E. Walczak, T. J. Mitchison, and A. Desai, “XKCM1: A Xenopus kinesin-related protein that regulates microtubule dynamics during mitotic spindle assembly,” *Cell*, vol. 84, no. 1, pp. 37–47, 1996.

[11] B. A. A. Weaver, Z. Q. Bonday, F. R. Putkey, G. J. P. L. Kops, A. D. Silk, and D. W. Cleveland, “Centromere-associated protein-E is essential for the mammalian mitotic checkpoint to prevent aneuploidy due to single chromosome loss,” *J. Cell Biol.*, vol. 162, no. 4, pp. 551–563, 2003.

[12] G. Goshima and R. D. Vale, “The roles of microtubule-based motor proteins in mitosis: Comprehensive RNAi analysis in the Drosophila S2 cell line,” *J. Cell Biol.*, vol. 162, no. 6, pp. 1003–1016, 2003.

[13] J. Matulienė and R. Kuriyama, “Role of the midbody matrix in cytokinesis: RNAi and genetic rescue analysis of the mammalian motor protein CHO1,” *Mol Biol Cell*, vol. 15, no. 7. pp. 3083–3094, 2004.

[14] G. Mao, J. Chan, G. Calder, J. H. Doonan, and C. W. Lloyd, “Modulated targeting of GFP-AtMAP65-1 to central spindle microtubules during division,” *Plant J.*, vol. 43, no. 4, pp. 469–478, 2005.

[15] M. Sasabe and Y. Machida, “MAP65: a bridge linking a MAP kinase to microtubule turnover,” *Curr. Opin. Plant Biol.*, vol. 9, no. 6, pp. 563–570, 2006.

[16] A. P. Smertenko, H.-Y. Chang, S. Sonobe, S. I. Fenyk, M. Weingartner, L. Bögre, and P. J.

Hussey, “Control of the AtMAP65-1 interaction with microtubules through the cell cycle.,” *J. Cell Sci.*, vol. 119, no. Pt 15, pp. 3227–3237, 2006.

[17] D. Pellman, M. Bagget, H. Tu, and G. R. Fink, “Two microtubule-associated proteins required for anaphase spindle movement in Saccharomyces cerevisiae [published erratum appears in J Cell Biol 1995 Oct;131(2):561],” *J. Cell Biol.*, vol. 130, no. 6, pp. 1373–1385, 1995.

[18] Y. L. Juang, J. Huang, J. M. Peters, M. E. McLaughlin, C. Y. Tai, and D. Pellman, “APC-mediated proteolysis of Ase1 and the morphogenesis of the mitotic spindle.,” *Science*, vol. 275, no. 5304, pp. 1311–1314, 1997.

[19] W. Jiang, G. Jimenez, N. J. Wells, T. J. Hope, G. M. Wahl, T. Hunter, and R. Fukunaga, “PRC1: a human mitotic spindle-associated CDK substrate protein required for cytokinesis.,” *Mol. Cell*, vol. 2, no. 6, pp. 877–85, 1998.

[20] S. C. Schuyler, J. Y. Liu, and D. Pellman, “The molecular function of Ase1p: Evidence for a MAP-dependent midzone-specific spindle matrix,” *J. Cell Biol.*, vol. 160, no. 4, pp. 517–528, 2003.

[21] J. a Ubersax, E. L. Woodbury, P. N. Quang, M. Paraz, J. D. Blethrow, K. Shah, K. M. Shokat, and D. O. Morgan, “Targets of the cyclin-dependent kinase Cdk1.,” *Nature*, vol. 425, no. 6960, pp. 859–864, 2003.

[22] R. Subramanian, E. M. Wilson-Kubalek, C. P. Arthur, M. J. Bick, E. A. Campbell, S. A. Darst, R. A. Milligan, and T. M. Kapoor, “Insights into antiparallel microtubule crosslinking by PRC1, a conserved nonmotor microtubule binding protein,” *Cell*, vol. 142, no. 3, pp. 433–443, 2010.

[23] Y. Kurasawa, W. C. Earnshaw, Y. Mochizuki, N. Dohmae, and K. Todokoro, “Essential roles of KIF4 and its binding partner PRC1 in organized central spindle midzone formation.,” *EMBO J.*, vol. 23, no. 16, pp. 3237–3248, 2004.

[24] S. P. Wheatley and Y. L. Wang, “Midzone Microtubule Bundles Are Continuously Required for Cytokinesis in Cultured Epithelial Cells,” *J. Cell Biol.*, vol. 135, no. 4, pp. 981–989, 1996.

[25] J. C. Canman, D. B. Hoffman, and E. D. Salmon, “The role of pre- and post-anaphase microtubules in the cytokinesis phase of the cell cycle,” *Curr. Biol.*, vol. 10, no. 10, pp. 611–614, 2000.

[26] R. Dosch, D. S. Wagner, K. A. Mintzer, G. Runke, A. P. Wiemelt, and M. C. Mullins, “Maternal control of vertebrate development before the midblastula transition: Mutants from the zebrafish I,” *Dev. Cell*, vol. 6, no. 6, pp. 771–780, 2004.

[27] S. Nair, F. Marlow, E. Abrams, L. Kapp, M. C. Mullins, and F. Pelegri, “The Chromosomal Passenger Protein Birc5b Organizes Microfilaments and Germ Plasm in the Zebrafish Embryo,” *PLoS Genet.*, vol. 9, no. 4, 2013.

[28] M. V Danilchik, W. C. Funk, E. E. Brown, and K. Larkin, “Requirement for microtubules in new membrane formation during cytokinesis of Xenopus embryos.,” *Dev. Biol.*, vol. 194, no. 1, pp. 47–60, 1998.

[29] S. Jesuthasan, “Furrow-associated microtubule arrays are required for the cohesion of zebrafish blastomeres following cytokinesis.,” *J. Cell Sci.*, vol. 111 (Pt 2, pp. 3695–3703, 1998.

[30] L. E. Urven, T. Yabe, and F. Pelegri, “A role for non-muscle myosin II function in furrow maturation in the early zebrafish embryo.,” *J. Cell Sci.*, vol. 119, no. Pt 20, pp. 4342–4352, 2006.

[31] S. Shrestha, L. J. Wilmeth, J. Eyer, and C. B. Shuster, “PRC1 controls spindle polarization and recruitment of cytokinetic factors during monopolar cytokinesis.,” *Mol. Biol. Cell*, vol. 23, no. 7, pp. 1196–207, 2012.

[32] S. M. Quartuccio and K. Schindler, “Functions of Aurora kinase C in meiosis and cancer.,” *Front. cell Dev. Biol.*, vol. 3, no. August, p. 50, 2015.

[33] G. Bellipanni, M. Varga, S. Maegawa, Y. Imai, C. Kelly, A. P. Myers, F. Chu, W. S. Talbot, and E. S. Weinberg, “Essential and opposing roles of zebrafish beta-catenins in the formation of dorsal axial structures and neurectoderm.,” *Development*, vol. 133, no. 7, pp. 1299–1309, 2006.

[34] C. Kelly, a J. Chin, J. L. Leatherman, D. J. Kozlowski, and E. S. Weinberg, “Maternally controlled (beta)-catenin-mediated signaling is required for organizer formation in the zebrafish.,” *Development*, vol. 127, pp. 3899–3911, 2000.

[35] H. Nojima, S. Rothhämel, T. Shimizu, C. Kim, S. Yonemura, F. L. Marlow, and M. Hibi, “Syntabulin , a motor protein linker , controls dorsal determination,” vol. 933, pp. 923–933, 2010.

[36] X. Ge, D. Grotjahn, E. Welch, J. Lyman-Gingerich, C. Holguin, E. Dimitrova, E. W. Abrams, T. Gupta, F. L. Marlow, T. Yabe, A. Adler, M. C. Mullins, and F. Pelegri, “Hecate/Grip2a Acts to Reorganize the Cytoskeleton in the Symmetry-Breaking Event of Embryonic Axis Induction,” *PLoS Genet.*, vol. 10, no. 6, 2014.

[37] D. W. Houston, “Cortical rotation and messenger RNA localization in Xenopus axis formation,” *Wiley Interdiscip. Rev. Dev. Biol.*, vol. 1, no. 3, pp. 371–388, 2012.

[38] L. D. Tran, H. Hino, H. Quach, S. Lim, a. Shindo, Y. Mimori-Kiyosue, M. Mione, N. Ueno, C. Winkler, M. Hibi, and K. Sampath, “Dynamic microtubules at the vegetal cortex predict the embryonic axis in zebrafish,” *Development*, vol. 139, pp. 3644–3652, 2012.

[39] E. Welch and F. Pelegri, “Cortical depth and differential transport of vegetally localized dorsal and germ line determinants in the zebrafish embryo,” *Bioarchitecture*, vol. 5, no. 1–2, pp. 13–26, 2015.

[40] F. Lu, C. Thisse, and B. Thisse, “Identification and mechanism of regulation of the zebrafish dorsal determinant,” *Proc. Natl. Acad. Sci. U. S. A.*, vol. 108, no. 38, pp. 15876–15880, 2011.

[41] J. M. Mason and K. M. Arndt, “Coiled coil domains: Stability, specificity, and biological implications,” *ChemBioChem*, vol. 5, no. 2, pp. 170–176, 2004.

[42] E. H. Kellogg, S. Howes, S.-C. Ti, E. Ramírez-Aportela, T. M. Kapoor, P. Chacón, and E. Nogales, “Near-atomic cryo-EM structure of PRC1 bound to the microtubule.,” *Proc. Natl. Acad. Sci. U. S. A.*, vol. 113, no. 34, pp. 9430–9, 2016.

[43] A. Guse, M. Mishima, and M. Glotzer, “Phosphorylation of ZEN-4/MKLP1 by aurora B regulates completion of cytokinesis,” *Curr. Biol.*, vol. 15, no. 8, pp. 778–786, 2005.

[44] R. Neef, U. R. Klein, R. Kopajtich, and F. A. Barr, “Cooperation between mitotic kinesins controls the late stages of cytokinesis,” *Curr. Biol.*, vol. 16, no. 3, pp. 301–307, 2006.

[45] Y. Minoshima, T. Kawashima, K. Hirose, Y. Tonozuka, A. Kawajiri, Y. C. Bao, X. Deng, M. Tatsuka, S. Narumiya, W. S. May, T. Nosaka, K. Semba, T. Inoue, T. Satoh, M. Inagaki, and T. Kitamura, “Phosphorylation by Aurora B converts MgcRacGAP to a RhoGAP during cytokinesis,” *Dev. Cell*, vol. 4, no. 4, pp. 549–560, 2003.

[46] F. Pelegri, H. Knaut, H. M. Maischein, S. Schulte-Merker, and C. Nüsslein-Volhard, “A

mutation in the zebrafish maternal-effect gene nebel affects furrow formation and vasa RNA localization," *Curr. Biol.*, vol. 9, no. 24, pp. 1431–1440, 1999.

[47] C. Thisse and B. Thisse, "High-resolution in situ hybridization to whole-mount zebrafish embryos.," *Nat. Protoc.*, vol. 3, no. 1, pp. 59–69, 2008.

[48] A. R. Bassett, C. Tibbit, C. P. Ponting, and J. L. Liu, "Highly Efficient Targeted Mutagenesis of Drosophila with the CRISPR/Cas9 System," *Cell Rep.*, vol. 4, no. 1, pp. 220–228, 2013.

[49] L.-E. Jao, S. R. Wente, and W. Chen, "Efficient multiplex biallelic zebrafish genome editing using a CRISPR nuclease system.," *Proc. Natl. Acad. Sci. U. S. A.*, vol. 110, no. 34, pp. 13904–9, 2013.

[50] M. A. Moreno-Mateos, C. E. Vejnar, J. Beaudoin, J. P. Fernandez, E. K. Mis, M. K. Khokha, and A. J. Giraldez, "CRISPRscan: designing highly efficient sgRNAs for CRISPR-Cas9 targeting in vivo.," *Nat. Methods*, vol. 12, no. 10, pp. 982–8, 2015.

[51] A. Dereeper, V. Guignon, G. Blanc, S. Audic, S. Buffet, F. Chevenet, J. F. Dufayard, S. Guindon, V. Lefort, M. Lescot, J. M. Claverie, and O. Gascuel, "Phylogeny.fr: robust phylogenetic analysis for the non-specialist.," *Nucleic Acids Res.*, vol. 36, no. Web Server issue, pp. 465–469, 2008.

[52] A. Dereeper, S. Audic, J.-M. Claverie, and G. Blanc, "BLAST-EXPLORER helps you building datasets for phylogenetic analysis.," *BMC Evol. Biol.*, vol. 10, p. 8, 2010.

[53] C. M. Yates, I. Filippis, L. A. Kelley, and M. J. E. Sternberg, "SuSPect: Enhanced prediction of single amino acid variant (SAV) phenotype using network features," *J. Mol. Biol.*, vol. 426, no. 14, pp. 2692–2701, 2014.

Chapter 5: Summary, Future Directions and closing remarks

Elaine L. Welch and Francisco Pelegri*

Laboratory of Genetics, University of Wisconsin-Madison, Madison, WI, USA

*Correspondence to: fjpelegri@wisc.edu

Summary

In this dissertation I have described the process of vertebrate axis induction in the zebrafish. Induction of primary embryonic axis involves a rotation of the embryo cortex relative to the cytoplasm termed the cortical rotation. Cortical rotation has been extensively described in *Xenopus laevis* to occur minutes after fertilization and is mediated by a parallel network of microtubules. A similar process has been described in the zebrafish where dorsal determinants that are initially localized to the base of the vegetal cortex are shifted at a time when vegetal cortex microtubules become maximally aligned and parallel. This movement is inhibited when the embryo is treated with the microtubule depolymerizing drug nocodazole, as well as in *hecate/grip2a* mutants that are defective in dorsal axis induction, suggesting the role of parallel microtubules in this process. Additionally, we identified and characterized the zebrafish maternal effect mutation *tmi* and mapped it to Prc1l, a homolog of human PRC1. Prc1l is necessary for meiosis, mitosis and cytokinesis and in our studies, is implicated in reorganizing vegetal microtubules that are necessary for transport of dorsal determinants, and in turn for axis induction. Our data give us great insights into processes involved in early embryo patterning and how the maternal genome greatly contributes to this process.

Future directions: Rescue and complementation of Prc1l

The mutation in *tmi* has been identified to encode Prc1l, and appears to be a null mutation; however, we have not yet verified gene identity. To do this we are utilizing the CRISPR-mediated gene knockout of prc1l to generate a mutation in the prc1l gene that

should recapitulate the cytokinesis defects we see in *tmi* mutant embryos. We have already started the process by injecting the Cas9 and guide RNAs, grew up the injected fish, mated the P0, and will sequence the F1 generation for any anomalies. It can often prove difficult to rescue maternal mutations, so another option in addition to generation of CRISPR mutants is to prove gene identity through functional in vitro manipulation of zebrafish oocytes.

Midbody associated factors – future direction

We would like to look at other factors localized to the midbody and see what effects they have on prc1l. For example, in mammalian cells, Kif4 is necessary to translocate PRC1 to the midzone, we would like to see if the zebrafish homolog (kif23) has the same or similar function. We will also investigate the interaction of prc1l with motor proteins to see how it is being transported along microtubules. We will also continue to do high resolution imaging of microtubules, and potentially electron microscopy to see the interaction between microtubules, Prc1l, AurbK, Plk1 and Kif23. Understanding live microtubules dynamics will also shed some light on how microtubules become organized at the vegetal cortex in the early embryo. Making fluorescently labelled tags with all the proteins mentioned above, and inject into EMTB-GFP fish, would be a plausible way to go about live imaging to visualize microtubule dynamics and the interaction with other midbody-associated factors.

Asymmetric segregation of germ plasm – future direction

In addition to the results we have already obtained, we will continue to analyze the asymmetric segregation pattern of germ plasm RNPs and determine structures to which

they associate. We hope to track GP movement using fluorescent probes to label various GP RNPs, as well as repeat labeling the mitotic spindle and centrosomes with antibodies for these structures. It would be ideal to perform these experiments during cleavage stages to discern the pattern of segregation of GP components. This would include embryos at the 4 and 8 cell stage as well as somite stages, time points that encompass GP segregation. Additionally, we will employ in vivo studies to track live movement of germ plasm, which uses an in vitro system of oocyte maturation to inject fluorescently-labeled mRNAs including *nanos* and *bruno-like* into the developing oocytes of EMTB:GFP and centrin:GFP fish to label spindle and centrioles, respectively. This system allows for protein expression immediately after fertilization. Ideally, we would like to know if there is an association of GP with centrioles, and if this association correlates with the age of the centriole. Previously described mother centriole-specific proteins have been shown to first localize to new mother centrioles in S, G2 or M phase. Ninein, centriolin, pericentrin, γ-tubulin, and Polaris are known to localize symmetrically to the mother centrioles of both sister cells [1]. We will use antibodies against γ-tubulin and centrin together with GP markers to identify any patterns of colocalization to mother centrioles. Alternatively, we will examine potential localization with germ plasm RNPs with other cellular structures (e.g. ER, golgi, lysosomes) using appropriate antibodies and dyes. Another factor that can help to more closely identify specific segregation patterns is to be able to distinguish centriole age. For these studies, we will generate expressed fusions of centriole components such as Sas-6 [2] with the photoactivatable fluorescent protein Kaede [3] which should allow us to monitor newly formed centrioles and therefore determine centriole age. These data will help us

understand how cell are fated to become the germ line if we understand the basics of germ plasm segregation.

Closing remarks

Over the years I have found that zebrafish is an excellent model system for studying embryo patterning. The abundance of embryos a mother produces to the transparency or the embryos allows for quick functional manipulation. My projects were pretty similar in that they involved understanding how the primary axis is established, but I have learned so much about how to approach different questions and challenges, how to ask challenging questions and how to find ways to address them. Using forward genetics has helped me to learn that nothing is as straightforward as they initially seem, as we find new phenotypes for a particular mutation, and discover that a particular gene has several functions throughout the embryo. This has been an amazing experience and I am happy and grateful for all that I have learned on the journey.

References

[1] C. T. Anderson and T. Stearns, "Centriole Age Underlies Asynchronous Primary Cilium Growth in Mammalian Cells," *Curr. Biol.*, vol. 19, no. 17, pp. 1498–1502, 2009.

[2] T. Yabe, X. Ge, and F. Pelegri, "The zebrafish maternal-effect gene cellular atoll encodes the centriolar component sas-6 and defects in its paternal function promote whole genome duplication," *Dev. Biol.*, vol. 312, no. 1, pp. 44–60, 2007.

[3] R. Ando, H. Hama, M. Yamamoto-Hino, H. Mizuno, and A. Miyawaki, "An optical marker based on the UV-induced green-to-red photoconversion of a fluorescent protein.," *Proc. Natl. Acad. Sci. U. S. A.*, vol. 99, no. 20, pp. 12651–12656, 2002.

Appendix 1: Factors involved in early embryonic cytokinesis function in the reorganization of the vegetal microtubule array required for cortical rotation and axis induction

Elaine L. Welch and Francisco Pelegri*

Laboratory of Genetics, University of Wisconsin-Madison, Madison, WI, USA

*Correspondence to: fjpelegri@wisc.edu

A1.1. Introduction and Results

A1.1.1. Midbody-associated factors important for dorsal axis induction

It has been established that the microtubule cytoskeleton is an important component in establishing the vertebrate embryo axis. The gene *too much information* (*tmi*) that encodes protein regulator of cytokinesis 1-like (Prc1l) is important for cytokinesis in the zebrafish embryo. Our observations show that embryos derived from mothers that are heterozygous for the *tmi* mutation display a significant proportion of embryos with ventralized phenotypes of varying degrees according to the classes identified previously in [1]. This observation led us to investigate the potential role that prc1l plays in dorsoventral axis induction.

As a proxy to test for patterning defects in the zebrafish, we have used the proposed dorsal determinant Wnt8a and observe the mRNA localization via whole mount in situ hybridization and examine its asymmetric movement toward the dorsal region of the embryo. The off-center movement of *wnt8a* mRNA from the vegetal pole to the dorsal region is mediated by a parallel network or microtubules spanning the vegetal cortex. We noticed that embryos from *tmi* homozygous mothers, referred to as *tmi* mutants, fail to exhibit the off-center movement of wnt8a mRNA, as mentioned in the previous chapter. *tmi/prc1l* is part of the MAP/ASE1 family of proteins and homologous to mammalian PRC1. PRC1 is localized to the spindle midzone and helps to control the extent of overlap between antiparallel microtubules [2]. Examining the subcellular localization of Prc1l revealed that it is not similar to that of its homologs. We thought however that we would examine other midbody-associated factors that we have available including chromosomal passenger

proteins Aurora B kinase and Survivin as well as Polo-like kinase, to see what roles, if any, these genes play in patterning the vertebrate embryo.

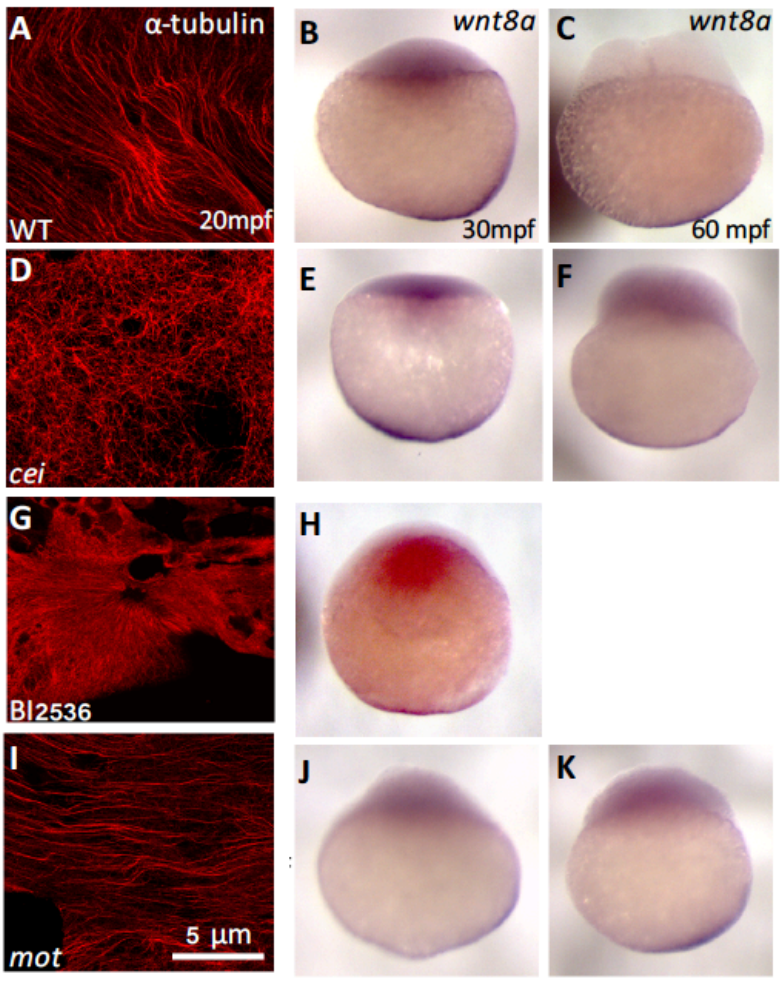

Figure 1: Vegetal microtubule reorganization and *wnt8a* localization.

A-C) Wild type embryo at 20 mpf show that microtubules spanning the vegetal cortex are arranged in a parallel orientation (A) and in situ hybridization show that the off-center movement of *wnt8a* mRNA is evident in embryos at 30 and 60 mpf. D-F) *cei* mutant embryo at 20 mpf display a disruption of the parallel vegetal microtubule array (D), and a consequent failure to transport *wnt8a* toward the dorsal region in embryos at 30 mpf (E) and 60 mpf (F). G-H) Embryo at 20 mpf in which Plk1 was inhibited shows microtubules radially emanating from an unknown structure (G), these embryos at 30 mpf also fail to undergo the off-center movement of *wnt8s* mRNA (H). I-K) *motley* mutant embryo at 20 mpf display a parallel arrangement of microtubules similar to that in wild type (I), and subsequently experience the off-center shift of *wnt8a* mRNA in 30 mpf (J) and 60 mpf (K) embryos. The scale bar in I represents 5 micron for all immunolabeled images.

Aurora B kinase is a member of the aurora family of serine/threonine kinases and a member of the chromosomal passenger complex (CPC). Aurora B is localized to centrosomes prior to mitosis, localized early in mitosis to centromeres and contributes to proper cell division by stabilizing the kinetochore and controls regulation of the spindle assembly checkpoint. It is later localized to the spindle midzone after chromatid segregation in anaphase [3]–[5].

In zebrafish, a maternal effect mutation *cellular island (cei)* was identified to encode Aurora B kinase that produces embryos with cytokinesis defects including delay in furrow initiation, as well as complete failure to form a mature cleavage furrow [4]. Using embryos from mothers that are homozygous for the *cei* mutation (*cei* mutant embryos), we investigated the localization of *wnt8a* as well as the organization of vegetal microtubules. Whole mount in situ hybridization revealed that wild type embryos at 30 and 60 mpf exhibit an off-center shift of *wnt8a* mRNA from the base of the vegetal pole toward the dorsal region of the embryo (Figure 1B-C). *cei/AurbK* mutant embryos at the same time in development failed to allow for the asymmetric dorsal movement of *wnt8a* mRNA (Figure 1E-F)). Since it has been determined that the off-center movement of dorsal factors, such as *wnt8a*, is mediated by a parallel array of microtubules at the vegetal cortex, we tested this phenomenon in *cei* mutant embryos. Using immunolabeling to detect alpha tubulin, we noticed that wild type embryos at 20 mpf display a nice bundling of parallel microtubules spanning the vegetal cortex (Figure 1A), on the other hand, *cei* mutant embryos display a branched meshwork of microtubules that does not become aligned as parallel bundles

(Figure 1D). In our studies, we also see AurbK protein is subcellular localized to the midbody matrix (Figure 2A-D).

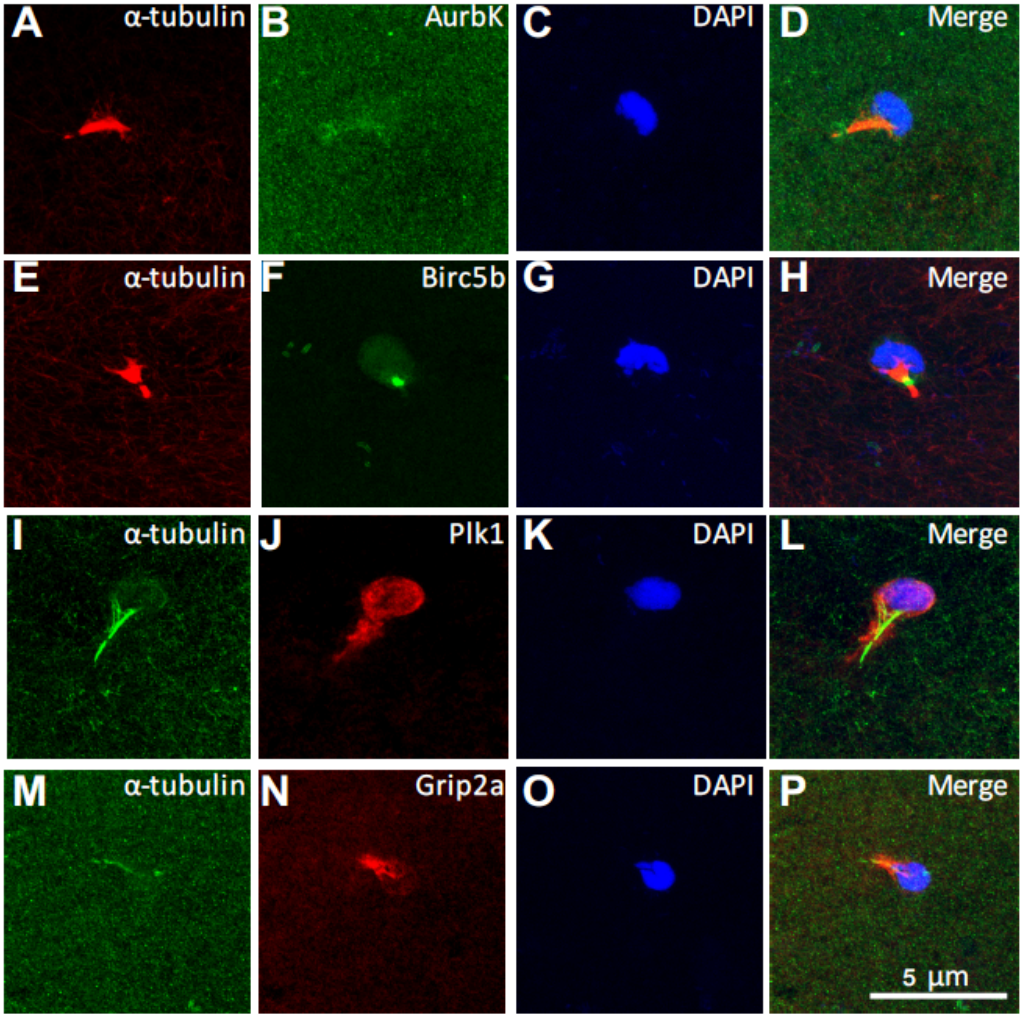

Figure 2: Subcellular localization of midbody associated-factors.

A-D) CPC component Aurora B kinase is localized to the midbody matrix, similar to that of Birc5b/Survivin (E-H). I-L) Plk1 is localized around the meiotic midbody as well as the polar body. M-P) The dorsal determinant Grip2a is also seen encasing the midbody and the polar body. In A-H, microtubules are labeled with mouse anti α-tubulin antibody (red), and in I-P microtubules are labaeled with a rabbit anti α-tubulin antibody (green). 5 micron scale bar in P is representative of all panels.

Similarly, we investigated the effects of Polo-like kinase 1, a conserved Polo family serine/threonine kinase that has various roles in mitotic entry, progression, exit and cytokinesis [2], [6]. Plk1 is also known to localize to significant mitotic structures as cell division progresses including the centrosomes and kinetochores from prophase to metaphase, the central spindle in anaphase and the spindle midzone in telophase [6]. It was shown that a Plk1 inhibitor, BI2536, blocked mitotic progression in developing zebrafish embryos [7]. In our studies, we used the Plk1 inhibitor, BI2536 to block the function of Plk1 in the early embryo. After treating dechorionated embryos in 100 μm of BI2536, we noticed that the embryos did not undergo cell division by failing to form a 2 cell embryo with a visible mature furrow by 45 mpf (not shown). Using in situ hybridization, we again looked at the spatial localization of *wnt8a* in drug treated embryos. We noticed that at 30 mpf Plk1-inhibited embryos failed to exhibit the off-center movement of *wnt8a* mRNA (Figure 1H). We also noticed that the organization of vegetal was different from that of wild type in that BI2536 treated embryos had a branched meshwork or microtubule bundles, and in some cases displayed a radial arrangement of microtubules (Figure 1G), similar to that seen in *hecate/grip2a* mutant embryos [1].

Another zebrafish maternal effect mutation, *motley*, was identified to encode *birc5b,* a zebrafish homolog of mammalian Birc5/Survivin, a member of the CPC [8]. Disruption of the CPC results in lagging chromosomes during metaphase that eventually cause chromosome segregation errors. Another effect is that cleavage furrows fail to ingress resulting in failure of cytokinesis [9], [10]. Data have shown that the subcellular localization of Birc5b is similar to that of a CPC protein [8] (Figure 2A-H). Embryos from mothers that are homozygous for the *motley* mutation (referred to as *motley* mutants),

display meiotic and mitotic chromosome segregation errors [8]. We tested motley mutants in whole mount in situ hybridization experiments to observe the spatial localization of *wnt8a* mRNA. We noticed that unlike *cei/aurbK*, *motley* embryos experience the asymmetric movement of *wnt8a* from the vegetal pole to the dorsal region of the embryo at 30 and 60 mpf (Figure 1J-K). We also tested the vegetal microtubule alignment in *motley* mutants, and they are similar to wild type in that they display a parallel alignment of microtubules along the vegetal cortex (Figure 1I), suggesting that *motley* likely doesn't play a role in dorsoventral patterning. Together these preliminary data suggest that members of the CPC act differently to regulate the same processes and others members of the complex have totally different functions.

Subsequently, we examined the subcellular localization of zebrafish Plk1 with an antibody designed against the N terminal region of the protein, as well as that of Grip2a. We notice that like Prc1l, Plk1 is localized around the polar body in the early embryo (Figure 2I-L). The dorsal determinant Grip2a also showed a similar localization to Plk1 in that it was also localized to the polar body at 20 mpf (Figure 2M-P), and the localization disappears with polar body extrusion (not shown). These data suggest that Plk1 and Grip2a have a potential role in polar body extrusion at the animal pole of the developing zebrafish embryo.

A1.1.2. Localization of midbody-associated factors along vegetal microtubules

It is known that vegetal microtubules are necessary for the process of cortical rotation (Houston, 2012), but very little is known about how this population of microtubules become polymerized and assembled. Given what we know about prc1l and its

potential role in axis induction, we have investigated the protein localization at the vegetal cortex and how it interacts with microtubules. Microtubules at the vegetal cortex begin to align into parallel bundles beginning at approximately between 12-17 mpf. At this time, we see Prc1 at the edges of microtubules (Figure 3A-F). By 20 mpf, at the time when microtubules are maximally parallel, we notice Prc1l localization along tracks of microtubules (Figure 3G-I). By 27 mpf microtubules begin to lose their parallel arrangement and Prc1l still attached to the microtubules pieces that are still intact (Figure 3J-L). In *tmi* mutant embryos, as mentioned previously, the microtubules do not form parallel bundles, and we do not see the localization of Prc1l present, as expected (Figure 3M-R). Additionally, we investigated the protein localization of Plk1 and Grip2a and notice that they also localize closely with microtubules, but with the preliminary images, it is hard to say how they are actually interacting (Figure 3S-X). Together out results give possible insights into how vegetal microtubules become assembled in the zebrafish embryo.

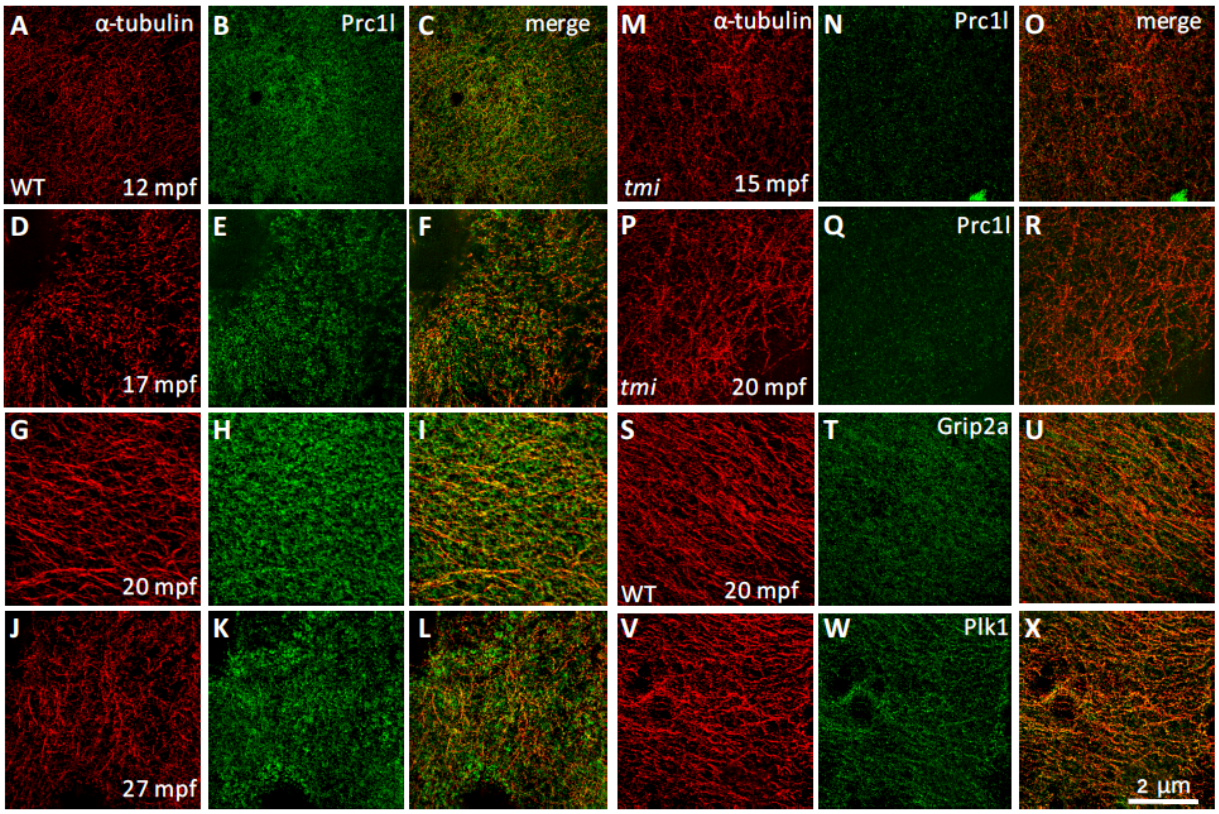

Figure 3: Vegetal microtubule reorganization.

A-F) Structured illumination microscopy show that in wild type embryos between 12 and 17 mpf, microtubules have not yet formed parallel bundles and Prc1l is seen attaching onto microtubules. G-I) By 20 mpf, microtubules form parallel bundles and Prc1l is localized along these parallel tracks. J-L) By 27 mpf the parallel begins to dissociate and Prc1l is still seen attached to intact microtubules. M-R) In *tmi* mutant embryos at 15 and 20 mpf, parallel arrangement is disrupted and Prc1l is not localized. S-U) Grip2a and (V-X) Plk1 are both localized along microtubule bundles in wild type embryos at 20 mpf. Scale bar represents 2 micron for all panels.

A1.2. References

[1] X. Ge, D. Grotjahn, E. Welch, J. Lyman-gingerich, C. Holguin, E. Dimitrova, E. W. Abrams, T. Gupta, F. L. Marlow, T. Yabe, A. Adler, M. C. Mullins, and F. Pelegri, "Hecate / Grip2a Acts to Reorganize the Cytoskeleton in the Symmetry-Breaking Event of Embryonic Axis Induction," vol. 10, no. 6, 2014.

[2] M. Petronczki, P. Lénárt, and J. M. Peters, "Polo on the Rise-from Mitotic Entry to Cytokinesis with Plk1," *Dev. Cell*, vol. 14, no. 5, pp. 646–659, 2008.

[3] V. Krenn and A. Musacchio, "The Aurora B Kinase in Chromosome Bi-Orientation and Spindle Checkpoint Signaling.," *Front. Oncol.*, vol. 5, no. October, p. 225, 2015.

[4] T. Yabe, X. Ge, R. Lindeman, S. Nair, G. Runke, M. C. Mullins, and F. Pelegri, "The maternal-effect gene cellular island encodes Aurora B kinase and is essential for furrow formation in the early zebrafish embryo," *PLoS Genet.*, vol. 5, no. 6, 2009.

[5] S. Ruchaud, M. Carmena, and W. C. Earnshaw, "Chromosomal passengers: conducting cell division," *Nat Rev Mol Cell Biol*, vol. 8, no. 10, pp. 798–812, 2007.

[6] F. a Barr, H. H. W. Silljé, and E. a Nigg, "Polo-like kinases and the orchestration of cell division.," *Nat. Rev. Mol. Cell Biol.*, vol. 5, no. 6, pp. 429–440, 2004.

[7] K. Jeong, J. Y. Jeong, H. O. Lee, E. Choi, and H. Lee, "Inhibition of Plk1 induces mitotic infidelity and embryonic growth defects in developing zebrafish embryos," *Dev. Biol.*, vol. 345, no. 1, pp. 34–48, 2010.

[8] S. Nair, F. Marlow, E. Abrams, L. Kapp, M. C. Mullins, and F. Pelegri, "The Chromosomal Passenger Protein Birc5b Organizes Microfilaments and Germ Plasm in the Zebrafish Embryo," *PLoS Genet.*, vol. 9, no. 4, 2013.

[9] R. R. Adams, H. Maiato, W. C. Earnshaw, and M. Carmena, "Essential roles of Drosophila inner centromere protein (INCENP) and aurora B in histone H3 phosphorylation, metaphase chromosome alignment, kinetochore disjunction, and chromosome segregation," *J. Cell Biol.*, vol. 153, no. 4, pp. 865–879, 2001.

[10] R. Honda, R. Körner, and E. Nigg, "Exploring the Functional Interactions between Aurora B, INCENP, and Survivin in Mitosis," *Molecular biology of the cell*, vol. 14, no. August. pp. 3325–3341, 2003.

Appendix 2: Patterns of segregation of known germ plasm components with respect to the cell division apparatus

Elaine L. Welch and Francisco Pelegri*

Laboratory of Genetics, University of Wisconsin-Madison, Madison, WI, USA

*Correspondence to: fjpelegri@wisc.edu

A2.1. Introduction and Results

Germ cells arise in early development by two distinct mechanisms. In some animals such as *D. melanogaster*, *C. elegans*, *X. laevis* and zebrafish, PGCs arise through a process known as preformation, which is a cell autonomous mechanism mediated by specialized cytoplasmic localization called germ plasm. Other animals such as mice [1] rely on epigenesis, which is the specification of germ cells involving their induction from pluripotent stem cells by extracellular signals [2], [3]. Zebrafish embryos use the preformation mechanism for PGC induction, as originally evidenced by the segregation pattern of the germ line gene *vasa* [4]. *vasa* mRNA GP RNPs are synthesized during oogenesis and localize to cleavage furrows. Subsequently, they form four large masses that segregate into four cells by the 32 cell stage [4], [5]. Other components of the zebrafish germ plasm, include *dead end* [6], *nanos* [7], *deleted-in-azoospermia-like (dazl)*, and *bruno-like (celf1)* [8], as well as Bruno-Like protein. We have also identified associations between germ plasm RNPs and components of the CPC such as the protein Survivin, which appears to mediate a link between astral microtubule tips and germ plasm RNPs that is essential for RNP multimerization [9].

The maternal inheritance of germ plasm is a common means by which animal species initiate the zygotic gene expression program of germ line specification. In the early zebrafish embryo, germ plasm (GP) inheritance involves the sequential aggregation of cortical GP ribonucleoparticles (RNPs) so that by the 4-cell stage, they form four multimerized masses (Figure 1). Once formed, these masses segregate asymmetrically during cell division in the cleavage stage embryo, so that it is inherited in its entirety by only one daughter cell [10] (see figure 1). Inheritance of the full-size GP aggregate by a

single daughter cell likely insures optimal germ cell specification once the zygote genome becomes activated at the mid-blastula transition. This process of asymmetric segregation has not been previously studied at the cellular level, but studying this process can give us insights about the processes involved in specifying cells that will become the germ line.

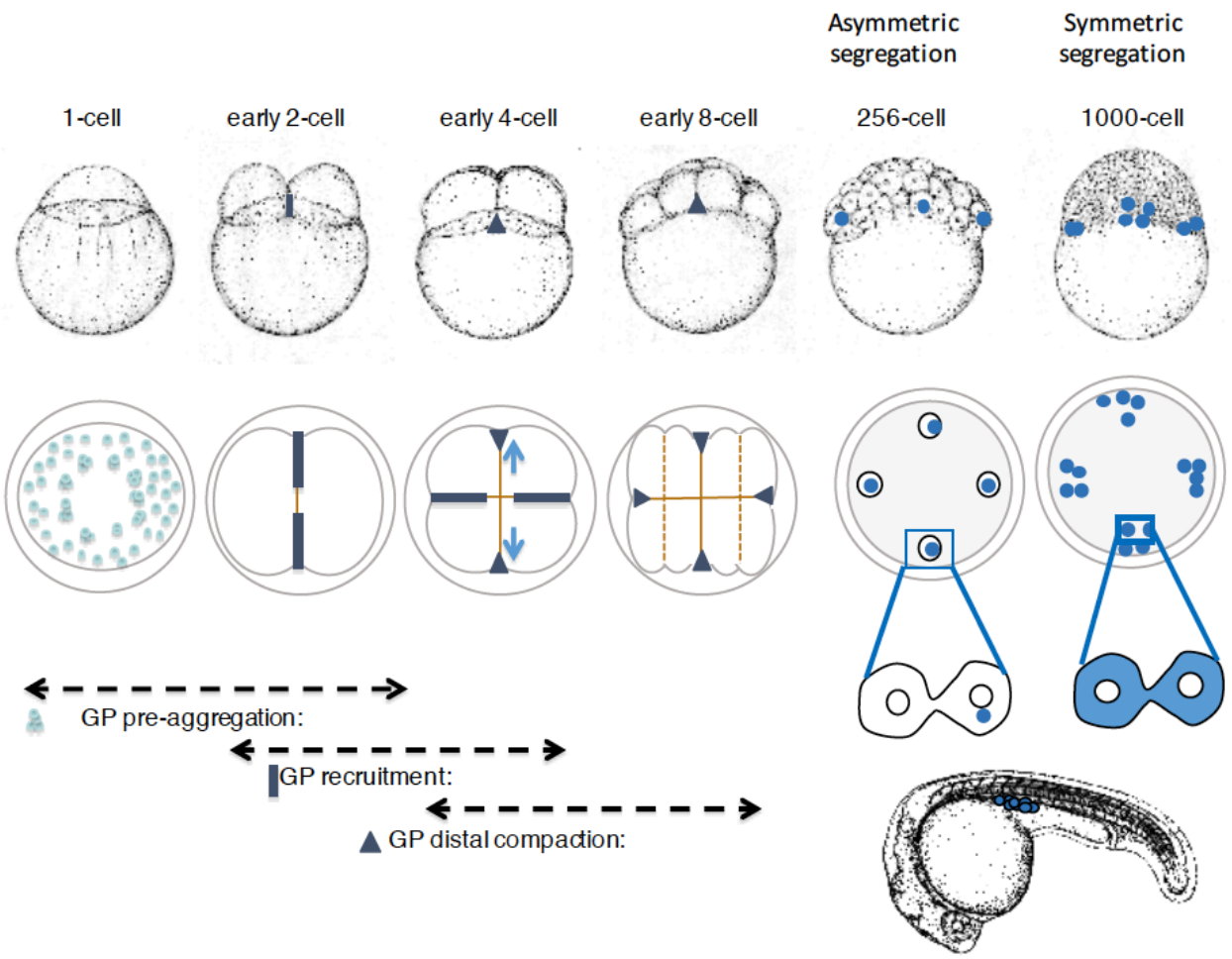

Figure 1: Schematic of zebrafish germ plasm segregation.

Germ plasm undergoes several stages of multimerization. In the one cell embryo, pre-aggregation takes place where RNPs gather prior to furrow initiation. At the 2 cell stage, pre-aggregated RNPs gather at the furrow. By the 4 cell stage, the second furrow has formed, and aggregates from the first furrow starts to distally compact toward the corners of the mature furrow. At the 8 cell stage, 4 RNP aggregates have compacted at the first and second furrow. The four germ plasm masses which formed during the first two cell cycles do not undergo degradation, but are translocate from their location at the blastomere-yolk cell boundary to the inside of each of four corners of the blastodisc. At the 256 cell stage, GP RNP is recruited to only one daughter cell, by 1000 cell stage it spreads into the cytoplasm where it is now symmetrically localized, and by 24 hpf, GP is localized to the gonads.

The fact that only one daughter cell inherits the GP aggregate led us to investigate the mechanism that allows for this to occur. We surmised that these RNPs become connected to the spindle pole either through the connection with the mother or daughter centriole. To address this, we first looked at the association between germ plasm RNPs and centrosomes. We used FISH combined with immunofluorescence to label the GP component *dead end (dnd)* as well as the spindle and centrosomes at various stages of development. Our imaging studies revealed that *dnd* is indeed seen toward one of the spindle poles (Figure 2A'-D'), however, based on 3D rendering of the image, we do not think that the RNP is directly attached to the centrosome (not shown). We premise that there is potentially another element of connection that brings the GP RNP toward the spindle pole and remains tethered to keep the RNPs there. Our preliminary data tells us that RNPs indeed segregate to one spindle pole and are being tethered by an unknown mechanism. This will be investigated further in the future.

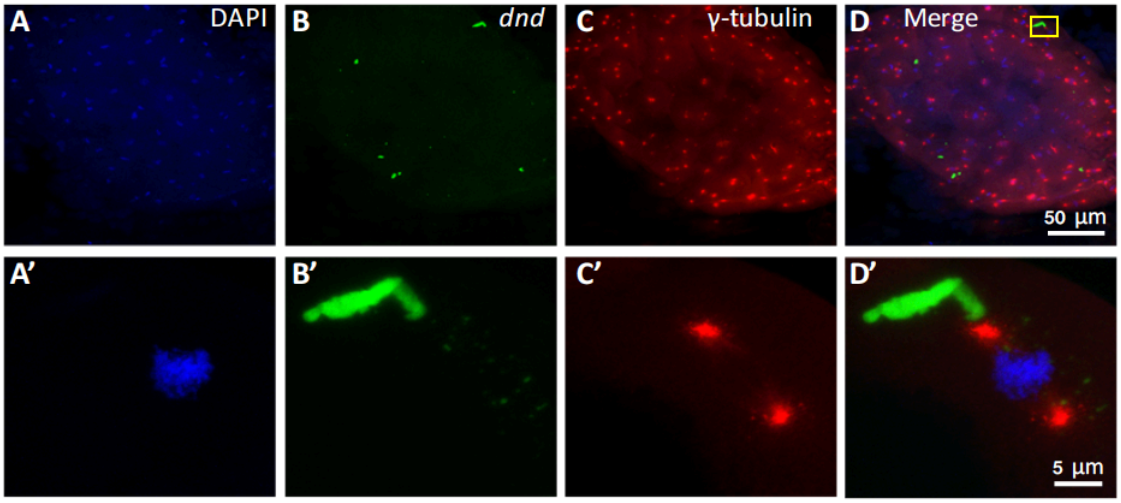

Figure 2: Asymmetric segregation of germ plasm.

A-D) Wild type embryos at 512 cells show RNPs for the germ plasm marker *dnd* (green) in the corners of the furrow seemingly touching centrosomes (red) (2D'). DNA is labeled in blue. A'-D' are higher magnification of inset in A-D.

A2.2. References

[1] C. G. Extavour and M. Akam, "Mechanisms of germ cell specification across the metazoans: epigenesis and preformation.," *Development*, vol. 130, no. 24, pp. 5869–5884, 2003.

[2] R. P. Elinson, M. C. Sabo, C. Fisher, T. Yamaguchi, H. Orii, and K. Nath, "Germ plasm in Eleutherodactylus coqui, a direct developing frog with large eggs," *Evodevo*, vol. 2, no. 1, p. 20, 2011.

[3] T. Evans, C. M. Wade, F. A. Chapman, A. D. Johnson, and M. Loose, "Acquisition of Germ Plasm Accelerates Vertebrate Evolution," *Science (80-.).*, vol. 344, no. 6180, pp. 200–203, 2014.

[4] C. Yoon, K. Kawakami, and N. Hopkins, "Zebrafish vasa homologue RNA is localized to the cleavage planes of 2- and 4-cell-stage embryos and is expressed in the primordial germ cells.," *Development*, vol. 124, no. 16, pp. 3157–65, 1997.

[5] A. K. Braat, T. Zandbergen, S. V. A. N. D. E. Water, H. J. T. H. Goos, and D. Zivkovic, "Characterization of Zebra sh Primordial Germ Cells: Morphology and Early Distribution of," *Dev. Biol.*, vol. 167, no. May, pp. 153–167, 1999.

[6] G. Weidinger, J. Stebler, K. Slanchev, K. Dumastrei, C. Wise, R. Lovel-Badge, C. Thisse, B. Thisse, and E. Raz, "dead end a novel vertebrate germ plasm component is required fir zebrafish primordial germ cell migration and survival," *Curr. Biol.*, vol. 13, pp. 1429–143478, 2003.

[7] M. Koprunner, C. Thisse, B. Thisse, and E. Raz, "A zebrafish nanos -related gene is essential for the development of primordial germ cells," *Genes Dev.*, vol. 15, pp. 2877–2885, 2001.

[8] Y. Hashimoto, S. Maegawa, T. Nagai, E. Yamaha, H. Suzuki, K. Yasuda, and K. Inoue, "Localized maternal factors are required for zebrafish germ cell formation," *Dev. Biol.*, vol. 268, no. 1, pp. 152–161, 2004.

[9] S. Nair, F. Marlow, E. Abrams, L. Kapp, M. C. Mullins, and F. Pelegri, "The Chromosomal Passenger Protein Birc5b Organizes Microfilaments and Germ Plasm in the Zebrafish Embryo," *PLoS Genet.*, vol. 9, no. 4, 2013.

[10] H. Knaut, F. Pelegri, K. Bohmann, H. Schwarz, and C. Nüsslein-Volhard, "Zebrafish vasa RNA but not its protein is a component of the germ plasm and segregates asymmetrically before germline specification," *J. Cell Biol.*, vol. 149, no. 4, pp. 875–888, 2000.